

MMIC Design JHU EE787
Fall 2001 Student Projects
Supported By TriQuint and Agilent Eesof
Instructors Craig Moore and John Penn

Driver Amplifier—Ricardo Kanney

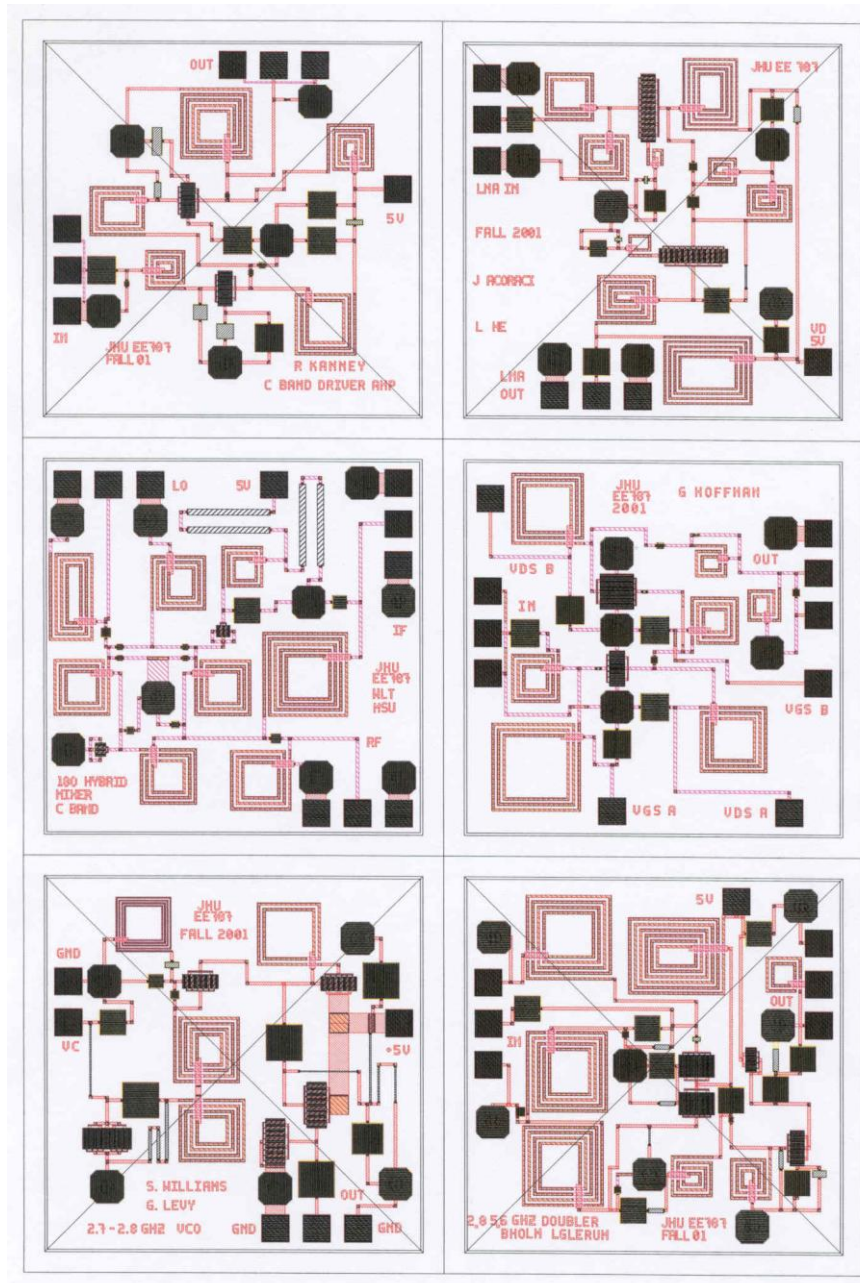
Low Noise Amplifier—Liewei He & Joe Acoraci

Mixer—Willie Thompson

Power Amplifier—Gary Hoffman

Voltage Controlled Oscillator—Steve Williams & Gary Levy

Frequency Doubler—Lonnie Glerum & Brent Holm



**MMIC DESIGN PROJECT
C BAND DRIVER AMPLIFIER**

BY

RICARDO KANNEY

DUE DATE: 12/10/01

INSTRUCTORS: C. MOORE & J. PENN

EE525.787

Table of Contents

Abstract	3
Introduction	5
Circuit Description	5
Design Philosophy	5
Trade-offs	6
Modeled Performance	6
Specification Compliance Matrix	6
Predicted Performance	7
Schematic Diagrams	13
DC Analysis	15
Test Plan	16
Linear Parameters	16
Power Measurements	16
Conclusion & Recommendations	16

Abstract

This report documents the design of a C band driver amplifier using the TriQuint TQS TRx process. The design was completed as part of the MMIC Design course offered by Johns Hopkins University. The amplifier was designed using the Advanced Design System (ADS) software which included the TriQuint elements library, and was laid out in a 60 x 60 mil Anachip. The driver amplifier is intended to be used in a simplex transceiver for the C band HiperLAN wireless local area network (WLAN) and industrial, scientific, and medical (ISM) frequencies, and will be used in conjunction with other projects designed in the class.

Introduction

Circuit Description

The driver amplifier is basically comprised of two cascaded GFET transistors biased class AB. Input and output matching circuitry was used to achieve the desired performance as stated in the circuit specifications. Where possible, components were used in both the matching circuitry and bias networks to reduce the total number of components used in the design.

Design Philosophy

In designing the driver amplifier the main focus was concentrated on output power and gain. These are critical parameters because the small amount of power exiting the variable amp must be amplified enough to drive the next stage which is the power amplifier. Also, it is desired in the specs to use only one 5v power supply, which calls for self-biased circuitry. For these reasons I chose the TriQuint 300um GFET for both stages.

The first step in the design was to determine the bias point for both stages. For the first stage I chose I_q to be about $1/3 I_{DSS}$ primarily to increase efficiency and lower the power to drive the second stage.

Stage 1: $V_{ds}=3.8v$; $V_{gs}=-1.2v$; $I_d=29mA$

This was done in ADS by connecting voltage sources to the gate and drain of the GFET and sweeping the voltages to obtain the parts IV curves.

Next, the bias for stage 2 was chosen to be about $1/2 I_{DSS}$ because this is where the main power amplification is taking place.

Stage 2: $V_{ds}=4.2v$; $V_{gs}=-0.8v$; $I_d=46mA$

The next step in the design was to determine the input and output matching circuitry for the first and second stages, individually. This was done using the Cripps method, where the output impedance of the GFET is determined using the linear s parameter file. Using this technique an output matching circuit can be developed. Next, by cascading the s2p file with the output matching network, a matching network can now be developed for the input of the transistor. Note that ideal elements were used for this iteration of the design process and each stage was modeled separately.

After the matching circuitry is designed for both stages and each stage is optimized for best output power, return loss, and gain, (this includes both linear and nonlinear modeling) the two stages are now combined and the overall performance of the amplifier is optimized. Upon determining that the overall performance of the ideal element model is satisfactory, it is now time to substitute in the TriQuint elements. I modeled TriQuint capacitors and inductors against their ideal counterparts to obtain comparable values. Since inductors contained high series resistance, I added them one at a time and tweaked the circuit at each iteration.

The final step was to add interconnects to the circuit and take the overall layout into consideration. Once the circuit was laid out in the 60 x 60 mil anachip using microstrip lines, the performance must again be evaluated. I found that the greatest impact came in adjusting the various inductances in the circuit because the interconnections coming from each inductor added increased the inductance.

Trade-offs

While a self-bias approach uses only one voltage supply and is relatively simple, the bias is not easily adjustable. A resistor ladder could have been added to compensate for variations in V_p but this would require more space.

Modeled Performance

Specification Compliance Matrix

The following table summarizes the design specification and the simulated results of both the simplified schematic and final layout schematic.

	Specification Goal	Simplified Schematic	Final Layout Schematic
Bandwidth	>725 MHz	1000 MHz	1000MHz
Gain	>12 dB	18.7dB	13.6dB
Gain Ripple	± 0.5 dB	0.37dB	0.49dB
Output Power	>+13dBm	14.77dBm	14.1dBm
VSWR	<1.5:1 input & output	1.24:1 input 2.44:1 output	1.32:1 input 2.32:1 output
Supply Voltage	± 5 v	+5v only	+5v only

Predicted Performance

The following plots show the modeled performance of the simplified schematic and the final layout schematic.

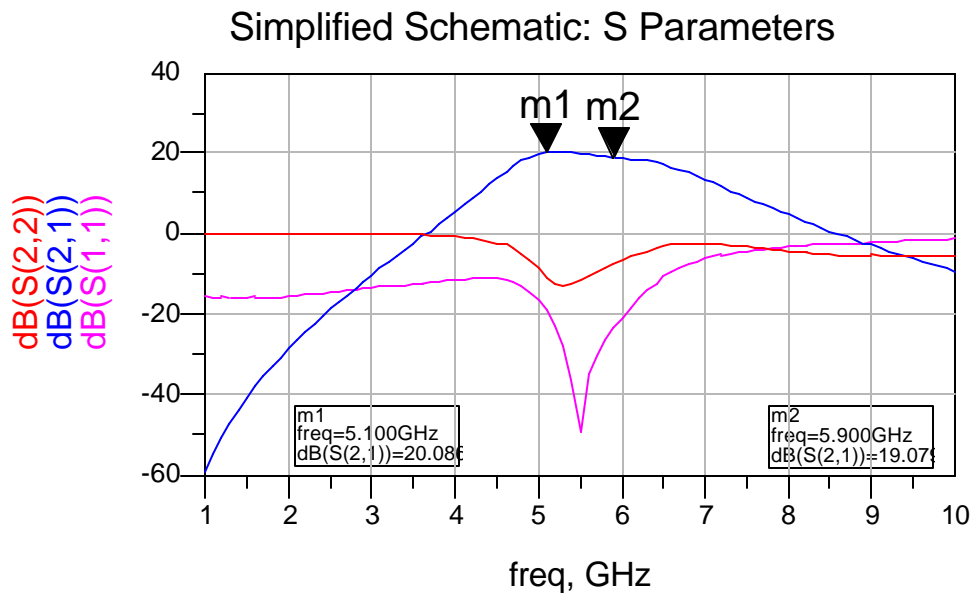


Figure 1: Simplified Schematic S Parameters

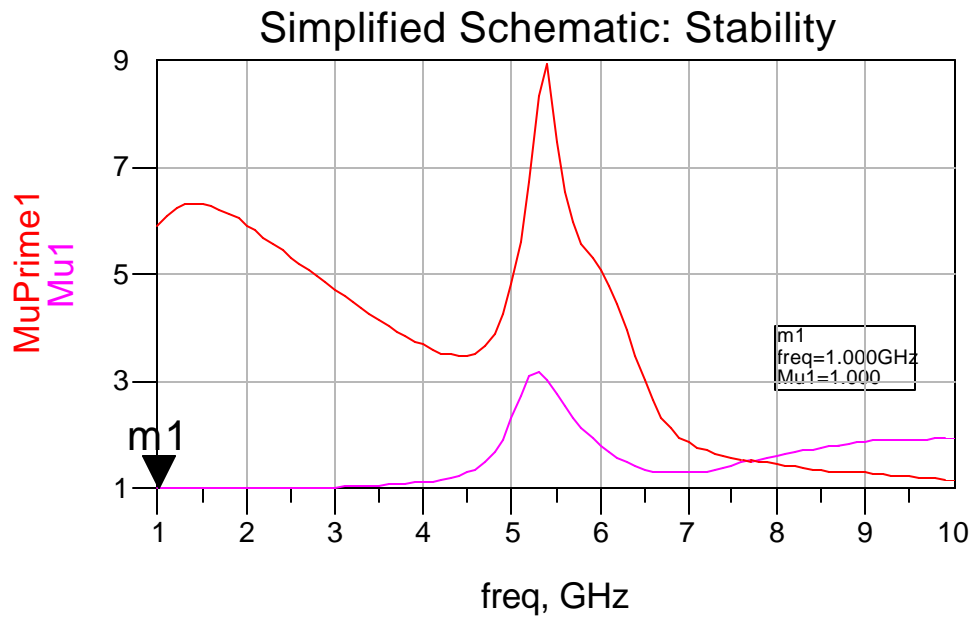


Figure 2: Simplified Schematic Stability

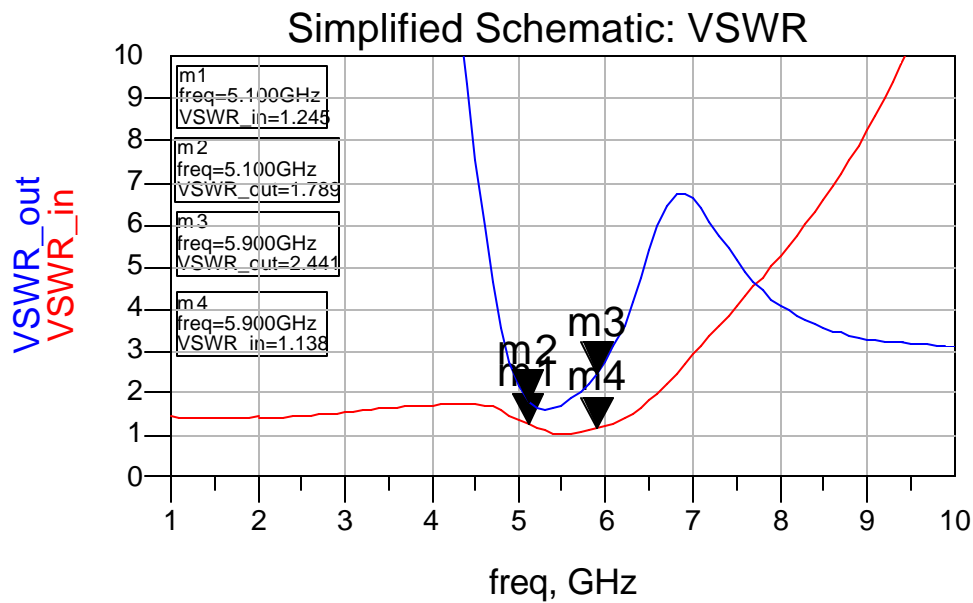
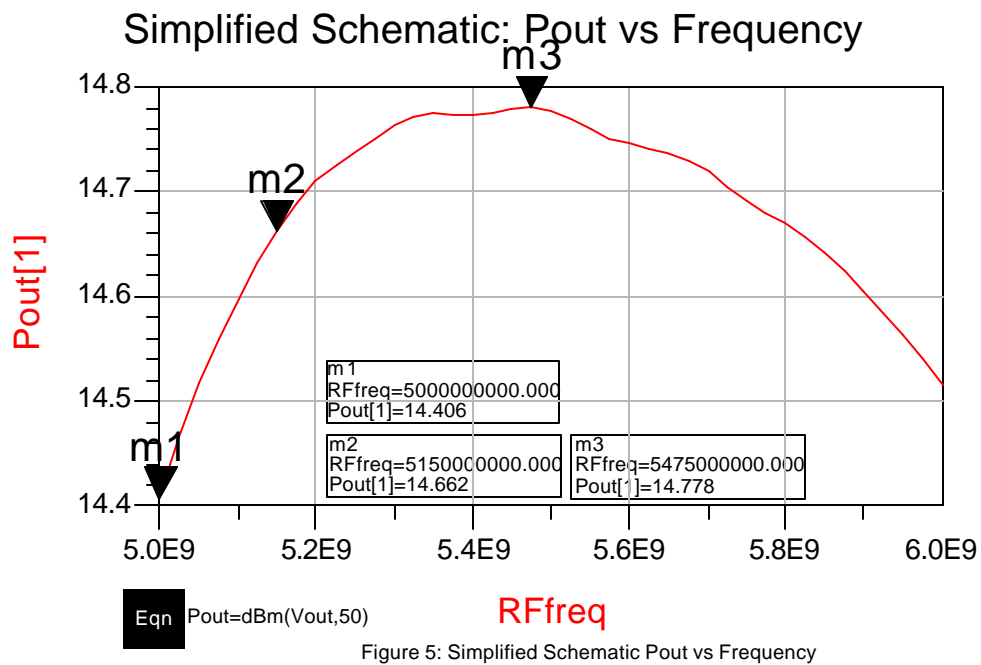
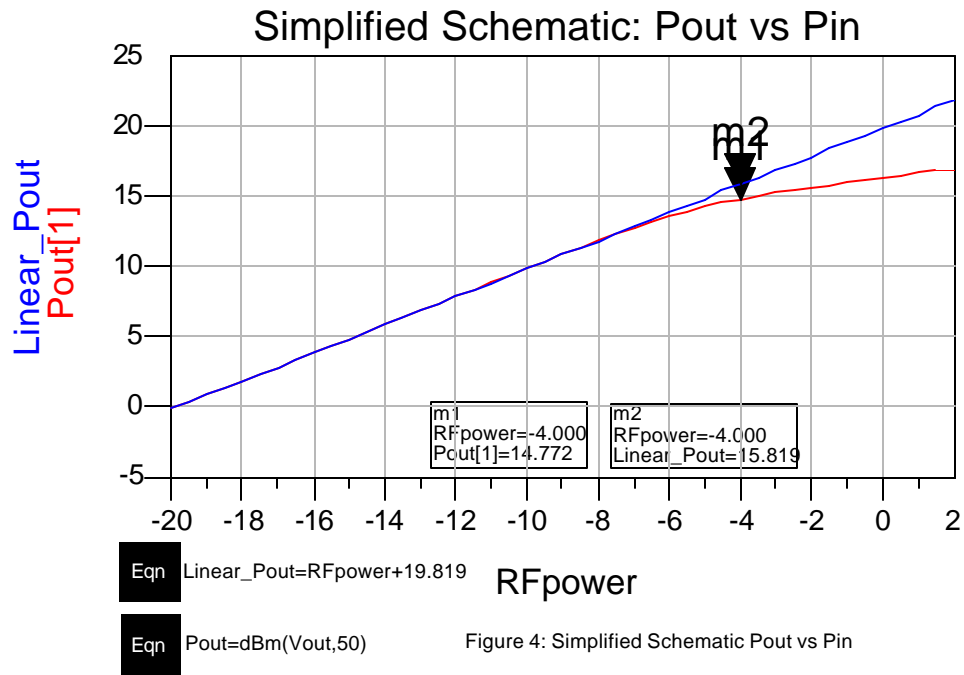


Figure 3: Simplified Schematic VSWR



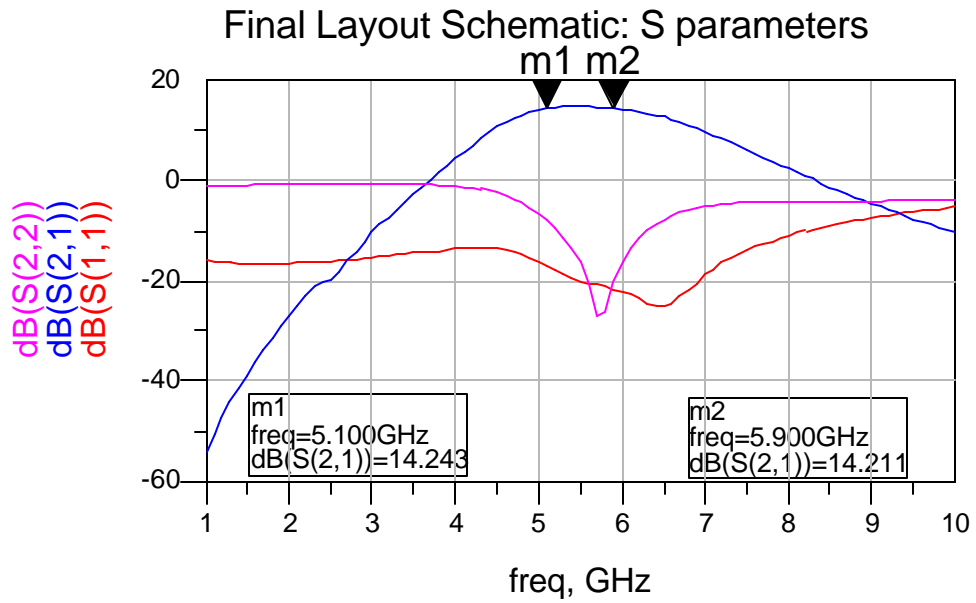


Figure 6: Final Layout Schematic S Parameters

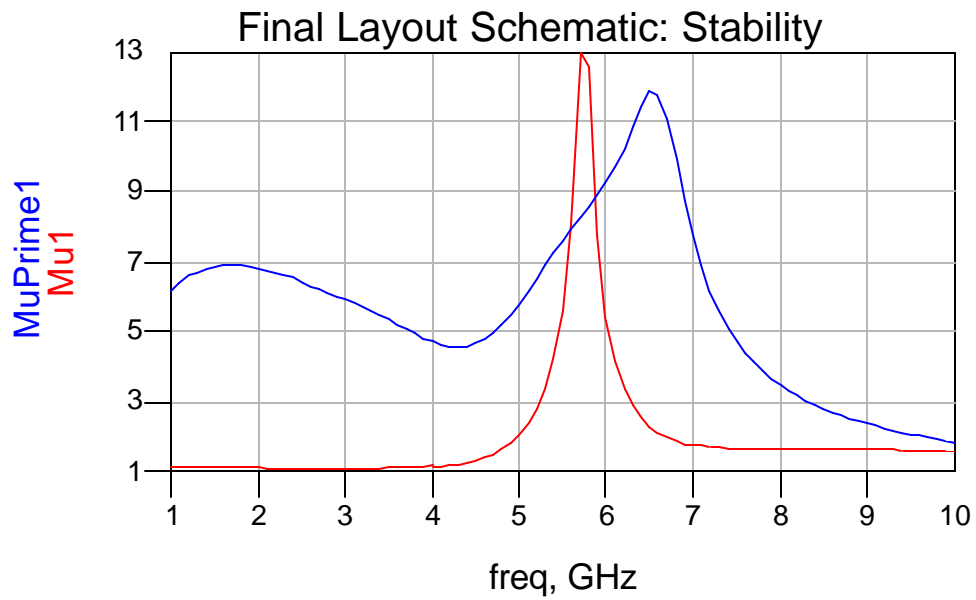


Figure 7: Final Layout Schematic Stability

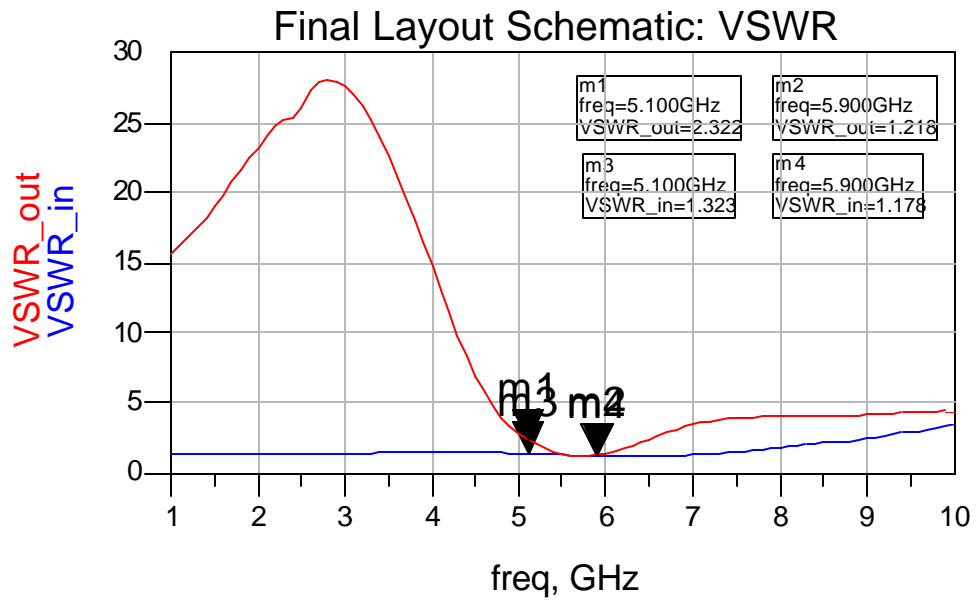


Figure 8: Final Layout Schematic VSWR

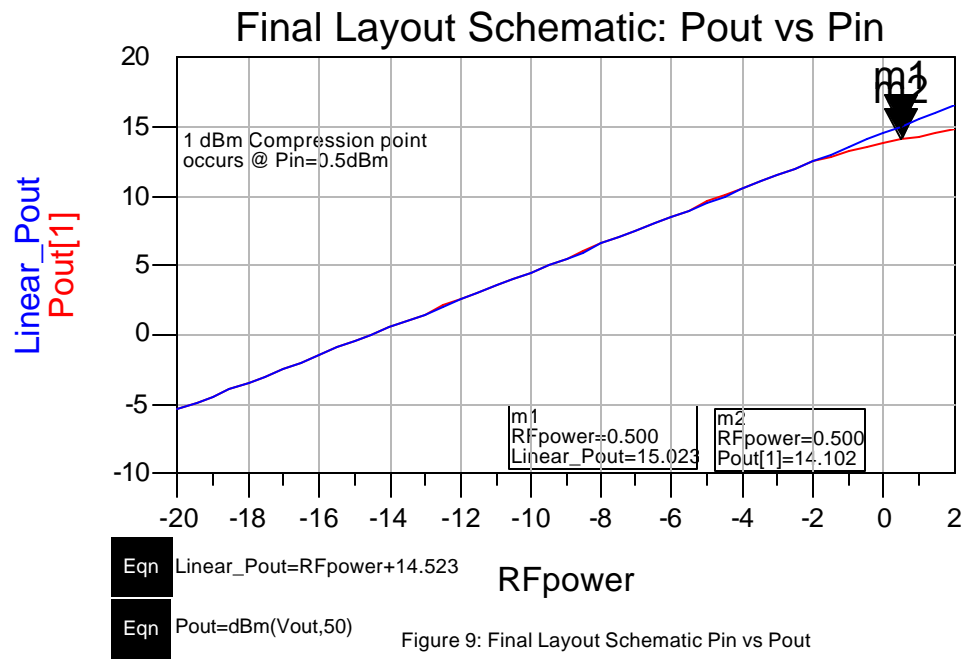


Figure 9: Final Layout Schematic Pin vs Pout

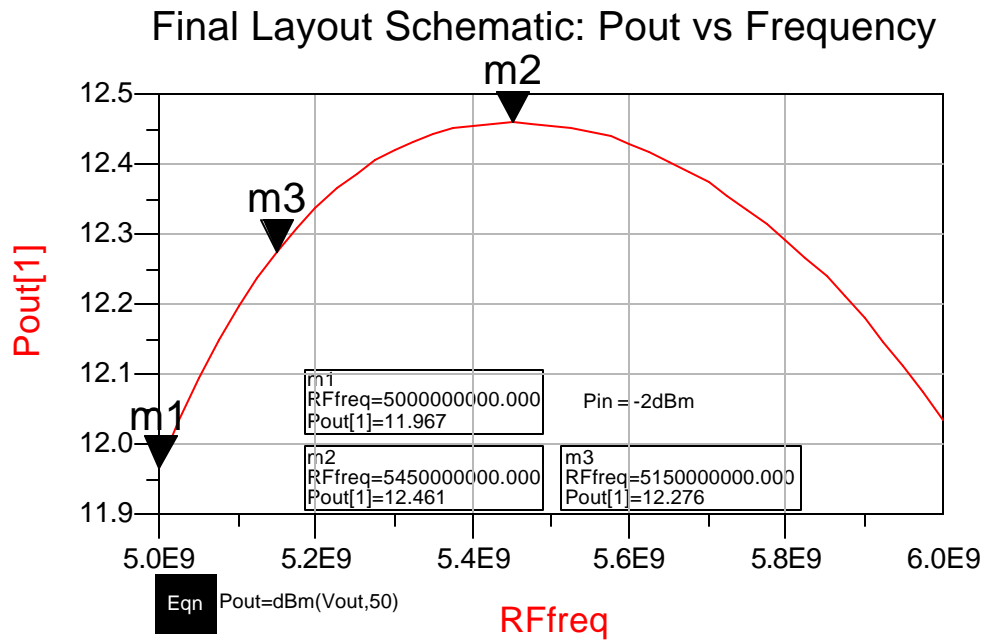


Figure 10: Final Layout Schematic Pin vs Frequency

Schematic Diagrams

The following diagrams are the schematics used for the simplified and final layout.

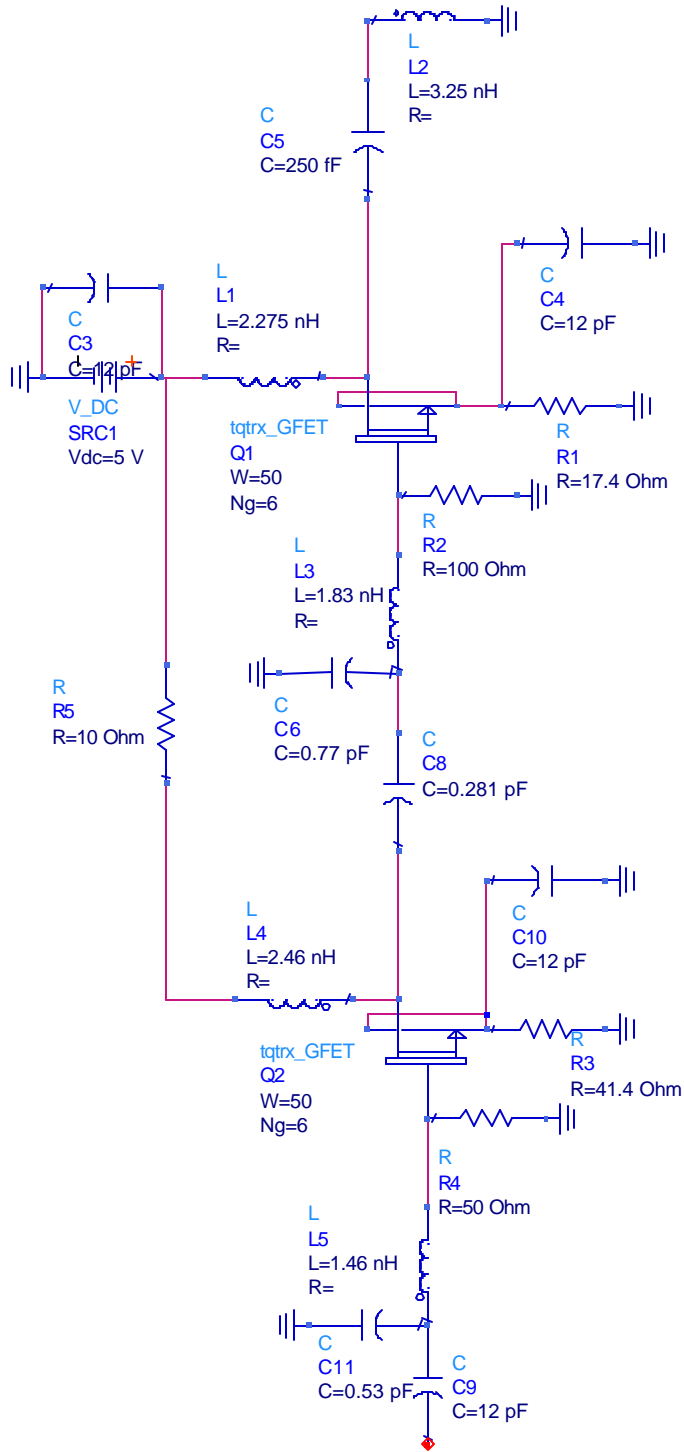


Figure 11: Simplified Schematic:

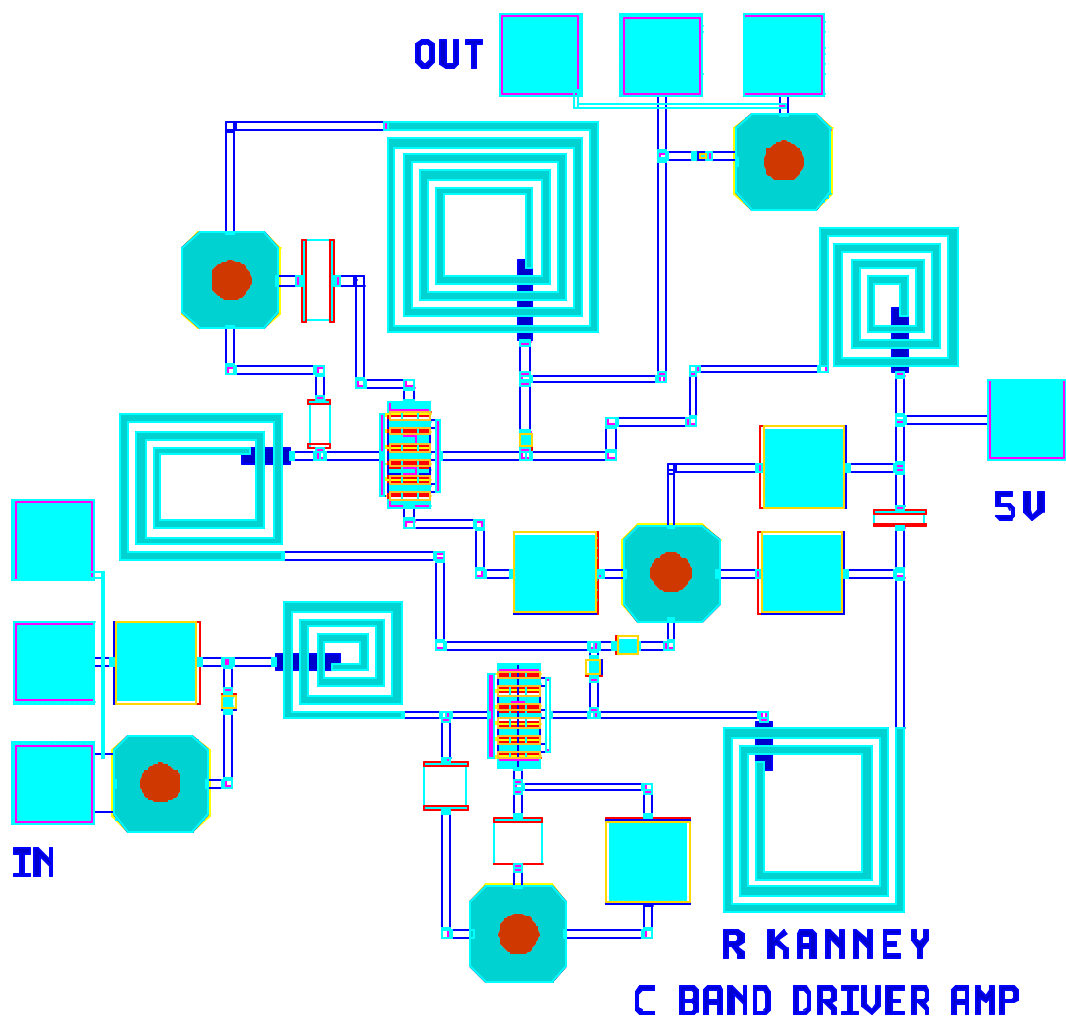


Figure 12: Final Layout Schematic

DC Analysis

The following is the simplified DC schematic without inductors and microstrip. Also listed in the table below is the bias check.

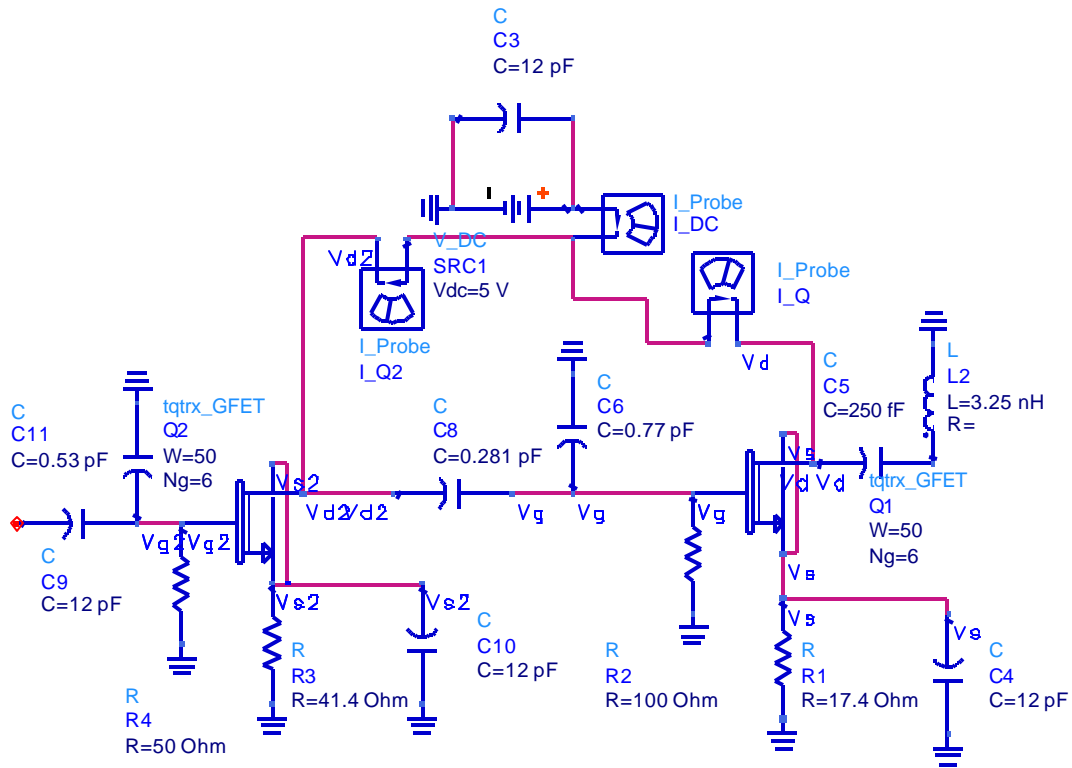


Figure 12: Simplified DC Schematic

DC Bias Check

	Stage 1	Stage 2
Id	28.91mA	45.85mA
Vds	3.8V	4.2V
Vgs	-1.2V	-0.8V

All components in the circuit are capable of handling the currents presented to them.

Test Plan

The following test procedures are recommended to test the C band driver amplifier.

Linear Parameters

An Agilent 8510 network analyzer is needed to measure the s parameters of the amplifier. It is also recommended that a 20dB attenuator pad be placed on the 2nd port of the analyzer to protect it.

1. Connect a 20dB attenuator to port 2 of the network analyzer.
2. Calibrate the analyzer from 1GHz to 10GHz.
3. Place the bias probe on the pad of the chip labeled “5V”.
4. Place probe tips on the designated pads. The input port is labeled “IN” and the output port is labeled “OUT”.
5. Turn on the 5V power supply.
6. Record data.

Power measurements

For power measurements it is recommended that a signal generator and spectrum analyzer be used.

1. Connect a 20dB attenuator to the input of the spectrum analyzer.
2. Connect the signal generator probe to the input pad of the amplifier chip, which is the port marked “IN”.
3. Connect the spectrum analyzer probe to the output pad of the amplifier chip, which is the port marked “OUT”.
4. Place the bias probe on the pad of the chip labeled “5V”.
5. Turn on the 5V power supply.
6. For Pin vs Pout set the generator to the frequency of interest and sweep the power up to, but not exceeding, 4dBm. Record measurements from spectrum analyzer after each interval.
7. For Pout vs Frequency set the Generator to 0.5dBm. Sweep the frequency and record measurements from the spectrum analyzer after each interval.

Conclusion & Recommendations

The C band amplifier design was a success and met and exceeded all of the specification goals except for output VSWR. Future recommendations

on this design would include improving the output match to improve output VSWR and to take the power added efficiency more into account. Also, a resistor ladder should be added to the design to compensate for changes in device characteristics.

C-Band Low Noise Amplifier (LNA)

Final Report

December 10, 2001

Prepared by

Liewei He
Joseph Acoraci

Liewei_He@Raytheon.com
Joseph_H_Acoraci@Raytheon.com

Student Project Prepared for

Microwave Monolithic Integrated Circuit (MMIC) Design Course

525.787

Fall 2001

Johns Hopkins University

Table of Contents

- 1.0 Summary
- 2.0 Introduction
 - 2.1 Circuit Description
 - 2.2 Design Philosophy
 - 2.3 Trade-offs
- 3.0 Modeled Performance
 - 3.1 Specification Compliance Matrix
 - 3.2 Predicted Performance
- 4.0 Schematic Diagrams
- 5.0 DC Analysis
- 6.0 Test Plan
 - 6.1 Test Equipment
 - 6.2 Turn On Procedure
 - 6.3 S-Parameter Measurement
 - 6.4 Noise Figure Measurement
- 7.0 Conclusion and Recommendations
- 8.0 Project File
- 9.0 GDSII (CALMA) Layout File

1.0 Summary

A Low Noise Amplifier (LNA) operating at C-Band (5150 to 5875 MHz) has been designed as part of a project for the MMIC Design course at the Johns Hopkins University. The project is a simplex transceiver for the C-band HiperLan wireless local area network (WLAN) operating at industrial, scientific, and medical (ISM) frequencies. The LNA is one of nine unique designs that make up the ten chip C-band transceiver. Each design is contained on a 60 mil square ANACHIP die using the TriQuint TQTRx design process. The design software used was Agilent Advanced Design System 1.5 (ADS). The predicted LNA design achieved all design goals including gain greater than 15 dB (15.4 dB minimum), noise figure less than 3 dB (1.7 dB maximum), input IP3 greater than +5 dBm (+20 dBm), and input/output VSWR goal of 1.5. The final LNA design will be fabricated and tested within the next six months of 2002.

2.0 Introduction

A Low Noise Amplifier (LNA) operating in C-Band (5150 to 5875 MHz) has been designed as part of a project for the MMIC Design course at the Johns Hopkins University. The project is a simplex transceiver for the C-band HiperLan wireless local area network (WLAN) operating at industrial, scientific, and medical (ISM) frequencies. The LNA is one of nine unique designs that make up the ten chip C-band transceiver. Figure 1 is the C-Band transceiver chip set with LNA shown highlighted.

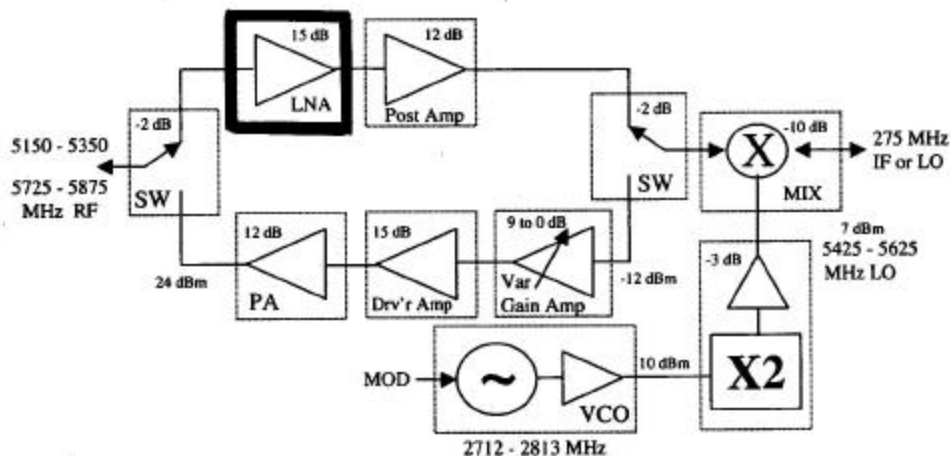


Figure 1. Chip Set for the 5150 – 5350 MHz WLAN and 5725 – 5875 MHz ISM Bands

2.1 Circuit Description

The LNA circuit design selected was a cascaded two-stage amplifier. Both stages utilized 600 μ m DFETs (12 fingers X 50 μ m). Self-biasing was used for both stages resulting with a single 5-volt voltage supply. An inductor at the DFET source was used for stabilization. Feedback and high pass filter input matching networks at the second stage achieved broadband performance for gain, noise figure and VSWR.

2.2 Design Philosophy

The TriQuint DFET was selected for the LNA based upon its low noise and gain characteristics. Achieving 15 dB gain with two stages was accomplished by using 600 μ m DFETs. The 600 μ m

DFETs resulted with a simpler input matching network for the first stage and higher output power for the second stage.

The design process was focused on achieving a stable design for the design goals of high gain, low noise figure, and input/output VSWR for the required frequency band. A concern throughout the design was predicting a reliable noise figure. The nonlinear DFET transistor model does not yield accurate noise figure data. Representative noise figure data was obtained by using S2P data files for linear models. The final design required switching back and forth from the nonlinear to linear models to obtain reliable noise figure data.

The design process was started by using ideal elements without any concern given to bends, tees, MLINs or real TriQuint elements that would be required for the layout of the final design. This approach was useful for determining the nominal DFET bias points, however numerous iterations and component value changes had to be made for the final layout. The bias points chosen for the final layout were:

Input Stage	Output Stage
Vd = 3.18V	Vd = 4.85V
Vgs = -0.27V	Vgs = -0.29V
Ids = 17.46mA	Ids = 18.58mA

The design started by determining the input matching network for the first stage. Next the network that would be the output matching network for the first stage and the input matching network for the second stage was determined. The required broadband performance of the LNA significantly influenced this network's design. A high pass filter type circuit evolved that gave acceptable broadband performance. Broadband performance was further improved by using feedback for the second stage. Design for the second stage output matching network followed. This composite design using ideal elements was then optimized. Finally, the ideal elements were replaced with TriQuint elements and the design was again optimized. After this step, the layout process was started.

The layout process involved interconnecting appropriate bends, tees, and MLINs to the optimized LNA design with TriQuint elements. General design guidelines included: keeping the separation between components and tracks to at least 3 line widths, sharing vias as much as possible, use of a single power supply and adhering to the minimum allowable resistor width of 1 μ m per 1ma current through the resistor. This process required going back and forth from the layout to the schematic to simulate and re-optimize performance. Numerous iterations were made to adjust component values to account for layout modifications.

2.3 Trade-offs

The major trade-off was between gain and noise figure. The lower noise figure resulted with less gain. The input VSWR was also compromised somewhat in order to meet the gain and noise figure goals. Also the small ripple for the gain across the entire band lowered the gain, raised the noise figure, and increased the VSWR.

3.0 Modeled Performance

3.1 Specification Compliance Matrix

Table 1 itemizes the design specifications and the predicted performance for the LNA.

Table 1. LNA Specification Compliance Matrix

Characteristic	Specification Goal	Simplified Schematic (no bends, tees, or MLINs)	Final Layout Predicted Performance
Frequency	5150 to 5875 MHz	5150 to 5875 MHz	5150 to 5875 MHz
Bandwidth	>725 MHz	-	800 MHz
Gain	>15 dB	12.8 dB	15.5 dB
Gain Ripple	±0.5 dB	±1.6 dB	±0.5 dB
Noise Figure	<5 dB, 3 dB goal	2.14 dB	1.74 dB
Input IP3	>+5 dBm	-	+20 dBm
VSWR, 50 Ohm	<1.5:1 (14 dB) input & output	-6.9 dB input -9.8 dB output	-14.2 dB input -15.2 dB output
Supply Voltage	+5 Volts only, goal	+5 Volts, one supply	+5 Volts, one supply
Size	60 X 60 mil ANACHIP	-	60 X 60 mil ANACHIP

3.2 Predicted Performance

The following plots included in this report show the characteristics and predicted performance of the LNA design.

- Figure 2. LNA Simplified Schematic S-Parameters
- Figure 3. LNA Simplified Schematic Stability Plot
- Figure 4. LNA Final Layout Schematic S-Parameters*
- Figure 5. LNA Final Layout Schematic Noise Figure (Linear DFET S2P file)
- Figure 6. LNA Final Layout Schematic Stability Plot
- Figure 7. LNA Final Layout Schematic Input IP3 Plot

* Figures 4 to 8 are for the LNA final layout schematic with bonding wires at the input, output and 5 volt supply.

Figure 2. LNA Simplified Schematic S-Parameters

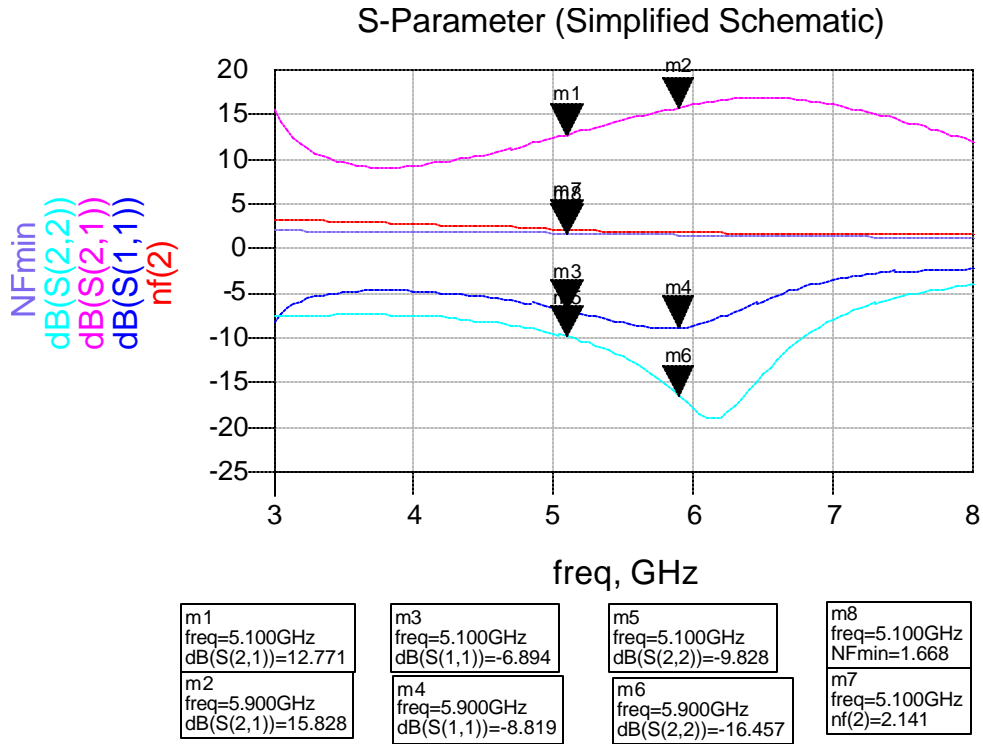


Figure 3. LNA Simplified Schematic Stability Plot

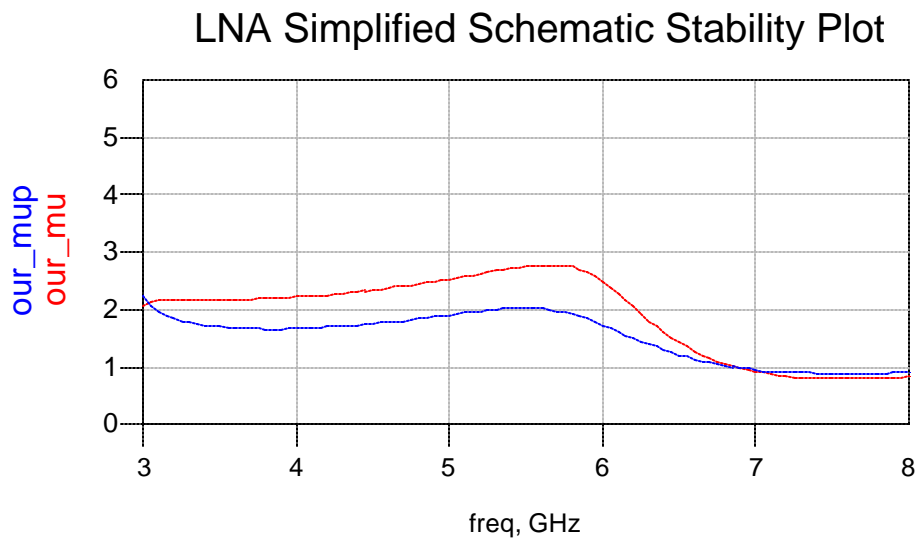


Figure 4. LNA Final Layout S-Parameters

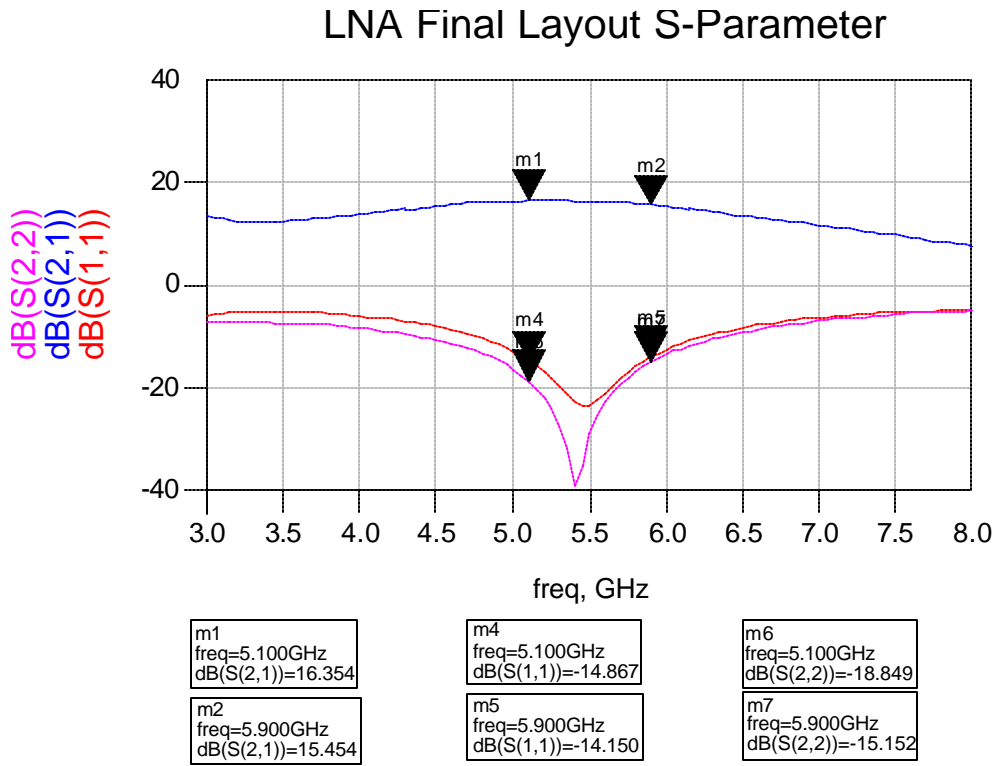


Figure 5. LNA Final Layout Schematic Noise Figure (Linear DFET S2P file)

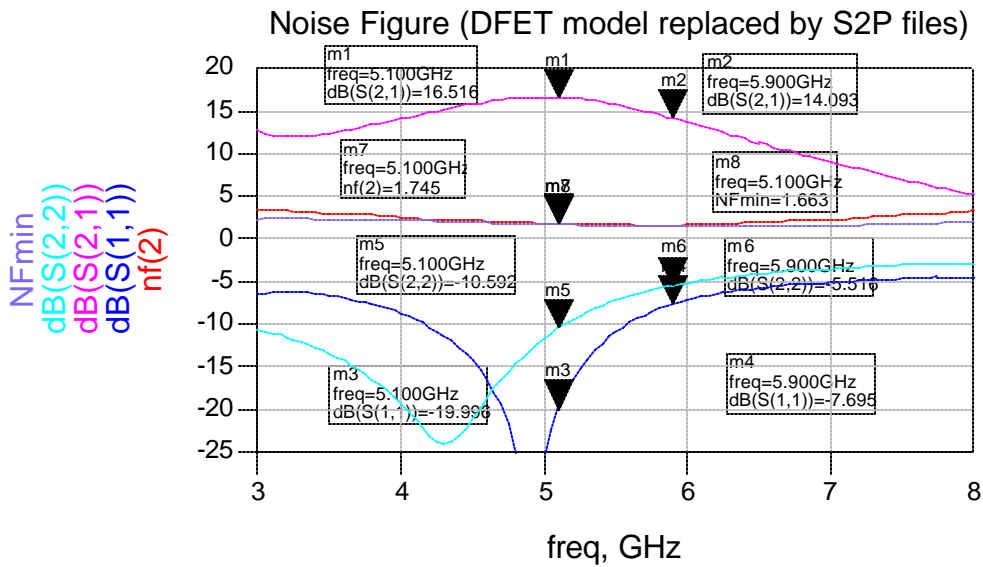


Figure 6. LNA Final Layout Schematic Stability Plot

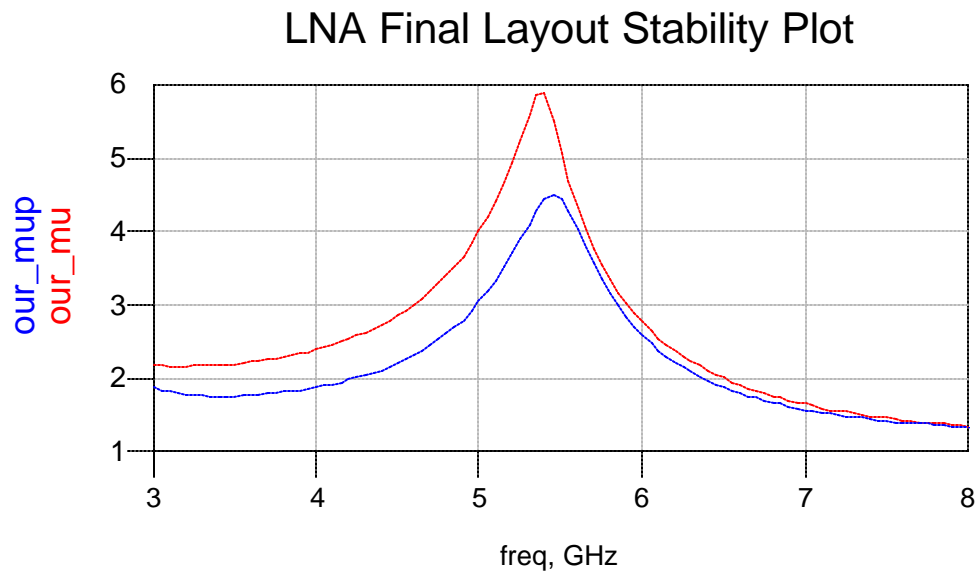
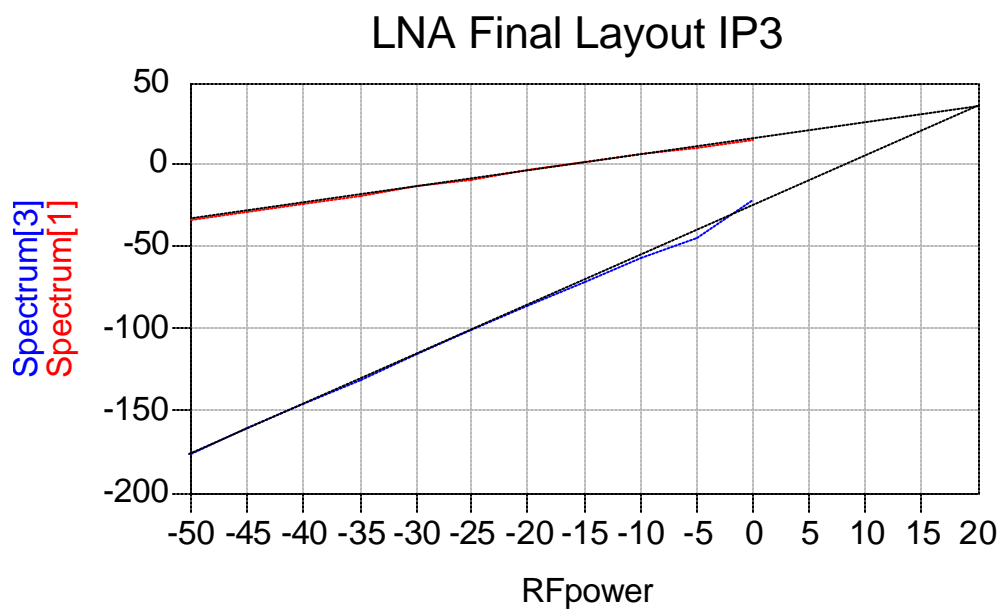


Figure 7. LNA Final Layout Schematic Input IP3 Plot



4.0 Schematic Diagrams

The following schematics are included in this report.

Figure 8. LNA Simplified Schematic

Figure 9. LNA Final Layout Schematic

Figure 10. LNA Final Layout Schematic with DFET model replaced by S2P file

Figure 11. LNA Final Layout in ANACHIP

5.0 DC Analysis

For the input and output stages, V_d , V_{gs} and I_{ds} were selected for the maximum gain and lowest noise figure that could be achieved simultaneously. Table 2 summarizes the DC bias check for the LNA.

Table 2. DC Bias Check

Input Stage	Output Stage
$V_d = 3.18V$	$V_d = 4.85V$
$V_{gs} = -0.27V$	$V_{gs} = -0.29V$
$I_{ds} = 17.46mA$	$I_{ds} = 18.58mA$

The currents through all resistors were checked to verify that the resistor widths selected adhered to the layout guidelines. The guideline followed was that the minimum allowable resistor width be $1\mu m$ per $1mA$ current through the resistor. In particular, the $100\ \Omega$ voltage dropping resistor for I_{ds} of the first stage was $25\mu m$ and drew $18mA$. Also the first and second stage $15\ \Omega$ source resistors were $25\mu m$ and drew $18mA$. The feedback resistor for the second stage was $5\mu m$ and drew only $1.3\mu A$.

Figure 12 is the simplified schematic showing the voltages and currents throughout the layout.

Figure 8. LNA Simplified Schematic

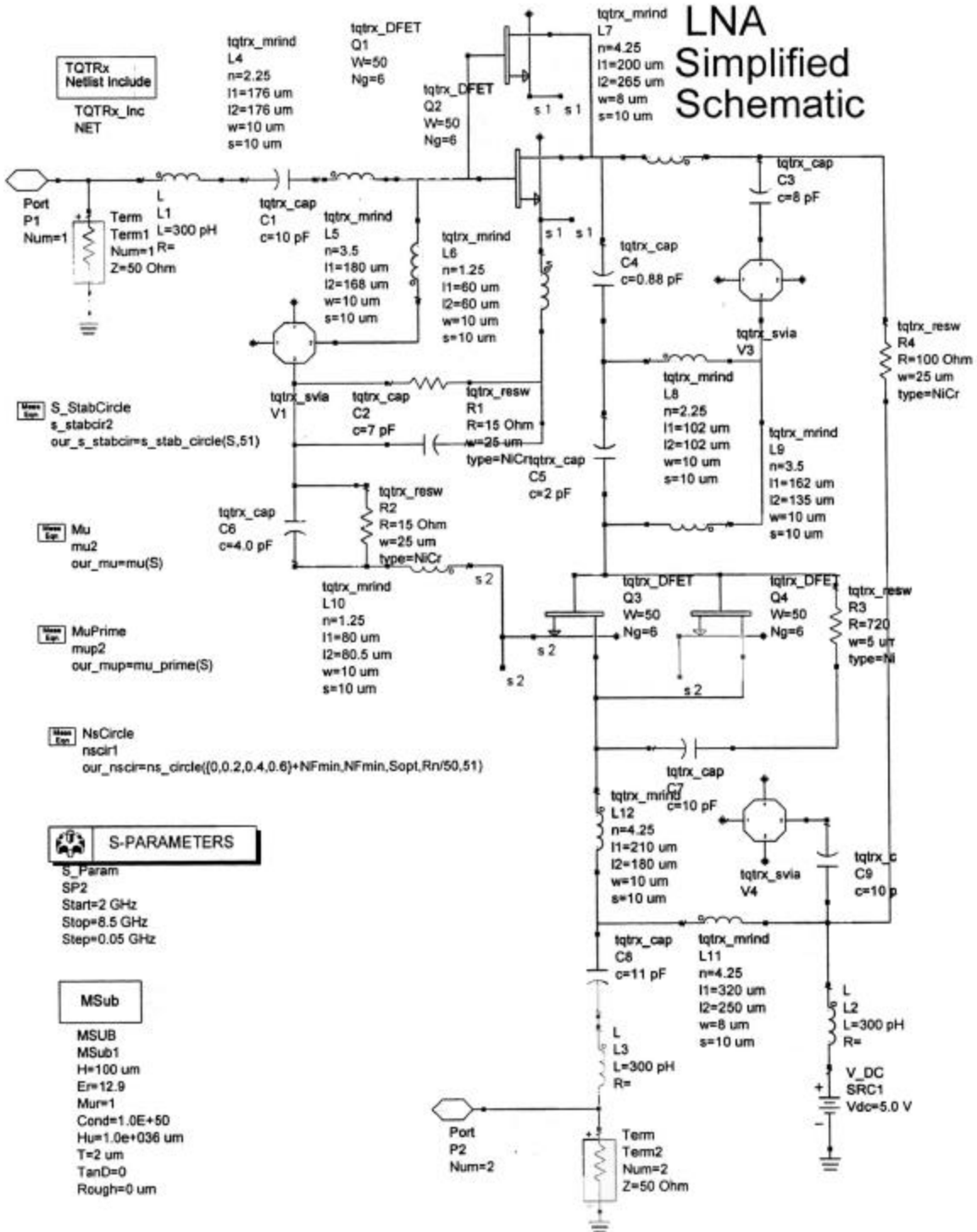


Figure 9. LNA Final Layout Schematic

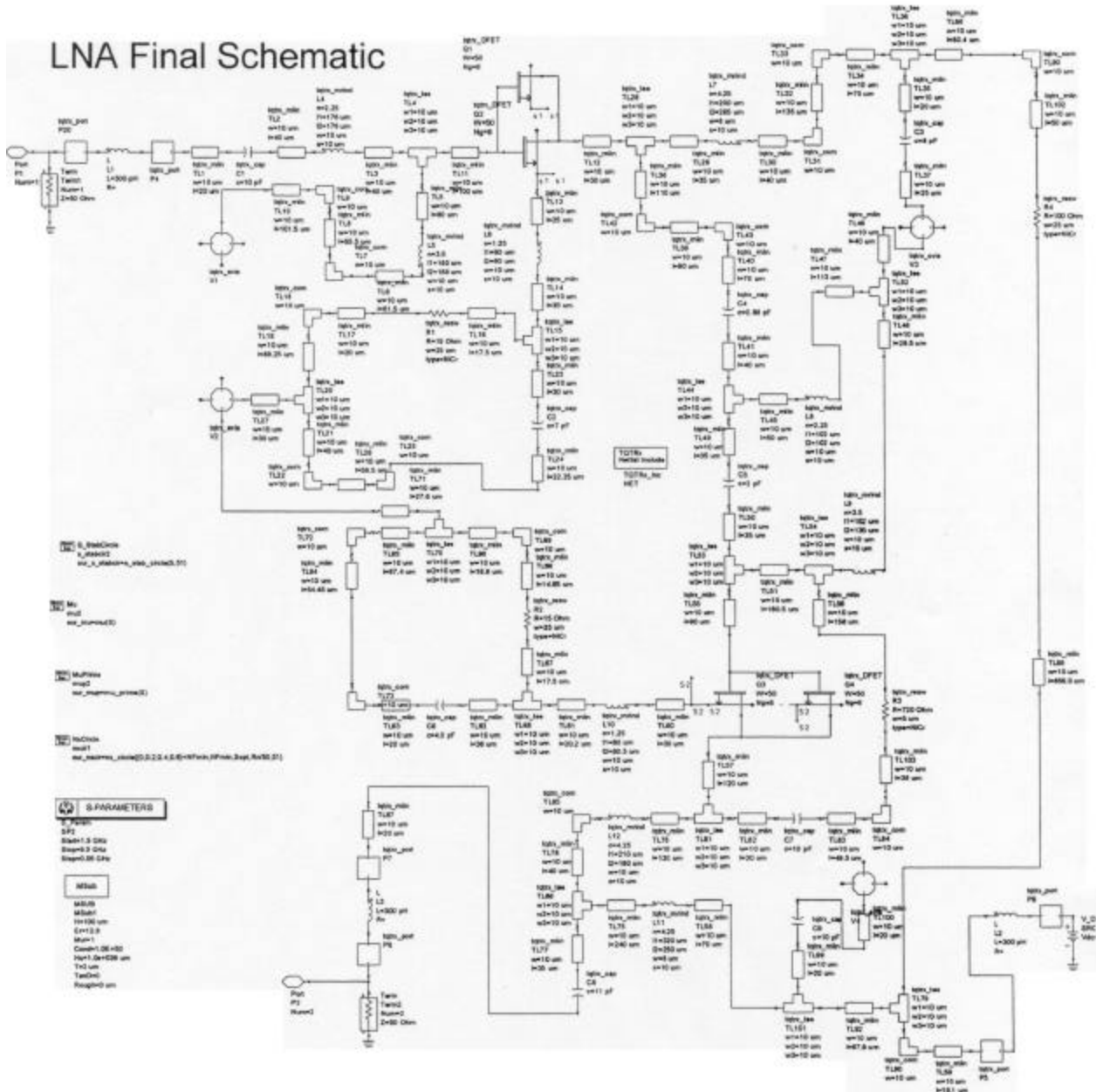


Figure 10. LNA Final Layout Schematic with DFET model replaced by S2P file

DFETs are replaced by S2P files

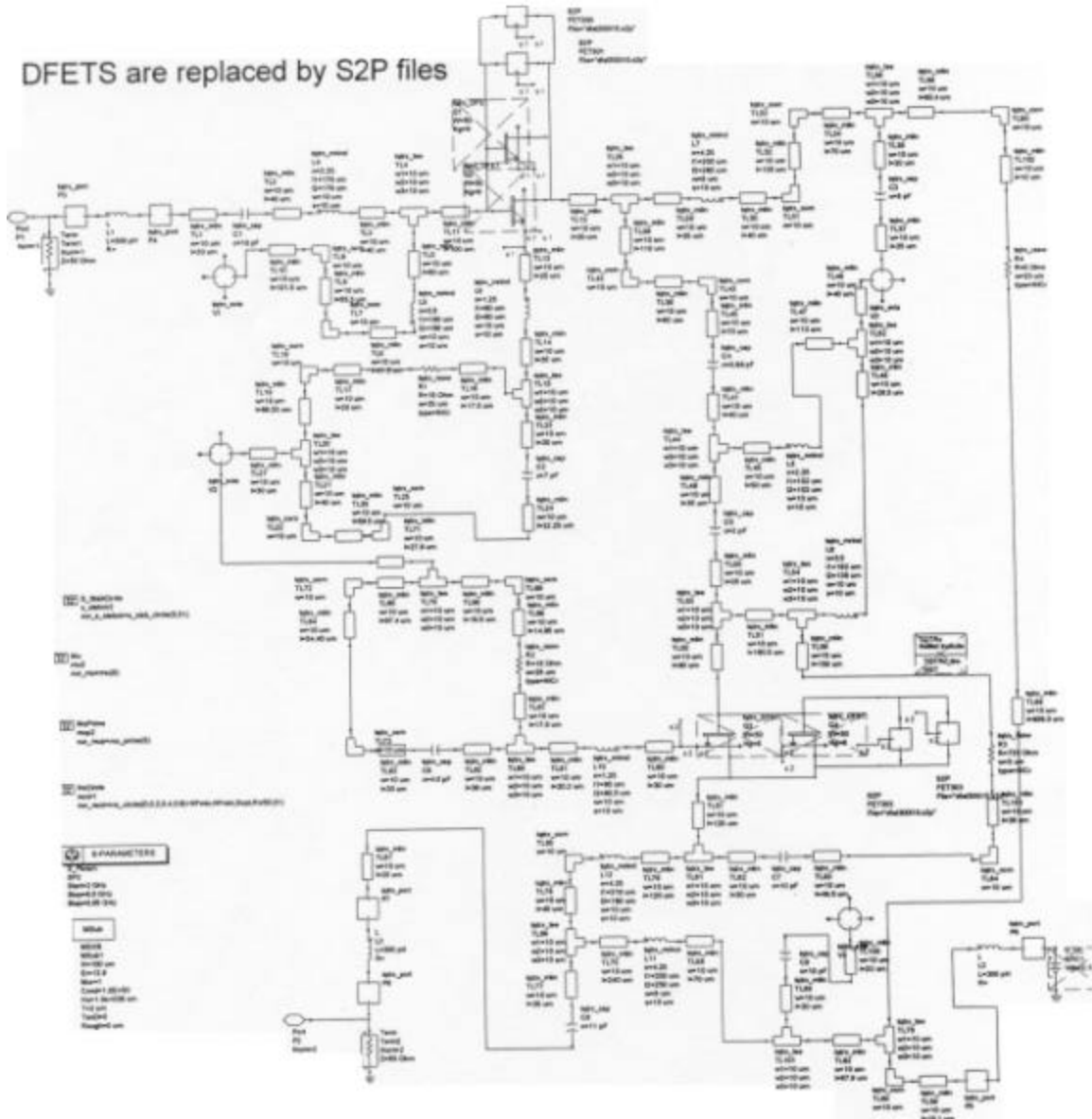


Figure 11 LNA Final Layout in ANACHIP

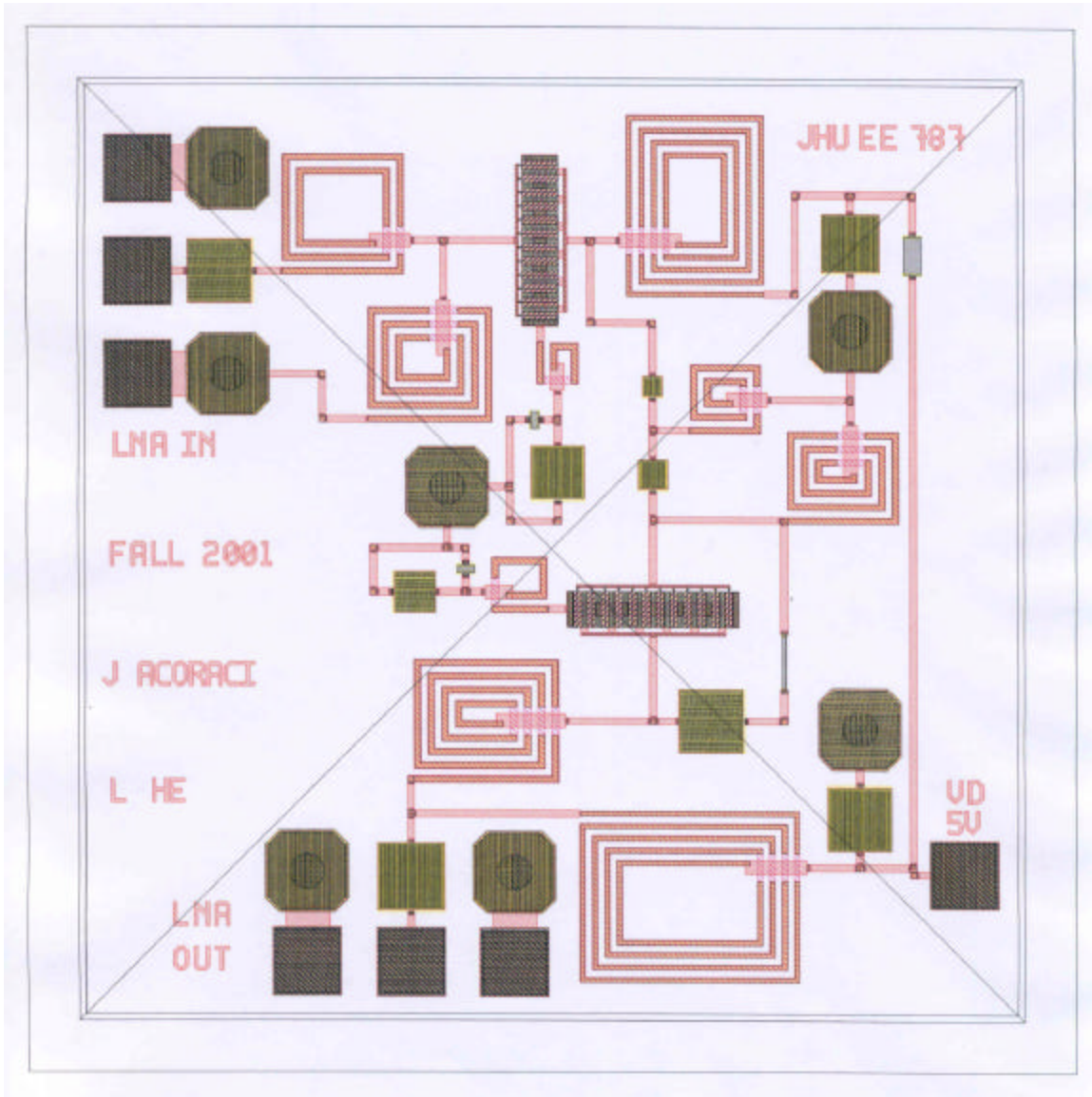
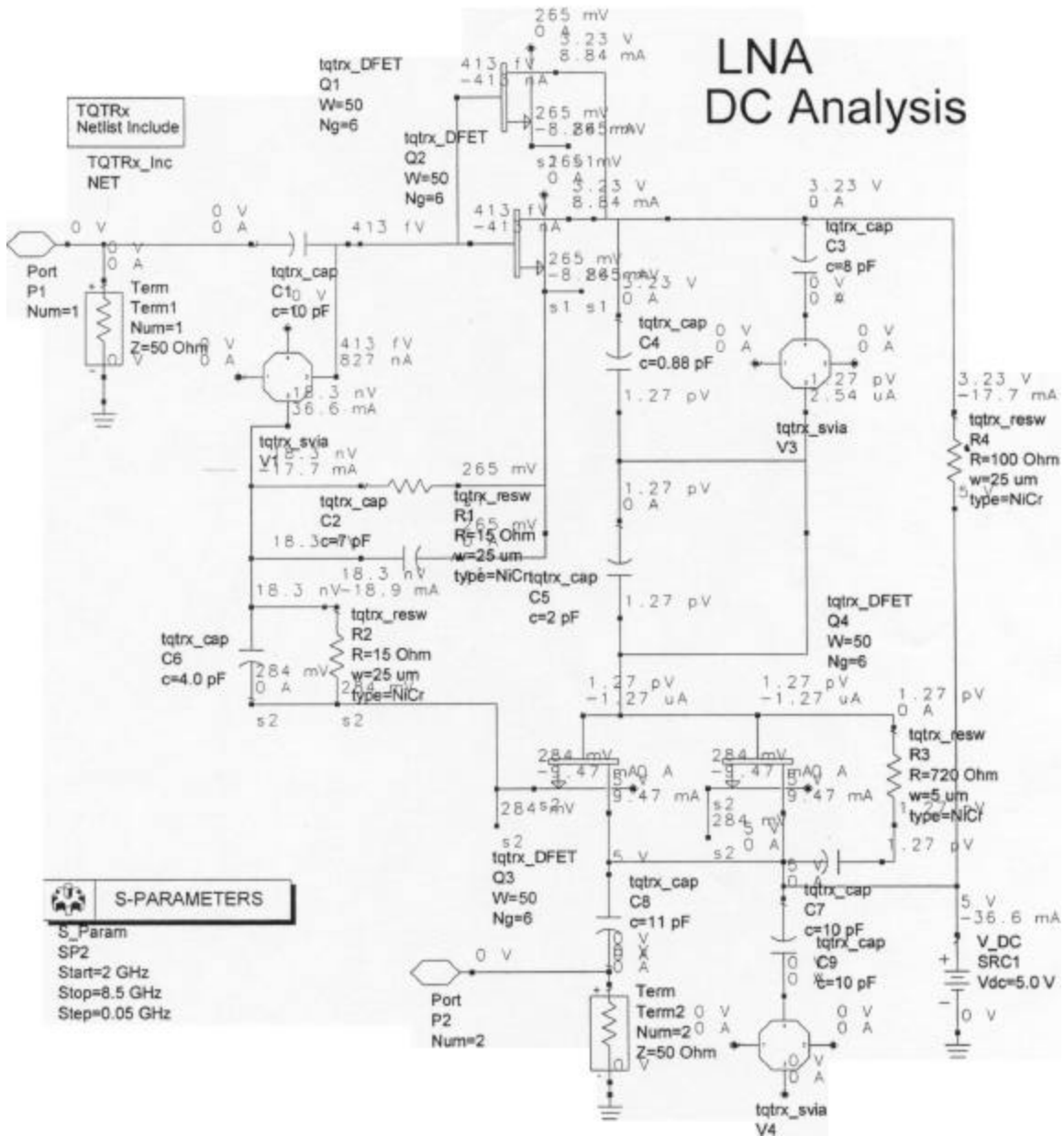


Figure 12. Simplified DC Schematic



6.0 Test Plan

6.1 Test Equipment

The following test equipment or equivalent is necessary to measure the LNA performance:

- Agilent 8510 Network Analyzer
- Agilent XXX Noise Figure Meter
- 5 volt DC power supply

6.2 Turn On Procedure

Extreme caution should be taken when turning on the 5 volt DC powers supply so as not to draw excessive current.

- The required voltage for the LNA is **+5 V DC**
- The required current for the LNA is **36.04 mA**

6.3 S-Parameter Measurement

- Calibrate the network analyzer from 1 to 10 GHz
- Position the bias probe on the "VD 5V" pad
- Position the input probes on the "LNA IN" input pads
- Position the output probes on the "LNA OUT" pads
- Make S11, S21, S12, S22 measurements and store all data on disk

6.4 Noise Figure Measurement

- Calibrate the noise figure meter
- Position the bias probe on the "VD 5V" pad
- Position the input probes on the "LNA IN" input pads
- Position the output probes on the "LNA OUT" pads
- Make noise figure measurements and store all data on disk

7.0 Conclusion and Recommendations

The LNA design process was very successful in that all design goals were met. In particular the noise figure of 1.7 dB was much lower than the goal of 3 dB. Also the input IP3 of +20 dBm was much higher the goal of +5 dBm. A recommendation to be more efficient in the design process is to spend less time with the ideal element design and more time with the TriQuint elements and the real layout with bends, tees, and MLINs.

8.0 Project File

The project file has been submitted on a 3 ½ HD Diskette.

9.0 GDSII (CALMA) Layout File

The GDSII layout file has been submitted on a 3 ½ HD Diskette

JOHN HOPKINS UNIVERSITY
WHITING SCHOOL OF ENGINEERING
PART-TIME PROGRAMS IN ENGINEERING
MMIC Design
JHU 525.787 (M 4:30-7:15 PM)

C-Band Up/Down Converter: Final Report

SUBMITTED BY:

Willie Lee Thompson, II
wlt@eng.morgan.edu

Morgan State University
Center of Microwave, Satellite and RF Engineering
Schaefer 353

ABSTRACT

A singly balanced 180-degree monolithic microwave integrated circuit (MMIC) is presented in this paper. The mixer exhibits up and down conversion capabilities for RF frequencies ranging from 5150 MHz to 5875 MHz, LO frequencies ranging from 5425 MHz to 5625 MHz and IF frequency of 275 MHz, respectively. Simulations exhibit a conversion loss of < 10 dB for a LO power of 3 dB for both up and down conversion with an LO-to-RF isolation > -22 dB. The MMIC circuit fits on a 60 mils x 60 mils chip with a +5 V power supply and will be implemented in a simplex transceiver for HiperLAN wireless local area network (WLAN).

CONTENTS

Abstract.....	ii
Contents.....	iii
1.0 Introduction.....	1
1.1 Circuit Architecture	1
1.2 Design Philosophy	2
1.3 Trade-offs.....	4
2.0 Modeled Performance.....	5
2.1 Specification Matrix	5
2.2 Predicted Performance	6
2.2.1 180-degree Hybrid Performance	6
2.2.2 Filters Performance	6
2.2.3 Down Converter Performance	7
2.2.4 Up Converter Performance.....	9
2.2.5 Isolation and VSWR Performance	11
3.0 Final Layout	12
4.0 DC Analysis	13
5.0 Test Plan.....	15
5.1 Spectrum Test Configuration.....	15
5.2 Isolation and VSWR Test Configuration.....	16
6.0 Conclusion	17
References.....	18

1.0 INTRODUCTION

The HiperLAN transceiver will be used to receive and send data within two RF bands. The lower band ranges from 5150 MHz to 5350 MHz, while the upper band ranges from 5725 MHz to 5875 MHz. The mixer is responsible for down converting the RF signal with the two bands to an IF signal in receive mode and up converting the IF signal to a RF signal within the bands in send mode. As a result, the circuit architecture used for the mixer must be able to up and down convert without any modification to the topology.

1.1 CIRCUIT ARCHITECTURE

The circuit architecture selected for the mixer is a singly balanced 180-degree mixer, best known as a “rat-race” mixer. The mixer consists of a lumped element 180-degree hybrid, two 80- μm DFETs diodes, a low-pass filter for IF port filtering and two high-pass filters for LO and RF port filtering, respectively. Figure 1.1 illustrates the general topology of a singly balanced 180-degree mixer.

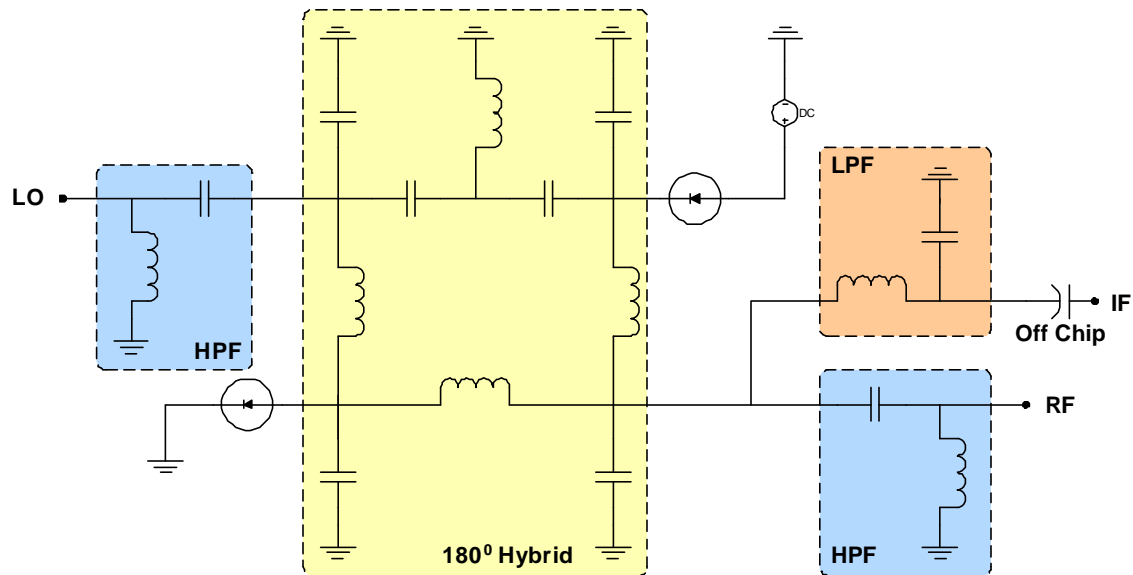


Figure 1.1.1: Singly balanced 180-degree mixer architecture.

This architecture utilizes the nonlinear conductance of the diodes for mixing. Diodes are more stable than field-effect transistors (FETs) and allows for mixing in both directions. The shunt configuration of the diodes allows for easier impedance matching to the 50- Ω at the hybrid's ports. Proper biasing and sizing of the DFETs can achieve impedance match. We concluded that an 80- μm DFET with 2 gate fingers connected in diode configuration provided the best impedance match.

LO signal is located at the Δ port and the RF/IF signals are located at the Σ port of the 180-degree hybrid, respectively. As a result, the hybrid splits the LO power between the two diodes ports with a 180-degree phase shift, while RF/IF powers are split between the diodes ports in phase. Filtering is implemented at the RF/IF port to separate the signals after mixing. In addition, filtering at the ports improves the RF-to-IF isolation and LO-to-IF isolation. LO-to-RF isolation is achieved by the properties of the hybrid, where the Δ and Σ ports are mutual isolated from each other.

Biasing of the diodes is used for starved LO operation of the mixer, which allows for smaller LO powers. The DC bias supply is coupled between the diodes via the hybrid and the blocking capacitors at each ports. An off chip blocking capacitor must be used due to low frequency of the IF signal, which requires a high value capacitor that cannot fit onto the chip.

1.2 DESIGN PHILOSOPHY

The design philosophy was determined by the specifications for the mixer. The specification of interested were:

- Up and down conversion abilities
- Layout Constraints
- High LO-to-RF isolation
- Low conversion loss

Concerning the above specifications, it was determine that the following architectures were candidates for the mixer: 1) 90-degree mixer, 2) singly balanced 180-degree mixer and 3) doubly balanced mixer.

One of the major advantages of balanced mixers has over single-component mixers is its inherent rejection of spurious responses. A spurious response is a mixing product between a harmonic of the RF and a harmonic of the LO, which can distort signals of interest if mixed to the proper frequencies. In addition, balanced mixer provides inherent port isolations. However, the 90-degree mixer exhibits poor spurious response and the port isolation is only as good as the VSWR at each port, while the singly balanced 180-degree mixer exhibits both characteristics well.

Next, the layout constraint of 60 mils x 60 mils was another important specification for developing the mixer. The doubly balanced mixer requires the use of a balun. A balun is a large coupling structure that cannot be implemented due to the layout constraints. In addition, the TriQuint design library does not have any models for a balun structure. To develop a library model would require the use of an electromagnetic simulator to model the coupling behavior of the balun, or fabrication of a structure for modeling. As a result, the doubly balanced mixer was not selected. However, the singly balanced 180-degree mixer requires a 180-degree hybrid, which can be easily implemented using lumped elements included within the TriQuint design library.

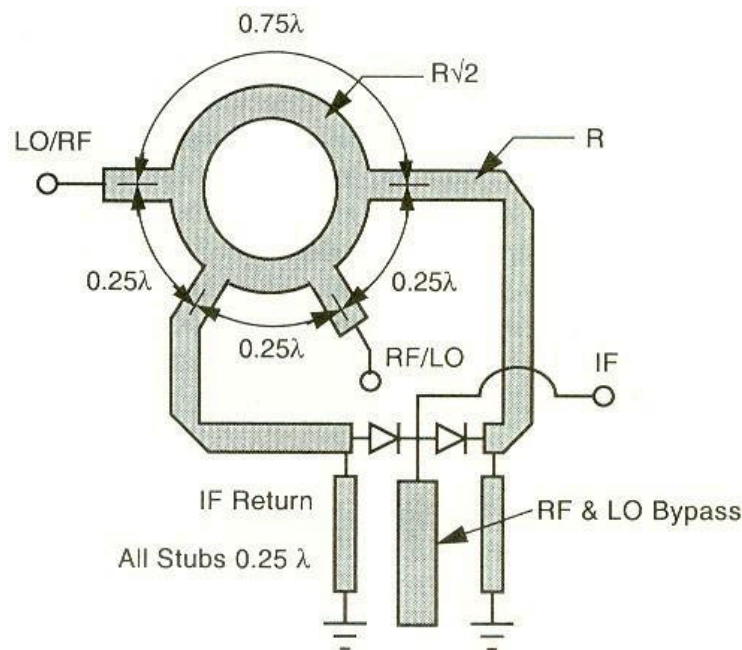


Figure 1.2: Classical architecture for a singly balanced 180-degree mixer.

The classical approach for implementing a singly balanced 180-degree mixer is illustrated in Figure 1.2. The diodes are tied together to form the IF port, while the LO

and RF are connected to the Δ and Σ ports, respectively. However, we implemented a novel approach for connecting the diodes. The diodes were connected in a shunt configuration as shown in Figure 1.1. The shunt configuration allows for good impedance matching of the diode independently for each other and easy implementation of DC bias via the hybrid.

1.3 TRADE-OFFS

The major trade-off for the design was the layout constraint of the MMIC. The doubly balanced mixer is an excellent general-purpose mixer design. It exhibits wide bandwidth, good spurious response injection and good port isolation. However, the implementation of a balun cannot be achieved. The 180-degree mixer exhibits a narrower bandwidth, which requires the RF/LO frequencies to be within 15% of each other. The bandwidth requirement is met by the frequency specifications for the mixer and the layout of the 180-degree hybrid is easily implemented with lumped elements.

A couple of minor trade-offs were made: 1) the sizing of the diodes for impedance matching, 2) layout design of the hybrid, and 3) inductor values for the RF/LO and IF filters. The input and output impedances of the diodes vary with DC bias and diode size. As a result, special interest was taken to bias and size the diodes to provide proper impedance to the hybrid's ports. Secondly, the hybrid requires the use of four shunt capacitors to ground. A layout design was implemented to share a center via to ground between the shunt capacitors. This configuration prevented the usage of multiple vias, which require significant amount of die area. Lastly, the optimum inductor values were calculated for each filter types. Due to layout constraints, the inductor values were modified with minimum effect on the overall transfer response of the filters. However, changing the inductors values affect the input impedance of the filters and the VSWRs of the ports. The VSWR specifications were still met, but were not ideal.

2.0 MODELED PERFORMANCE

2.1 SPECIFICATION MATRIX

Table 2.1 summarizes the design specifications and simulated performance of the singly balanced 180-degree mixer. All specifications for the design were met.

Table 2.1: Specification matrix and simulated performance results.

Specification	Goal	Acceptable	Simulated
Frequency Bandwidths	<u>Lower RF Band</u> 5150 – 5350 MHz	<u>Lower RF Band</u> 5150 – 5350 MHz	<u>Lower RF Band</u> 5150 – 5350 MHz
	<u>Upper RF Band</u> 5725 – 5875 MHz	<u>Upper RF Band</u> 5725 – 5875 MHz	<u>Upper RF Band</u> 5725 – 5875 MHz
	<u>LO Band</u> 5425 – 5625 MHz	<u>LO Band</u> 5425 – 5625 MHz	<u>LO Band</u> 5425 – 5625 MHz
	<u>IF Band</u> 275 MHz	<u>IF Band</u> 275 MHz	<u>IF Band</u> 275 MHz
LO-to-RF Isolation	-16 dB	- 10 dB	> -22 dB
Conversion Loss	-7 dB	- 10 dB	9.10 dB*
LO Power	0 dBm	+7 dBm	3 dBm**
VSWR	1.5:1	2.5:1	~1.75:1
Supply Voltage	5 V	0 – 5 V	5 V
Size	60 mils x 60 mils	60 mils x 60 mils	60 mils x 60 mils

*Conversion loss is an average of up and down conversion simulation results for both RF bands.

**LO power is the LO power that met conversion loss specification for both up and down conversions.

2.2 PREDICTED PERFORMANCE

2.2.1 180-DEGREE HYBRID PERFORMANCE

The simulated performance of the 180-degree hybrid is illustrated in Figure 2.1. As previously discussed, the LO signal is connected to the Δ port (S_{11}), the RF and IF signals are connected to the Σ port (S_{44}), and the diodes are connected the port 2 (S_{22}) and port 3 (S_{33}), respectively. The powers division of the Δ and Σ ports at the diode ports are approximately -3 dB and -4.2 dB, respectively. The phase differences at the diode ports are ~180 degree and ~0 degree across the operating band of the mixer, respectively.

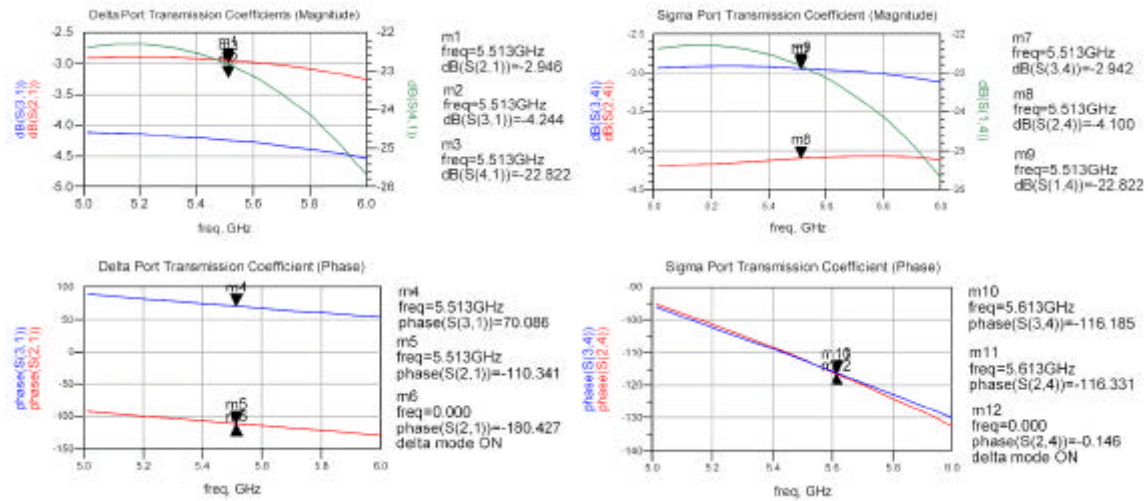


Figure 2.1: Simulated performance of the 180-degree hybrid.

2.2.2 FILTERS PERFORMANCE

The simulated performance of the filters is illustrated in Figure 2.2. The LO and RF filters are high-pass filters using series capacitor and shunt inductor configuration. The IF filters is a low-pass filter using series inductor and shunt capacitor configuration. Each filter was design to provide approximately -20 dB of attenuation for the undesired frequencies. As illustrated in Figure 2.2, the LO/RF filters provide approximately -30 dB of attenuation at the IF frequency of 275 MHz, while the IF filter provides at least -20 dB of attenuation across the operating band of the mixer.

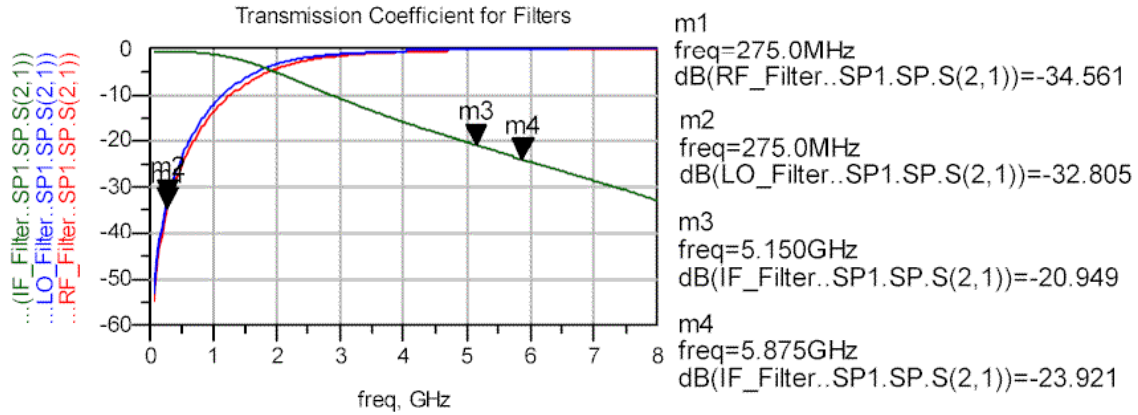


Figure 2.2: Simulated performance of the filters used in the singly balanced 180-degree mixer.

2.2.3 Down Converter Performance

The mixer’s performances as a down converter are illustrated in Figure 2.3 and Figure 2.4. In Figure 2.3, the mixer is configured for down converting frequencies in the lower band, while in Figure 2.4, it is configured for down converting frequencies in the upper band. The LO and RF powers were +3 dBm and –20 dBm for both configurations. The conversion losses were –8.22 dB and -8.75, respectively.

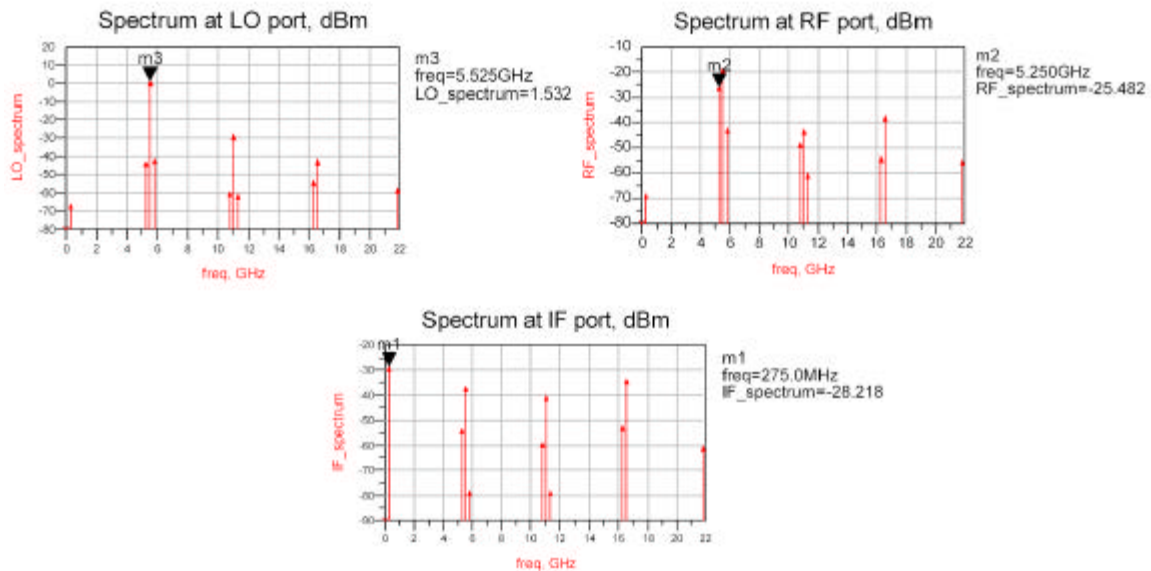


Figure 2.3: Simulated performance of mixer as a down converter for lower band frequencies.

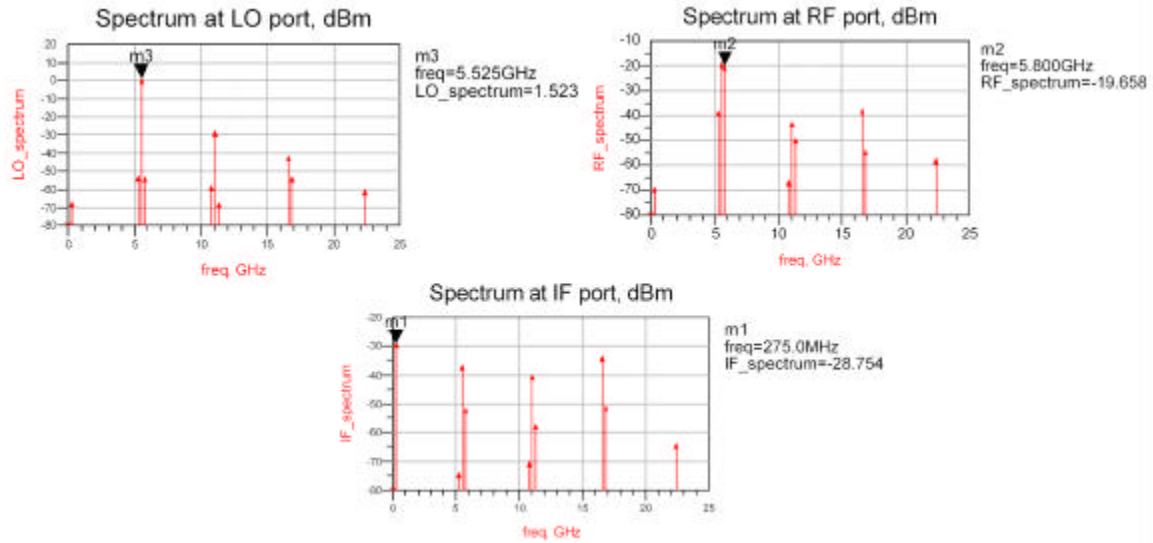


Figure 2.4: Simulated performance of mixer as a down converter for upper band frequencies.

The conversion loss is a function of LO power. To find optimum performance for the mixer, simulations of the conversion loss as a function of LO power were performed. The results of the simulations are plotted in Figure 2.5. The optimum LO powers for the down converter were +3 dBm for the lower band and +5.5 dBm for the upper band. In addition, several other simulations were performed for verification of design and are summarized in Table 2.2.

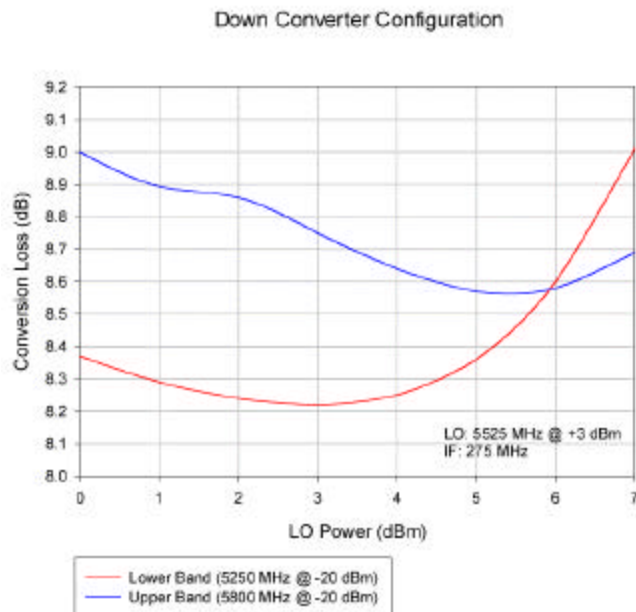


Figure 2.5: Simulation results of conversion loss as a function of LO power.

Table 2.2: Summary of simulated performances for down converter configurations.

RF Frequency	LO Frequency	IF Frequency	Conversion Loss
5250 MHz	5525 MHz	275 MHz	-8.22 dB
5800 MHz	5525 MHz	275 MHz	-8.75 dB
5150 MHz	5425 MHz	275 MHz	-8.21 dB
5875 MHz	5600 MHz	275 MHz	-9.22 dB

*LO power was +3 dBm and RF power was -20 dBm for all simulations.

2.2.4 Up Converter Performance

The simulated performance of the mixer as a up converter is illustrated in Figure 2.6. The up converter produces both lower and upper band RF frequencies for a given LO and IF configuration. The lower band is given by $f_{\text{LOWER}} = f_{\text{LO}} - f_{\text{IF}}$ and upper band is given by $f_{\text{UPPER}} = f_{\text{LO}} + f_{\text{IF}}$. The LO and IF powers for the simulation were +3 dBm and 0 dBm, respectively. Conversion loss as a function of LO power is illustrated in Figure 2.7 and Table 2.3 summarizes the simulated performance of several simulation configurations.

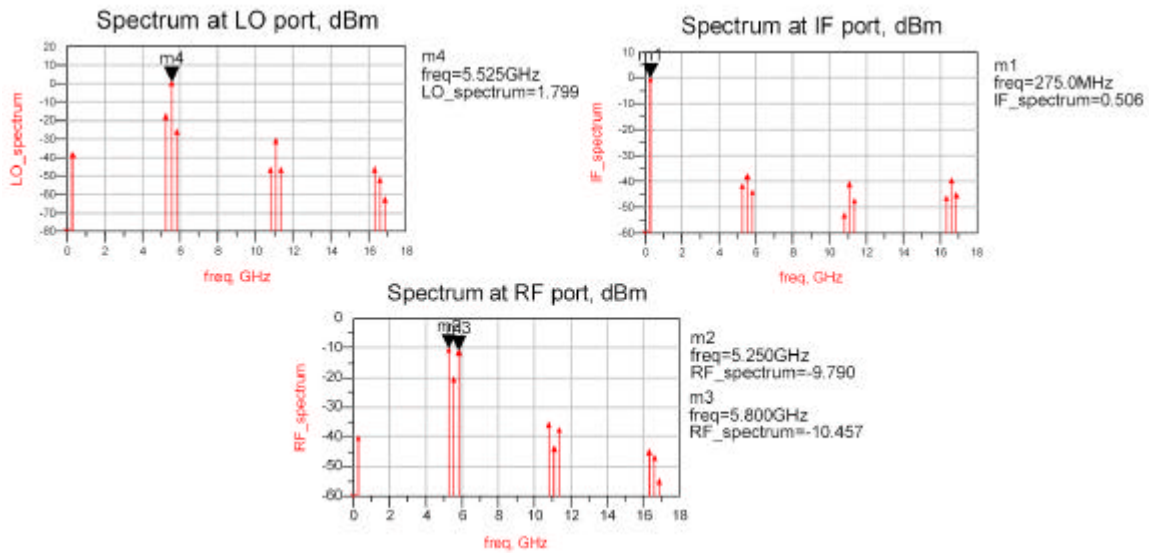


Figure 2.6: Simulated performance of mixer as a up converter.

Up Converter Configuration

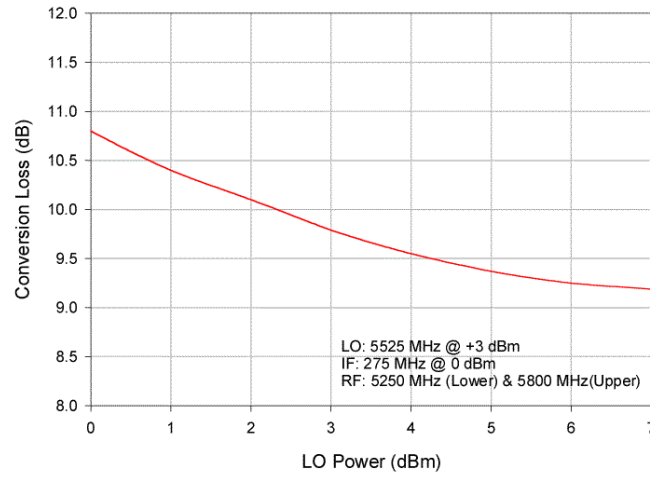


Figure 2.7: Simulation results for conversion loss as a function of LO power.

Table 2.3: Summary of simulated performances for up converter configurations.

LO Freq	IF Freq	Lower Freq	Upper Freq	Conversion Loss
5525 MHz	275 MHz	5250 MHz	5800 MHz	9.79 dB
5425 MHz	275 MHz	5150 MHz	5700 MHz	9.72 dB
5600 MHz	275 MHz	5325 MHz	5875 MHz	9.81 dB

*LO power was +3 dBm and IF power was 0 dBm for all simulations.

Figure 2.7 demonstrates that the up converter requires more LO power to obtaining the minimum specification of a conversion loss, while the down converter configuration met the specification with a LO power of 0 dBm. In addition, the optimum LO power for the up converter seems to be greater than the allowable LO power of 7 dB.

2.2.5 ISOLATION AND VSWR PERFORMANCE

The simulated performance for the LO isolation and VSWRs is illustrated in Figure 2.8. The LO-to-RF isolation is greater than -20 dB across the operating band and LO-to-IF isolation is greater than -35 dB across the operating band. The VSWR specification of 2.5:1 is met for each port.

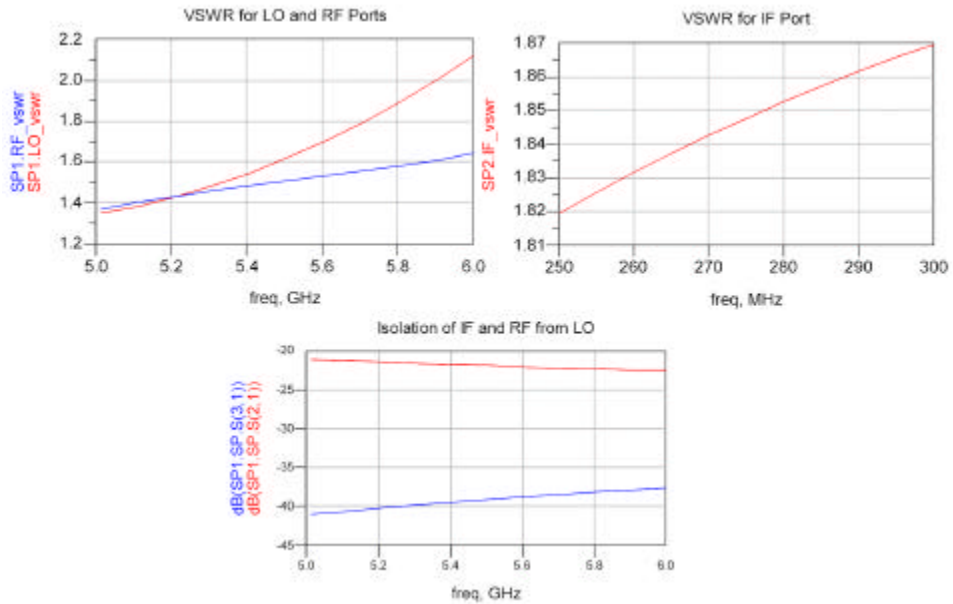


Figure 2.8: Simulated performance for LO isolation and VSWR for each port.

3.0 FINAL LAYOUT

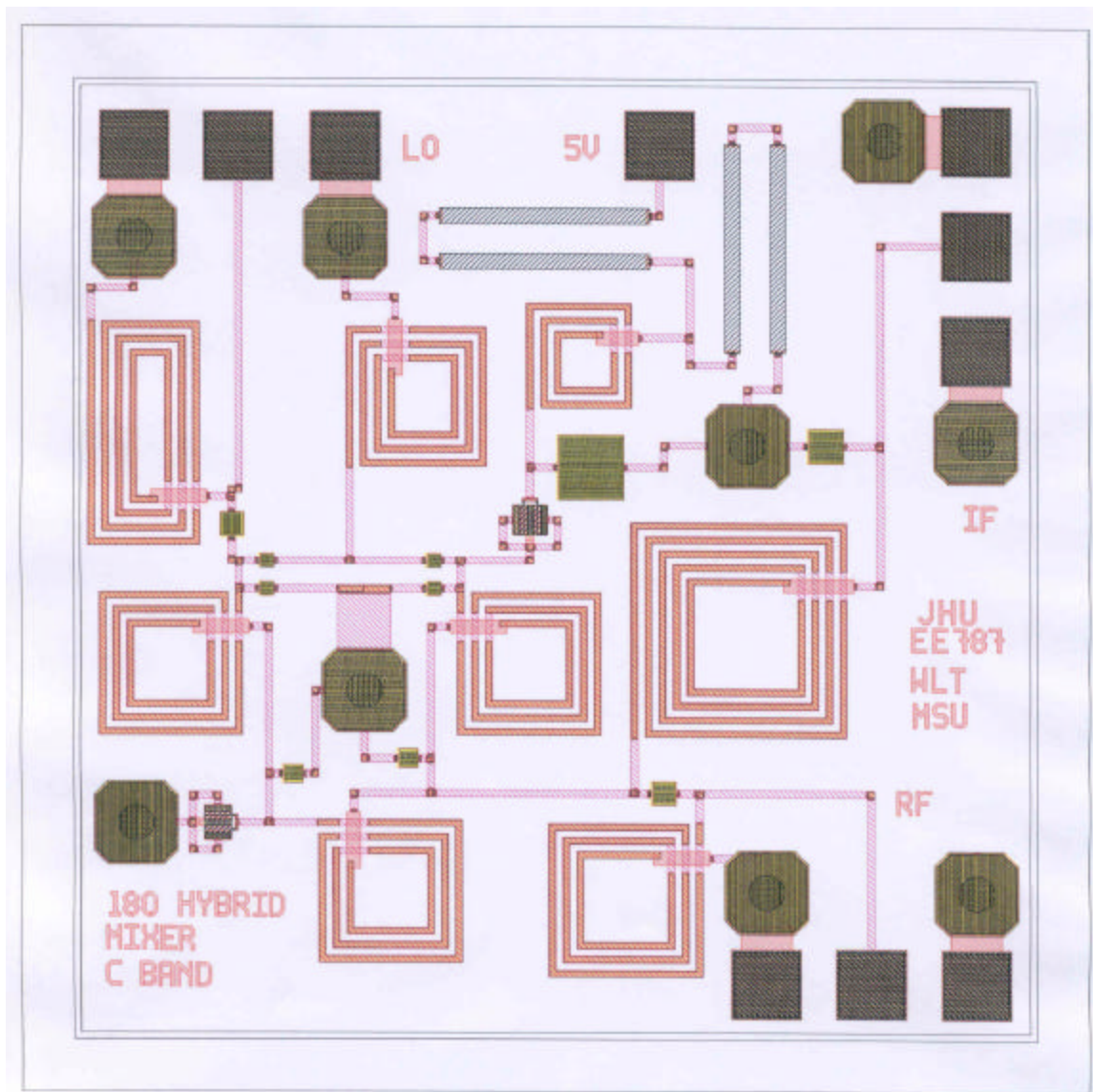


Figure 3.1: Final layout of singly balanced 180-hybrid mixer.

Implanted resistors were used for the voltage divider to provide the proper DC biasing of the DFET diodes. All interconnects, capacitors, inductors and resistors were sized for current capabilities that are twice the maximum circuit current. All inductors, microstrip lines, capacitors and vias were spaced ~ 3 times the line width from each other to minimize signal coupling.

4.0 DC ANALYSIS

The DC bias of the diodes is essential for starved LO operation of the mixer. The DFET diodes were bias at a DC voltage of 0.65 V and a DC current of $\sim 800 \mu\text{A}$. This bias point provided the best impedance match at the hybrid's ports and the nonlinear conductance that is required for mixing. Figure 4.1 – Figure 4.3 show the DC analysis results for a simplified schematic architecture of the singly balanced 180-degree mixer. The DC current and voltage is coupled between the diodes via the hybrid and the blocking capacitors at each port. A DC voltage of 1.3 V is supplied by a voltage divider and a +5V power supply. The 1.3 V will be approximately dropped evenly across both diodes resulting in biasing voltages of 0.65 V for each diode and DC current of $\sim 800 \mu\text{A}$.

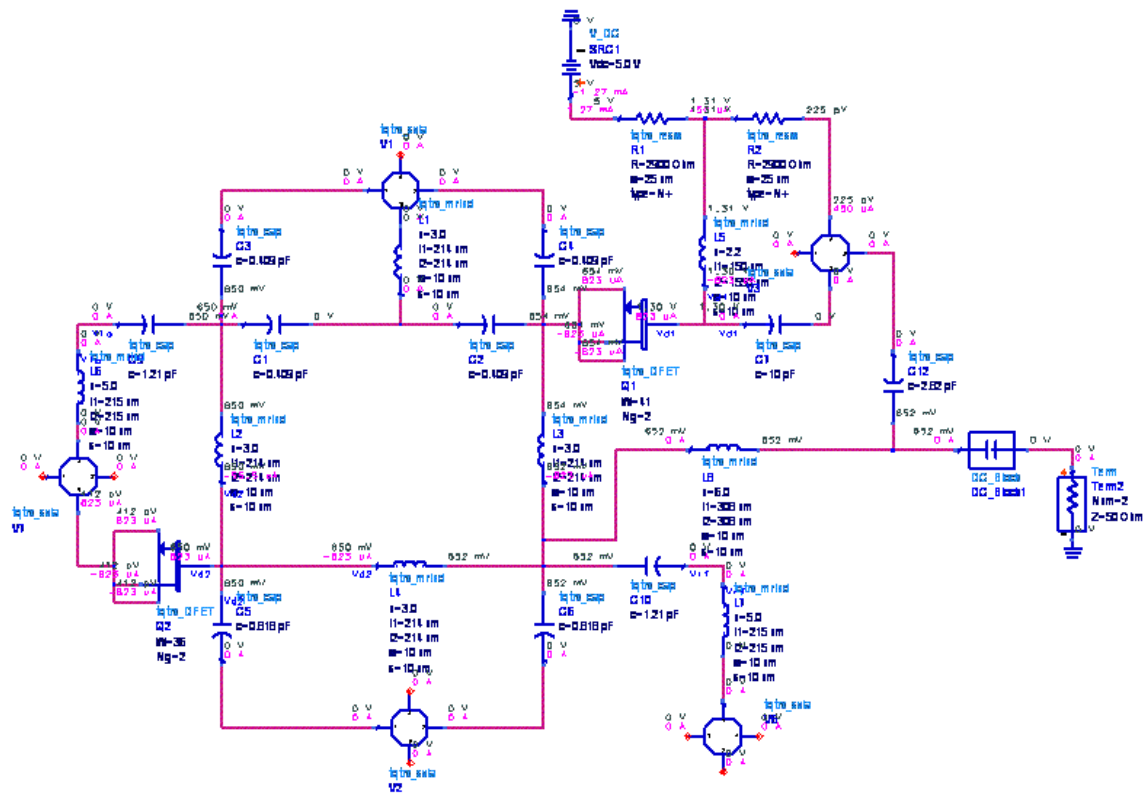


Figure 4.1: DC analysis results for a simplified schematic diagram of the singly balanced 180-degree mixer.

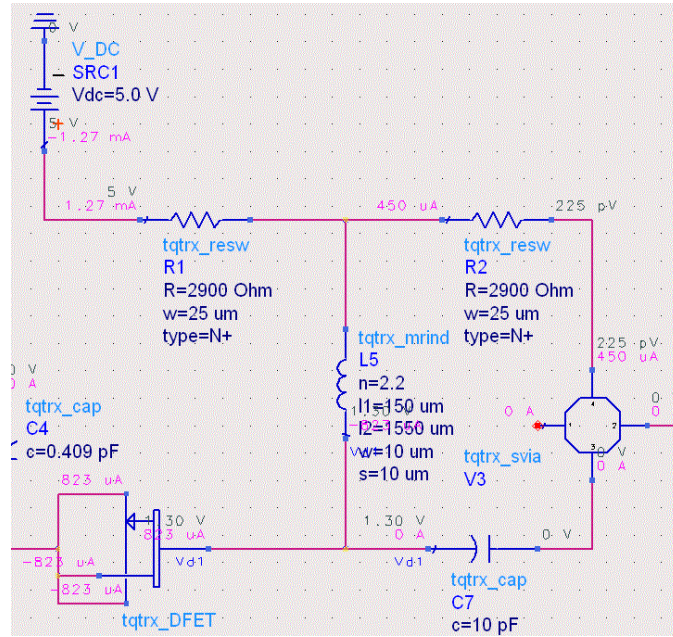


Figure 4.2: DC analysis results for voltage divider and DFET diode @ port 3.

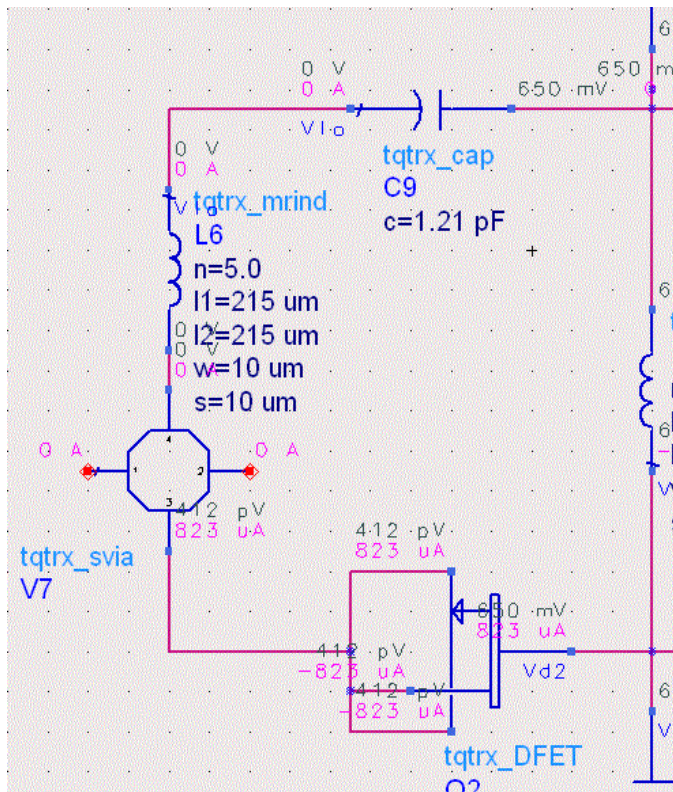


Figure 4.3: DC analysis results for DFET diode @ port 2.

5.0 TEST PLAN

5.1 SPECTRUM TEST CONFIGURATION

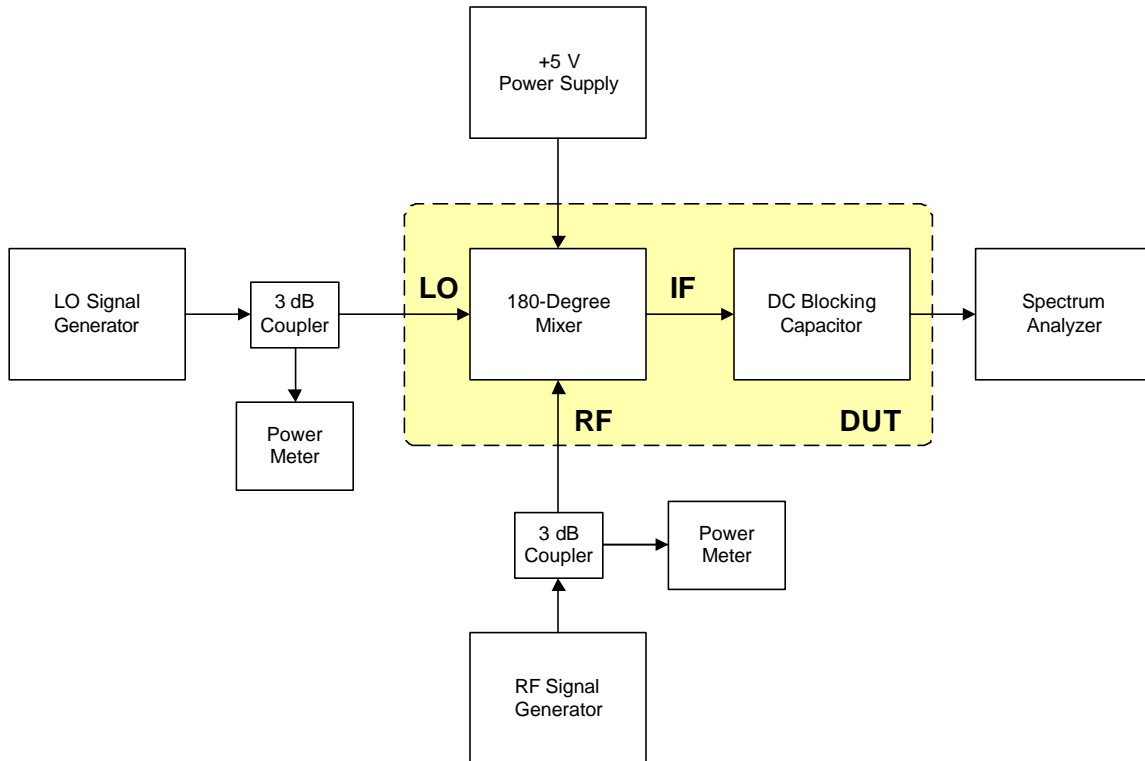


Figure 5.1: Test configuration for spectrum measurement in the down converter configuration.

To properly analyze the mixing capabilities of a mixer requires the measurement of the mixer's output spectrum. The spectrum contains all the frequency components and their power levels within the output signal. Figure 5.1 illustrates the test configuration for measuring the spectrum of the down converter configuration. The LO and RF signals are inserted into the mixer using signal generators and the output spectrum is measured by a spectrum analyzer. The 3 dB couplers and power meters are used to measure the LO and RF power levels, respectively.

To measure the output spectrum for the up converter configuration, the spectrum analyzer would be connected to the RF port of the mixer and the signal generator with the coupler and power meter would be connected to the IF port of the mixer. The LO branch would remain the same.

5.2 ISOLATION AND VSWR TEST CONFIGURATION

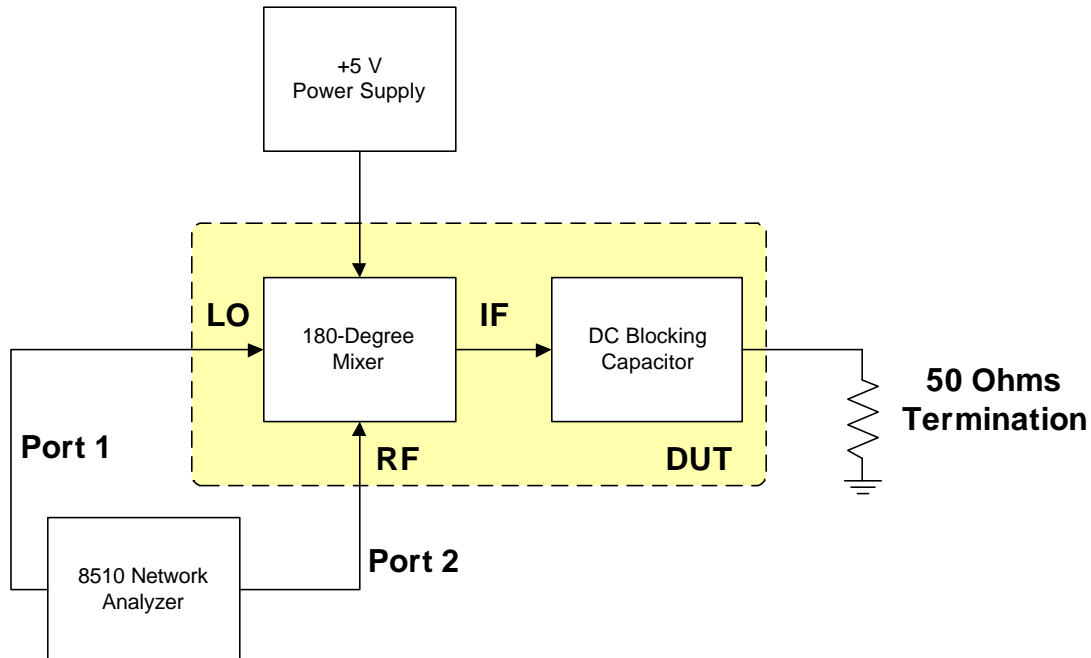


Figure 5.2: Test configuration for measurement of LO isolation and VSWRs

The LO isolation and VSWRs can be measured by using a network analyzer. The network analyzer will measure the LO isolation and VSWRs as a function of frequency. The LO-to-RF isolation can be obtained by measuring the forward transmission coefficient (S_{21}) and the VSWRs at each port can be obtained by measuring the input and output reflection coefficients (S_{11} and S_{22}) as illustrated in Figure 5.2. The 8510 network analyzer is a two-port measurement instrument and requires the proper termination of the IF port of the mixer for the down converter configuration. VSWR is calculated using the following equation:

$$\text{VSWR} = \frac{1 + |\Gamma|}{1 - |\Gamma|} \quad (5.1)$$

where Γ is the reflection coefficient at that port.

The LO-to-IF isolation and VSWRs for the up converter configuration can be measured by connecting the network analyzer to the IF port and terminating the RF port.

6.0 CONCLUSION

A complete MMIC design for a C-Band singly balanced 180-degree mixer was presented with a conversion loss of < 10 dB @ LO power of +3 dBm for both up and down conversion configurations. All other specifications for the mixer were met as demonstrated in Section 2 of this report. The novel shunt diode architecture was used to improve the impedance matching of the diodes at the hybrid's ports, which allowed for better conversion loss.

The conversion loss was a strong function of LO power. It was demonstrated that a LO power of +3 dBm was optimum for both up and down converting to meet the conversion loss specification. The up converter configuration required more LO power than the down converter configuration.

An improvement to this design could be better matching of the filters to 50Ω , which may decrease the conversion loss even further for both configurations. Also using better filter architectures (i.e. 3 section Butterworth filter) could improve the LO isolation and conversion loss, but requires more die area.

REFERENCES

- S. A. Mass, Microwave mixers, 2nd Ed Artech House: Boston, 1993.**
- S. A. Mass, The RF and microwave circuit design cookbook, Artech House: Boston, 1998.**
- R. Gabany, "C band MMIC up/down converter final report", JHU/APL Project Report, 2000.**
- C. Moore and J. Penn, Class Handouts, JHU/APL, 2000.**

C-BAND POWER AMPLIFIER

525.787 Microwave Monolithic Integrated Circuits (MMIC) Design

Gary S. Hoffman
Fall 2001

ABSTRACT – MMIC Class-F, cascade C-Band power amplifier designed for final class project using TriQuint parts. Frequency band of 5.15 to 5.875 GHz, or a bandwidth of 725.0 MHz, with a center frequency of 5.5125 GHz. Amplifier small signal gain >12.0 dB across the band with an output power > +24.0 dBm at center frequency, 1.0 dB compression point. On-chip resonant circuits in series and parallel, tuned to center frequency and its 3rd harmonic respectively, shape the output waveform and improve Power Added Efficiency (PAE). On-chip input and output matching networks into 50.0 Ohms, minimize VSWR to <1.5:1 across the band.

1. INTRODUCTION

CIRCUIT DESCRIPTION – With reference to a simplified final layout shown in Schematic #1 on page 6A, this C-Band power amplifier is a cascade Class-F power amplifier, which has a Class-A biased pre-amplifier (Q2) with a Class-AB biased post-amplifier (Q1). This design allowed for an overall small signal gain >12.0 dB to be divided between two amplifier stages. Center frequency of amplifier is 5.5125 GHz with a 725.0 MHz bandwidth (5.15-5.875 GHz). On-chip input matching (L12, L16), output matching (L4) with resonant circuits in series (L8, C8) and parallel (L7, C7), plus DC blocking and by-pass capacitors (C2, C4, C5, C9, C11, C12, C13). 1.0 mH inductors (L18 - L21) shown in DC bias paths are bond wire models, while input and output tqtrx_ports (P1, P2) are models of G-S-G signal-probe pads [5, 6].

For individual TriQuint GFET amplifiers; Class-A biased pre-amplifier, as given by marker #1 in IV Curves of Plot #1 on page 5A, has a DC bias point of -0.5 V for VGS, +7.0 V for VDS and 63.0 mA for IDS. Schematic #2 on page 6B gives the number of gates and gate widths for this 330.0 um GFET as 6 and 55.0 um respectively. Class-AB biased post-amplifier, as given by marker #1 in the IV Curves of Plot #2 on page 5B, has a DC bias point (25.0% of the IDSS value shown at marker #2) of -1.5 V for VGS, +7.0 V for VDS, and 49.0 mA for IDS. Schematic #3 on page 6C for this 720.0 um GFET gives number of gates and gate widths as 6 and 120.0 um respectively [5, 6].

Returning to Schematic #1 on page 6A, Input Matching Network (IMN) formed by L12 and L16 match pre-amplifier (Q2) to a 50.0 Ohm source impedance. L17, C2 and L15 form an inductive pi-network between pre-amplifier Q2 and post-amplifier Q1. L4 on output of post-amplifier Q1 has an R_{Cripp} load value of 50.0 Ohms and matches Q1 to an output load impedance of 50.0 Ohms through an output resonant network of series circuit L8 and C8, plus parallel circuit of L7 and C7 [5, 6].

This output resonant network shapes the output waveform and improves overall Power Added Efficiency (PAE). It is composed of resonant circuit L8 and C8 tuned to 16.54 GHz (3rd harmonic of 5.5125 GHz), and resonant circuit L7 and C7 tuned to center frequency (i.e. 5.5125 GHz). With these two resonant circuits, this network provides an OPEN to the 3rd harmonic (16.54 GHz) and a SHORT to the 2nd harmonic (11.03 GHz) but prevents their appearance at the load. For center frequency of 5.5125 GHz, this resonant network provides a MATCH to a 50.0 Ohm load. C4 is a DC blocking capacitor, but is also part of this resonant network and tunes-out any added inductance between the Q1 drain and load presented by this output resonant network [1, 2, 3, 4].

Plot #3 on page 5C along with Schematic #4 on page 6D, show the full final layout for this C-Band, cascade Class-F amplifier. Stated design specifications for this C-Band cascade Class-F power amplifier.

FREQUENCY BAND: 5.15 to 5.875 GHz [center frequency of 5.5125 GHz],
BANDWIDTH: > 725.0 MHz,
GAIN, small signal: > 12.0 dB Min [15.0 dB goal],
GAIN RIPPLE (flatness): ± 0.5 dB Max,
OUTPUT POWER: > +24.0 dBm @ 1.0 dB compression point,
EFFICIENCY: > 20.0% @ 1.0 dB compression point [25.0 % goal],
VSWR into 50.0 Ohms: < 1.5:1 [$\Gamma < 0.2$, Return Loss < -14.0 dB] for input and output,
SUPPLY VOLTAGES: +7.0 and - 5.0 VDC,
SIZE: 60.0 x 60.0 mil ANACHIP.

DESIGN PHILOSOPHY – Class-F amplifiers are also termed harmonic control amplifiers. This, from use of a frequency selective network on the amplifier output which is resonant at odd and even harmonics of the fundamental, but blocks these selected harmonics from appearing on the output load. By appearing as an open or a short to these odd/even harmonics, drain voltages and currents are optimized to reduce overall power dissipation in the GFET which results in a higher Power Added Efficiency (PAE). For this design, an open appears for the 3rd harmonic and a short appears for the 2nd harmonic. An open presented to the 3rd harmonic causes flattening of the drain voltage, which if more harmonics were involved, would eventually produce a square wave. A short for the 2nd harmonic causes a flattened sinusoid from added output current flow with a lowered output drain voltage and results in the higher PAE mentioned [1, 2, 3, 4, 5, 6].

Preliminary design of this cascade Class-F amplifier began with the output resonant network described in papers referenced in [1, 2, 3]. Shown in Schematic #5 on page 6E with accompanying Plot #4 on page 5D, resonant circuit L6 and C3 was designed for resonance at the center frequency, Fo, of 5.5125 GHz. At Fo this circuit appears as an open and only the 50.0 Ohm load appears on the output. C2 tuned-out any inductance from this resonant circuit at Fo. Schematic #6 on page 6F with accompanying Plot #5 on page 5E, shows resonant circuit L6 and C3 tuned to provide an open for the 3rd harmonic of Fo. By presenting an open, this circuit prevents 3rd harmonic from appearing across the load. C2 again swamped any residual inductance at resonance. Completed output network appears in Schematic #7 on page 6G with Plot #6 on page 5F, shows combined effect of these two resonant circuits. 2nd harmonic of Fo has a short presented to it through a series L/C resonant circuit consisting of an inductive dominate resonant circuit (L6 and C3) and a capacitive dominate resonant circuit (L7 and C4), with the result that the 2nd harmonic does not appear across the load.

Incorporation of this resonant network into the cascade Class-F amplifier design would require added tuning of resonant circuit values, but gave a starting point in overall circuit design. Design of the Input Matching Network (IMN) along with the Output Matching Network (OMN) followed.

Using procedures outlined in [5], marker #2 in Plot #7 on page 5G resulting from Schematic #8 on page 6H gave an approximate input value for S11 of the 330.0 um GFET pre-amplifier with which to design an IMN. Taking the conjugate of the value at marker #2 and using a Smith Chart while “looking towards the load and moving towards the GFET gate,” a series inductor (L12) with a shunt inductor (L16) was chosen for the IMN design as shown in Schematic #1 on page 6A. An added benefit of this IMN was the shunt inductor could be used for biasing the gate of this GFET. Bias values stated earlier for the pre-amplifier GFET were -0.5 V for VGS and +7.0 V for VDS and are the values used in Schematic #8 on page 6H.

Following Procedures for R_{Cripp} outlined in [5], Plot #8 on page 5H resulting from Schematic #9 on page 6J gave, in marker #1, an output S_{22} value for the 720.0 μm GFET post-amplifier with which to design an OMN using an R_{Cripp} of 50.0 Ohms. Starting with Plot #9 on page 5J from Schematic #10 on page 6K, a parallel resistor (R1) and capacitor (C1) circuit approximated the output S_{22} value at 5.5125 GHz from Plot #8 for the 720.0 μm GFET. To keep low Q by staying close to the real impedance axis of the Smith Chart, the capacitor value in this circuit was adjusted accordingly. Next, 50.0 Ohms was substituted for the value of R1 in Schematic #11 on page 6L with results shown by marker #2 in Plot #10 on page 5K. Conjugating capacitor C1 in Schematic #11 with an inductor in Schematic #12 on page 6M, gave the result shown by marker #3 in Plot #11 on page 5L. This gave a design point for a shunt inductor using a Smith Chart “while looking towards a 50.0 Ohm load and moving towards the GFET drain” which is given as L4 in Schematic #1 on page 6A.

Referring back to Schematic #1 on page 6A, the next step in this cascade Class-F amplifier design was to match the output of the 330.0 μm pre-amplifier GFET to the input of the 720.0 μm post-amplifier GFET. Looking again at S_{11} in Plot #8 on page 5H for the 720.0 μm post-amplifier, a matching network was designed to the conjugate of the S_{11} value at marker #2. From work with a Smith Chart, this resulted in the pi-network of L17, C2 and L15 shown in Schematic #1 on page 6A. Adjustments were made in this matching network to attain designed-for gain and power output from this cascade Class-F amplifier. Driving this approach to a between stage matching network was a single load line for this cascade Class-F amplifier on the output of the 720.0 μm GFET post amplifier.

TRADE-OFFS – Working from a stated design requirement of $> +24.0$ dBm at the 1.0 dB compression point, gate width of the post-amplifier GFET was gradually increased to its final value of 720.0 μm ($N = 6$, $W = 120$) as a power margin was sought in Plot #2 on page 5B. This meant that the maximum power output from this GFET was approximately +26.17 dBm at V_{sat} in Plot #2, or a +2.17 dB margin over the required design output power of $> +24.0$ dBm. Having a design value for the GFET post-amplifier gate width, bias was the next design item to examine for this post-amplifier.

With reference to [1, 2, 3, 4, 5, 6], a Class-F amplifier is traditionally biased as Class-B, or at the pinch-off voltage. This was tried with less than satisfactory results. As an alternative to Class-B biasing, Class-AB biasing at 25.0% of $IDSS$ (marker #2 in Plot #2) was used in the final circuit design. This gave (marker #1 in Plot #2) a VGS of -1.5 V with an IDS of 49.0 mA for a VDS of $+7.0$ V for this post-amplifier GFET.

Having bias and gate width for the post-amplifier GFET, an overall Class-F amplifier gain of 12.0 dB required addition of a pre-amplifier stage to this cascade Class-F amplifier design. Without this pre-amplifier stage, this Class-F amplifier could go into compression with a very low input power level. From STUDENT PROJECTS handout given in class [5], this input level could be as high as +12.0 dBm from input driver and variable gain amplifier stages. From this, +12.0 dBm was chosen as the input power level for an output 1.0 dB compression point $> +24.0$ dBm from this cascade Class-F power amplifier design.

Choosing Class-A bias for the pre-amplifier GFET, and with a maximum output power level from the post-amplifier of approximately 26.17 dBm, a gate width for the pre-amplifier which would split the overall power requirement was required. Taking as a guide [5], the pre-amplifier gate width was initially set to one-third the 720.0 μm gate width of the post-amplifier, or 40.0 μm . VDS was set to $+7.0$ V and VGS to -0.5 V. From this initial gate width, TUNE MODE in ADS was utilized until a gate width for this Class-A pre-amplifier GFET of 55.0 μm with 6 gate fingers was found which provided overall performance sought for this cascade Class-F amplifier.

2. MODELED PERFORMANCE

SPECIFICATION COMPLIANCE MATRIX –

PARAMETER	STATED RANGE	PRE-LAYOUT	FINAL LAYOUT
Frequency	5.15 - 5.875 GHz	>5.15 - 5.875 GHz	>5.15 - 5.875 GHz
Bandwidth	>725.0 MHz	>725.0 MHz	>725.0 MHz
Small Signal Gain	>12.0 dB Min	>12.0 dB	>12.0 dB
Gain Ripple	< +/- 0.5 dB Max	> +/- 0.5 dB	> +/- 0.5 dB
Output Power	>+24.0 dBm @ 1.0 dB Comp. Pt.	24.490 dBm @ 1.0 dB Comp. Pt.	25.26 dBm @ 1.0 dB Comp. Pt.
Efficiency (PAE)	>20.0% @ 1.0 dB Comp. Pt.	20.512 % @ 1.0 dB Comp. Pt.	23.824 % @ 1.0 dB Comp. Pt.
VSWR (input/output)	<1.5:1	<1.5:1	<1.5:1
Return Loss (input/output)	<-14.0 dB	<-14.0 dB	<-14.0 dB

PREDICTED PERFORMANCE -- S-Parameter simulations for pre-layout design are shown in Plot #12 on page 5M with corresponding Schematic #13 on page 6N. From Plot #12E, given stated VSWR requirement of < 1.5:1 (Return Loss < -14.0 dB), resulting bandwidth > 725.0 MHz. Mu-parameters in Plot #12D show this Class-F amplifier is unconditionally stable over the bandwidth. While Plot #12B show forward gain (S21), or the small signal gain, to be >12.0 over the bandwidth as well. Parameter goal not attained during simulations was the gain ripple requirement of ± 0.5 dB Max, and is discussed in: “**7. CONCLUSIONS & RECOMMENDATIONS.**”

Harmonic balance simulations on pre-layout design, Plot #13A on page 5N with corresponding Schematic #14 on page 6P, show a 1.0 dB compression point > 24.41 dBm with a PAE of 20.51 % for an input power level of 11.0 dBm. Highest PAE was 20.82 % at an output power level of 24.64 dBm for an input power level of 12.0 dBm. Plot #13B shows dynamic load line to be Class-F. Plot #13C shows fundamental output power level along with output power levels for its 2nd and 3rd harmonics. Plots #13D - #13J are plots of currents and voltages at the input (Vin, I_in), post-amplifier drain (VDS, IDS), and on the output (Vout, I_out). Specifically, Plot #13E shows a slight flattening of voltage waveform due to the 3rd harmonic, and Plot #13H shows a slight flattening of the current sinusoid waveform due to the 2nd harmonic

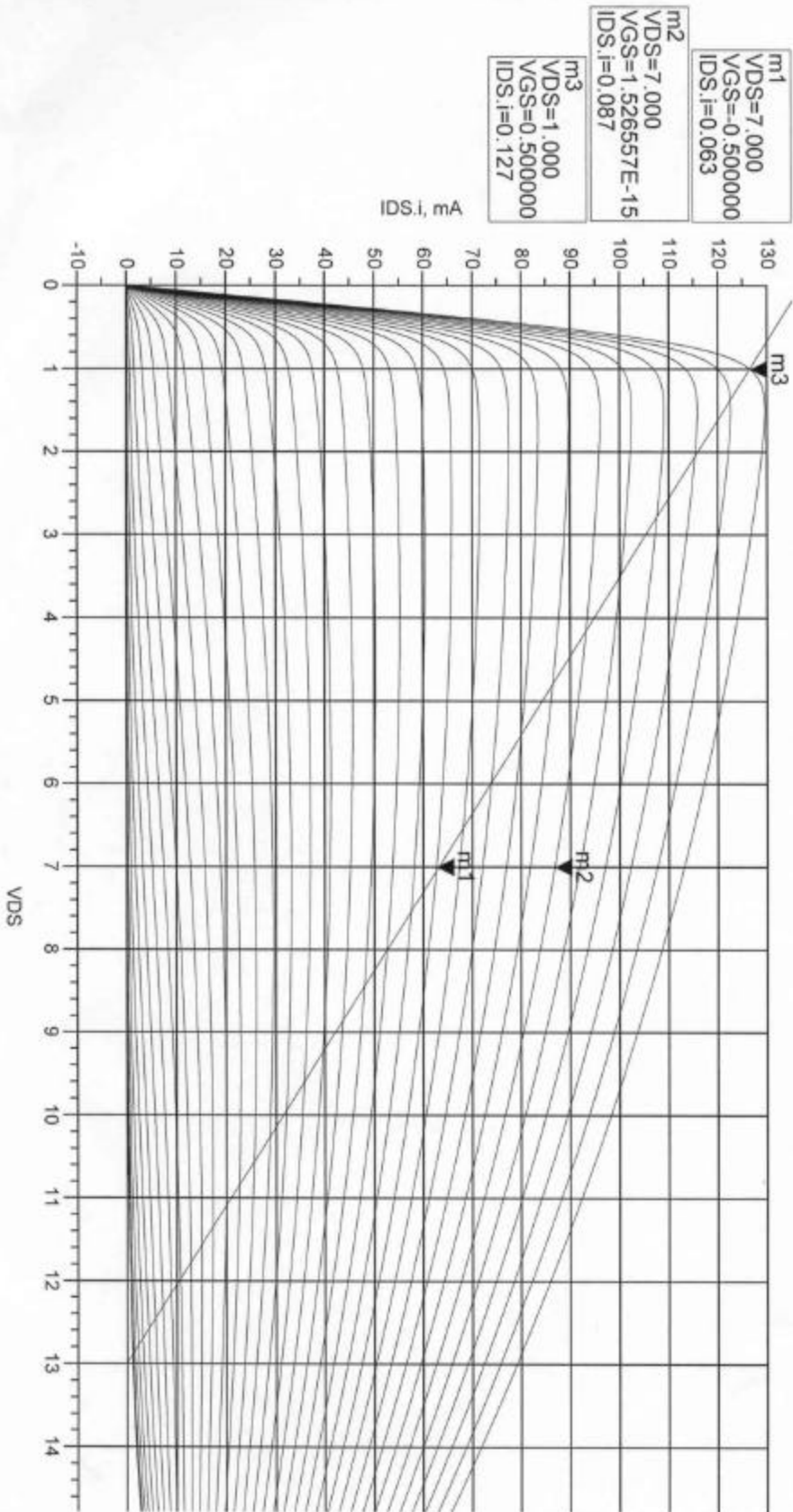
Final layout S-parameter simulations are shown in Plot #14, on page 5P. Schematic #4 on page 6D shows final layout schematic used for S-parameter simulations. Plot #14E gives S11 and S22 results. Aside from attaining a VSWR < 1.5:1 (Return Loss < -14.0 dB) across the band for S11 and S22, there is some distortion present on S22. Plot 14D of mu-parameters does show this amplifier unconditionally stable across the bandwidth. Plot #14B has small signal gain (S21) >12.0 dB across the required bandwidth.

Final layout harmonic balance simulations are shown in Plot #15, on page 5Q. Schematic #4 on page 6D shows final layout schematic used for harmonic balance simulations. Plot #15A shows, for an input power level of 12.0 dBm, an output 1.0 dB compression point of 25.26 dBm with a PAE of 23.82 %. Highest PAE was 24.12 % for an input power level of 13.0 dBm and an output power level of 25.38 dBm. Plot #15B shows dynamic load line to be Class-F. Plot #15C has output power levels for the fundamental as well as those for its 2nd and 3rd harmonics. Plots #15D - #15J are voltage and current waveforms for the input (Vin, I_in), post-amplifier drain (VDS, IDS), and the output (Vout, I_out). Plot #15E shows a slight flattening of the VDS voltage waveform due to the 3rd harmonic, and Plot #15H shows a slightly flattened sinusoid IDS current waveform due to the 2nd harmonic.

3. SIMULATION PLOTS

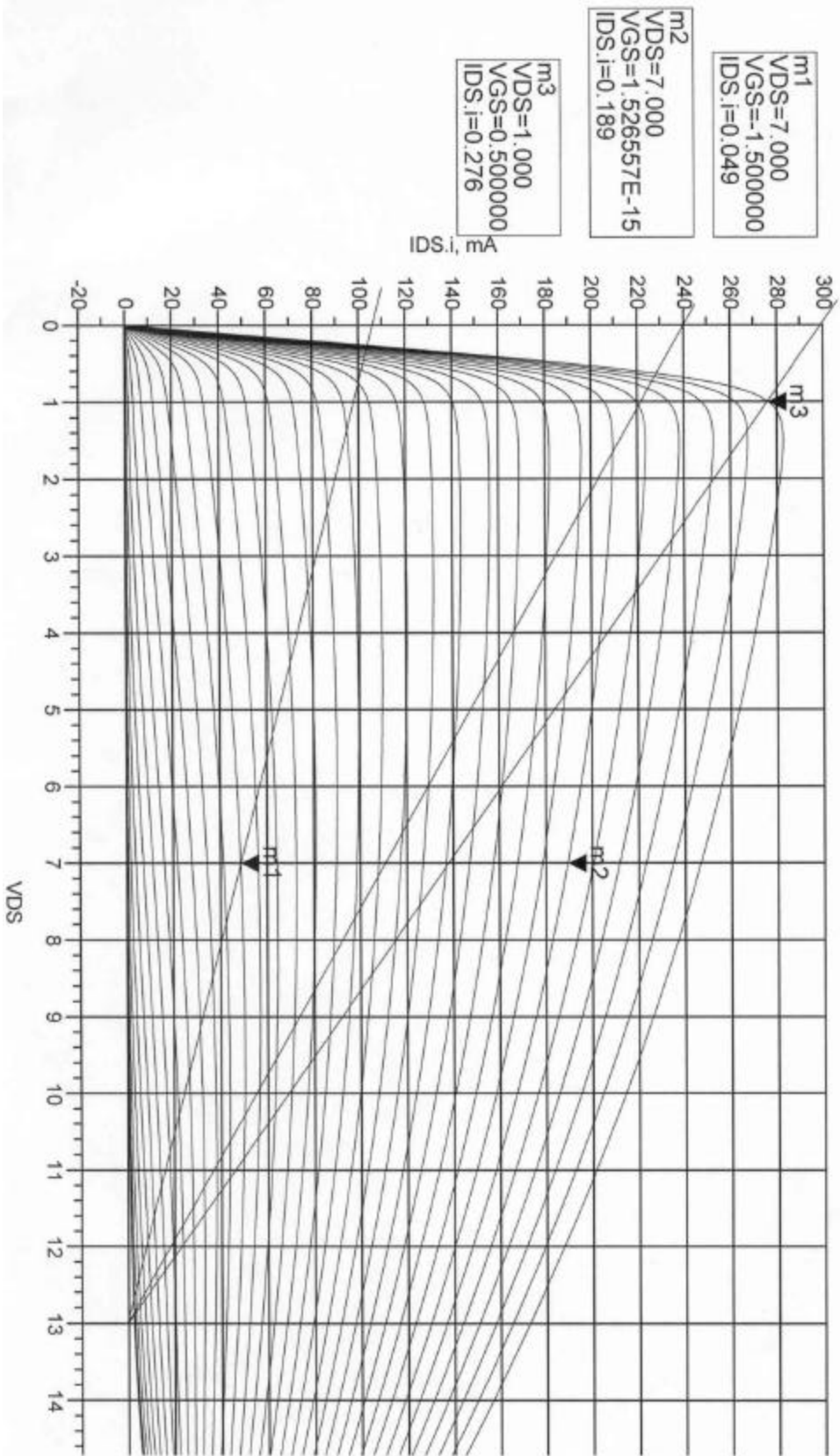
Simulation plots used in all discussions follow. Numbering for each simulation plot and its respective schematic is given in the upper left-hand corner.

Plot # 1. Schematic # 2. 330.0 um (N = 6, W = 55) Class A Pre-Amplifier GFET IV Curves



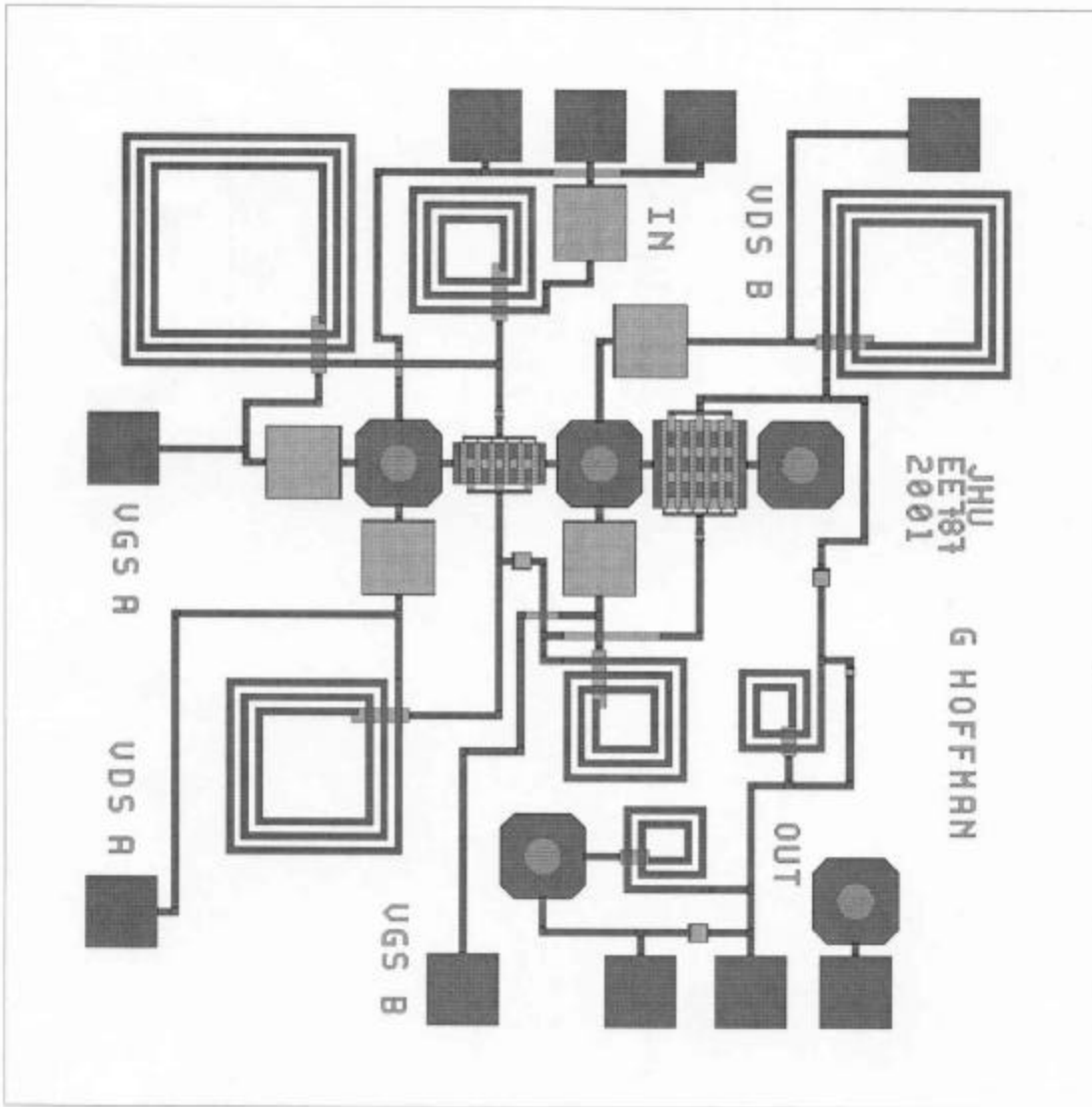
5A

Plot # 2. Schematic # 3. 720.0 um (N = 6, W = 120) Class F Post Amplifier GFET IV Curves



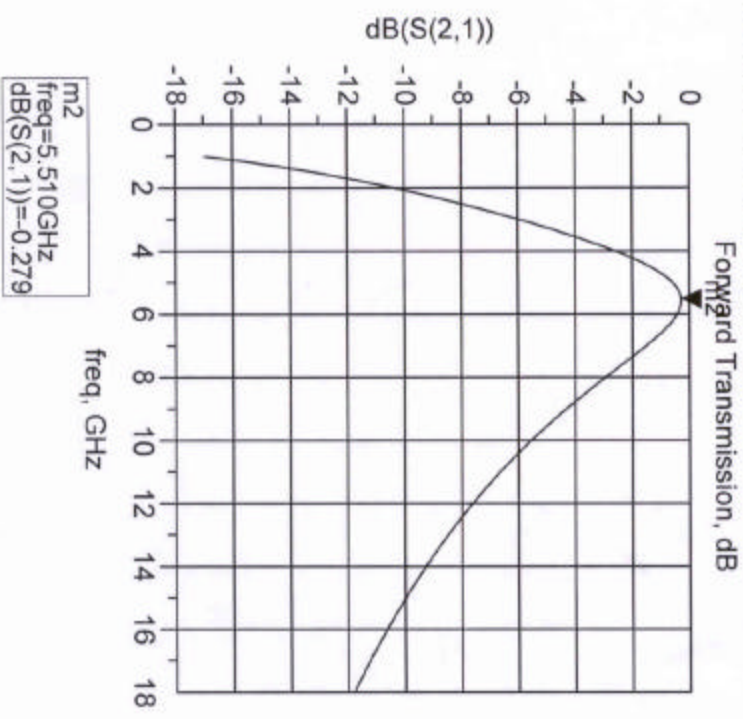
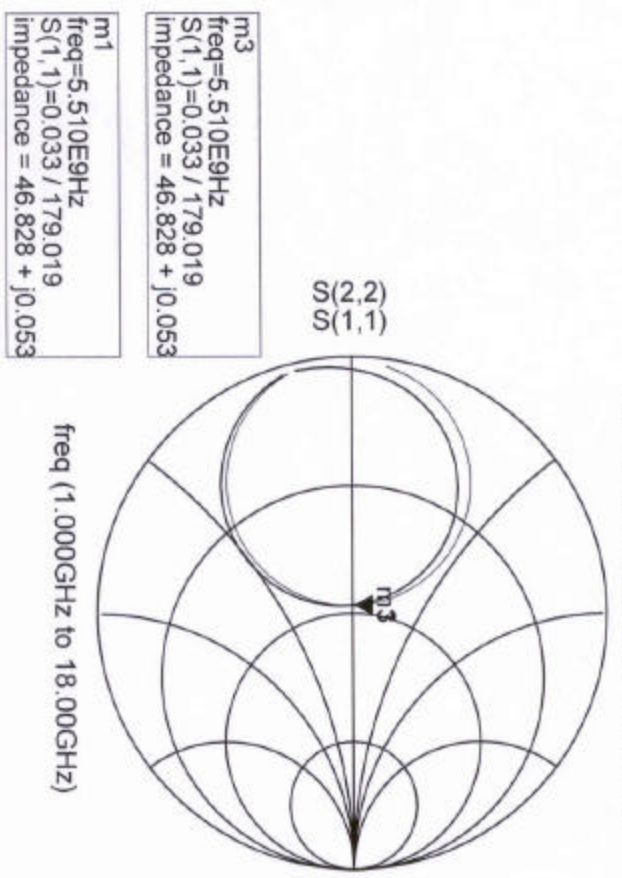
5B

Plot. #3. Schematic #4. Final layout



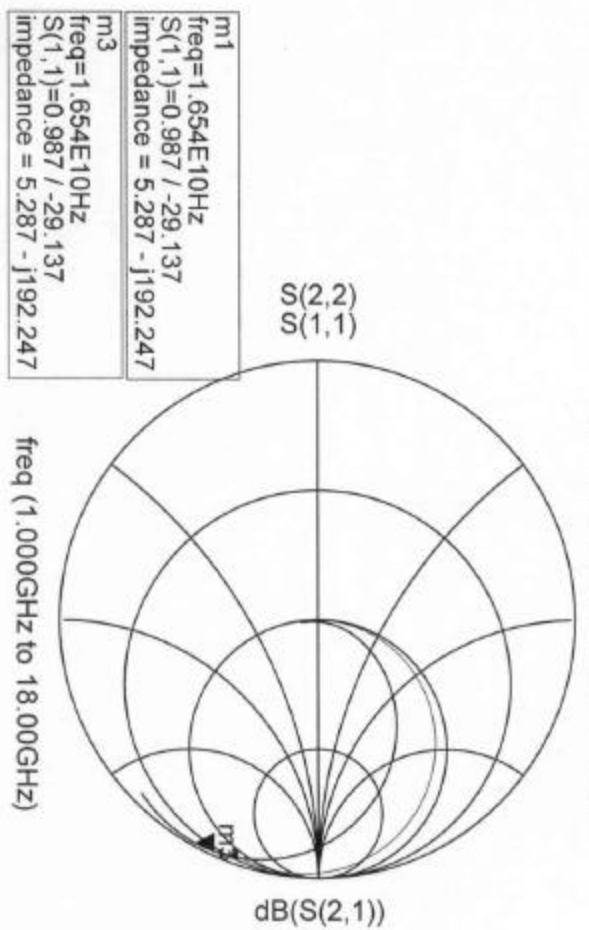
5C

Plot # 4. Schematic # 5. Class F Parallel Fundamental Frequency Resonant Tank Test Bed
Input/Output Reflection Coefficients

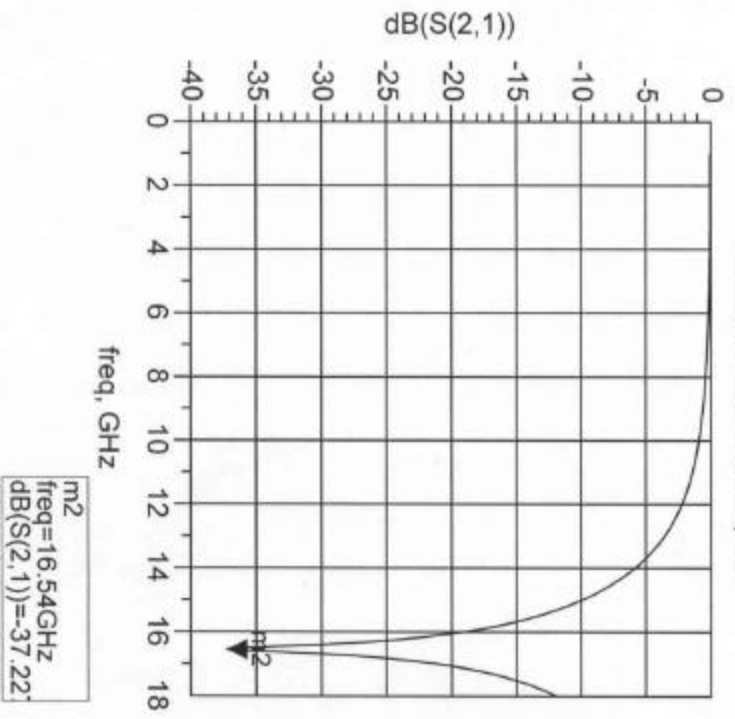


Plot # 5. Schematic # 6. Class F Series 3rd Harmonic of Fundamental Frequency Resonant Tank Test Bed

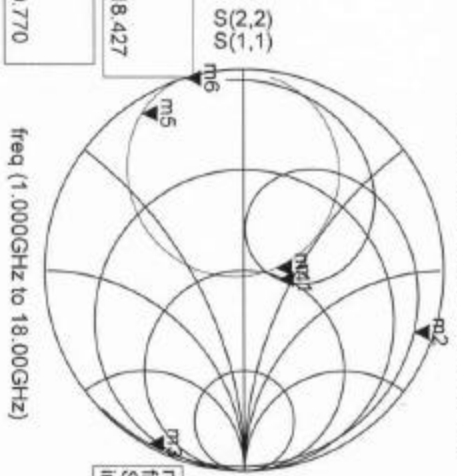
Input/Output Reflection Coefficients



Forward Transmission, dB



Plot # 6. Schematic # Z. Class F Series and Parallel Resonant Tank Test Bed
 Input/Output Reflection Coefficients



m1
 freq=5.510E9Hz
 S(1,1)=0.180 / 76.144
 Impedance = 51.137 + j18.427

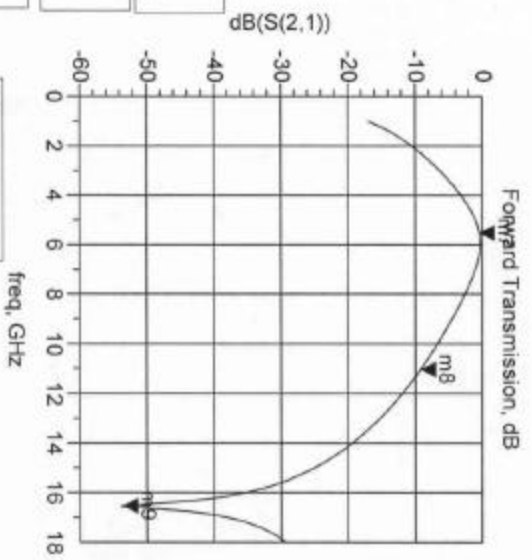
m2
 freq=1.103E10Hz
 S(1,1)=0.904 / 70.071
 Impedance = 7.583 + j70.770

m3
 freq=1.654E10Hz
 S(1,1)=0.987 / -29.144
 Impedance = 5.323 - j192.203

m4
 freq=5.510E9Hz
 S(2,2)=0.164 / 94.634
 Impedance = 46.191 + j15.513

m5
 freq=1.103E10Hz
 S(2,2)=0.933 / -146.790
 Impedance = 1.893 - j14.891

m6
 freq=1.653E10Hz
 S(2,2)=0.999 / -163.168
 Impedance = 0.016 - j7.398



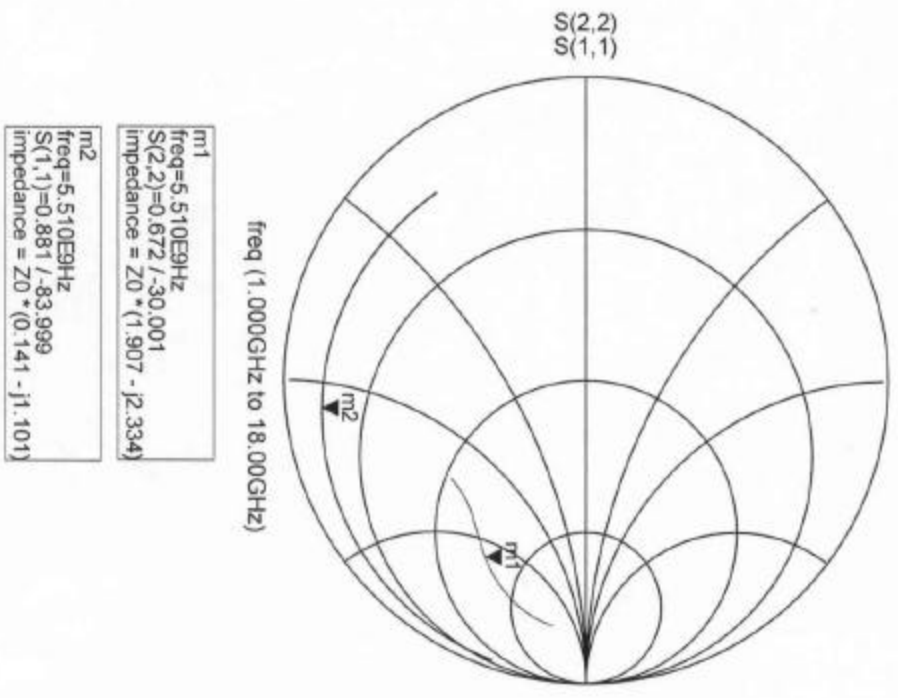
m7
 freq=5.510GHz
 dB(S(2,1))=-0.474

m8
 freq=11.03GHz
 dB(S(2,1))=-9.176

m9
 freq=16.53GHz
 dB(S(2,1))=-53.636

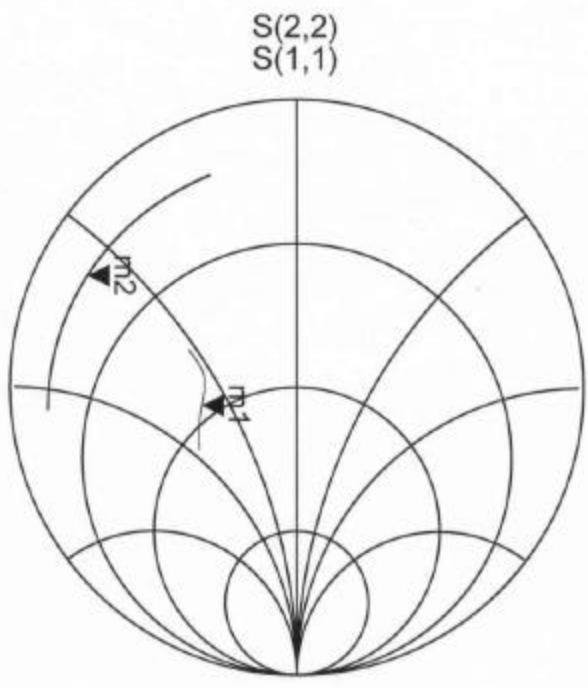
Plot # 7. Schematic # 8. Class F Pre-Amplifier GFET S22 and S11 S-Parameters Use with S-Parameter Simulation

Input Reflection Coefficient



Plot # 8. Schematic # 9. Class F Post Amplifier GFET S22 and S11 S-Parameter Simulations

Input/Output Reflection Coefficients

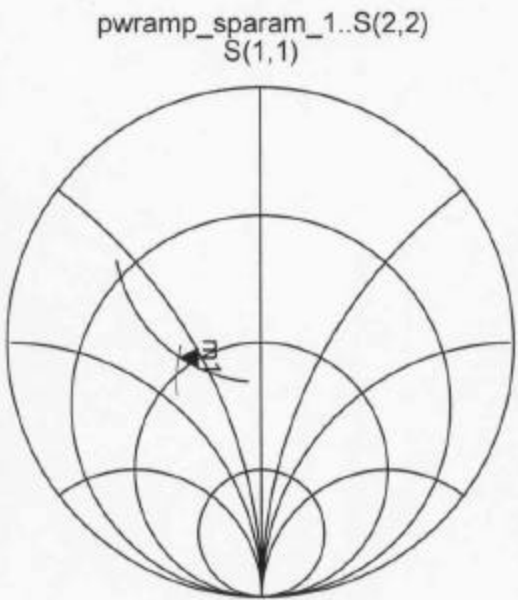


freq (3.000GHz to 18.00GHz)

m1
freq=5.510E9Hz
S(2,2)=0.337 / -79.180
Impedance = 44.893 - j33.555
m2
freq=5.510E9Hz
S(1,1)=0.827 / -117.939
Impedance = 6.432 - j29.713

54

Plot # 9. Schematic # 10. Class F Retripp Output Matching Circuit to Post Amplifier
720.0 um (N = 6, W = 12.0) GFET S22 S-Parameters
Input Reflection Coefficient



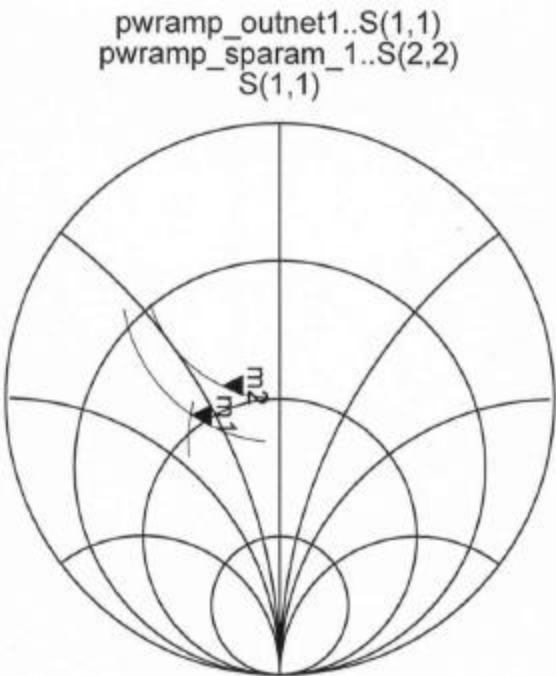
freq (1.000GHz to 18.000GHz)
freq (3.000GHz to 7.000GHz)

m1
freq=5.510E9Hz
pwramp_sparam_1..S(2,2)=0.331 / -79.758
impedance = 44.893 - j32.830

5J

Plot # 10 : Schematic # 11 : Class F Rcripp Output matching Circuit to Post Amplifier
 720.0 um (N = 6, W = 120) GFET S22 S-Parameters

Input Reflection Coefficient



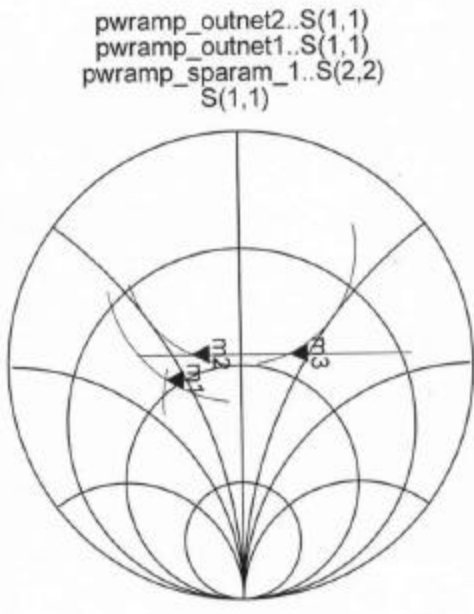
freq (1.000GHz to 18.000GHz)
 freq (3.000GHz to 7.000GHz)

m1
 freq=5.510E9Hz
 pwramp_sparam_1..S(2,2)=0.331 / -79.75
 impedance = 44.893 - j32.830

m2
 freq=5.510E9Hz
 S(1,1)=0.218 / -102.588
 impedance = 41.686 - j18.61

5k

Plot # 11 Schematic # 12 Class F Rctrip Output Matching Circuit to Post Amplifier
 720.0 um (N = 6, W = 120) GFET S22 S-Parameters
 Input Reflection Coefficient



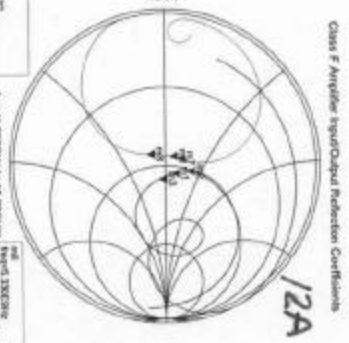
m1
 freq=5.510E9Hz
 pwramp_sparam_1..S(2,2)=0.331 / -79.758
 impedance = 44.893 - j32.830

m2
 freq=5.510E9Hz
 pwramp_outnet2..S(1,1)=0.218 / -102.588
 impedance = 41.686 - j18.617

m3
 freq=5.510E9Hz
 S(1,1)=0.218 / 102.587
 impedance = 41.686 + j18.617

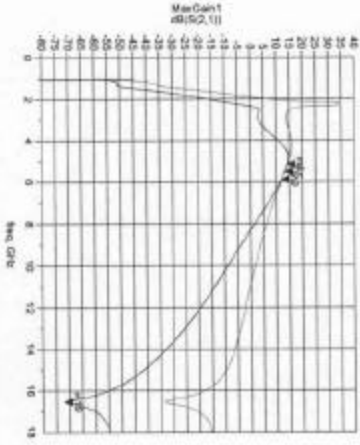
5L

Plot # 12 Schematic # 13 Class F Amplifier Pre-Layout S-Parameter Simulations



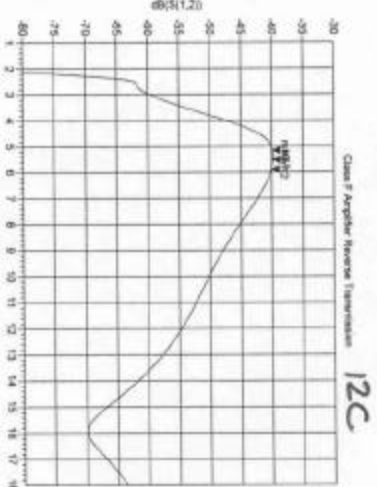
Port 1: S111
 Magnitude: 0.000000
 Phase: 0.000000
 Frequency: 20.000000 GHz

Port 2: S222
 Magnitude: 0.000000
 Phase: 0.000000
 Frequency: 20.000000 GHz



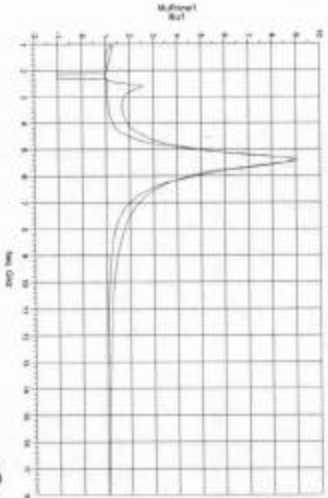
Port 1: S111
 Magnitude: 0.000000
 Phase: 0.000000
 Frequency: 20.000000 GHz

Port 2: S222
 Magnitude: 0.000000
 Phase: 0.000000
 Frequency: 20.000000 GHz



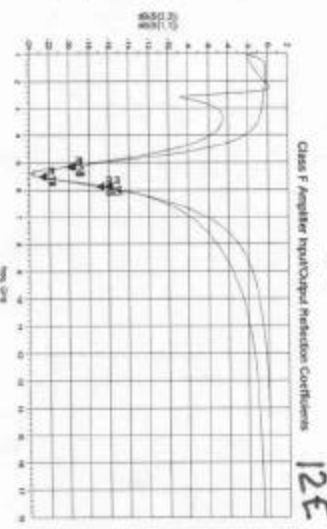
Port 1: S111
 Magnitude: 0.000000
 Phase: 0.000000
 Frequency: 20.000000 GHz

Port 2: S222
 Magnitude: 0.000000
 Phase: 0.000000
 Frequency: 20.000000 GHz



Port 1: S111
 Magnitude: 0.000000
 Phase: 0.000000
 Frequency: 20.000000 GHz

Port 2: S222
 Magnitude: 0.000000
 Phase: 0.000000
 Frequency: 20.000000 GHz



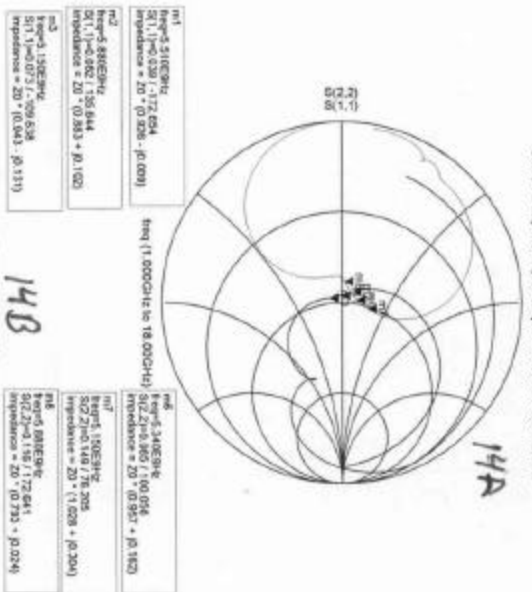
Port 1: S111
 Magnitude: 0.000000
 Phase: 0.000000
 Frequency: 20.000000 GHz

Port 2: S222
 Magnitude: 0.000000
 Phase: 0.000000
 Frequency: 20.000000 GHz

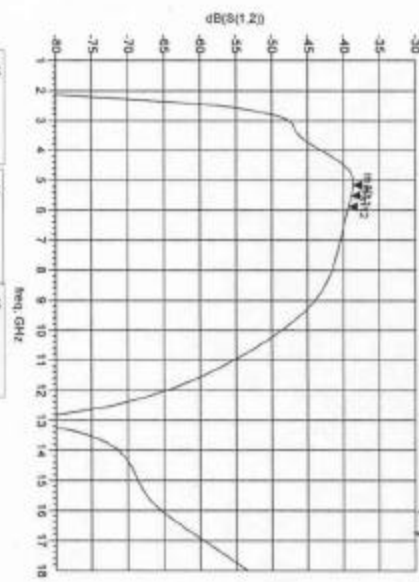
5M

Plot # 14. Schematic # None Class F Amplifier Final Layout S-Parameter Simulations

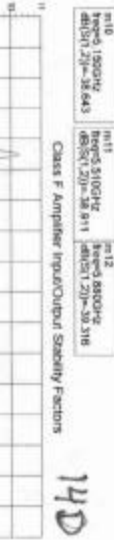
Class F Amplifier Input/Output Reflection Coefficients



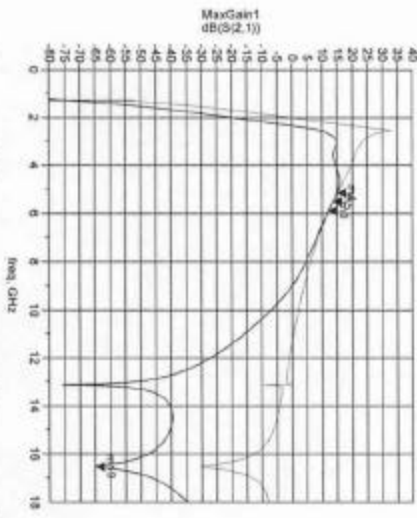
Class F Amplifier Reverse Transmission



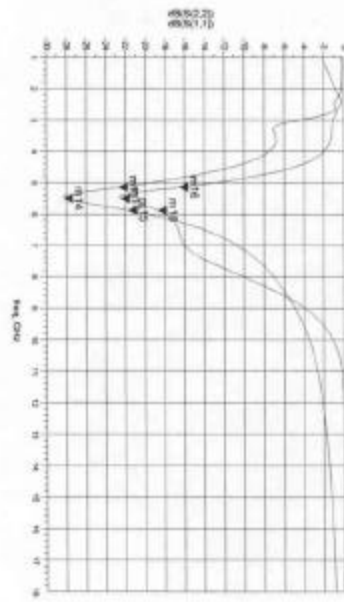
Class F Amplifier Input/Output Standing Factors



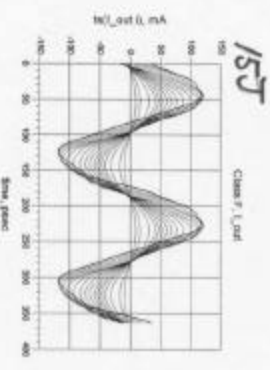
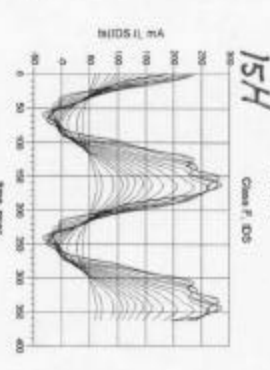
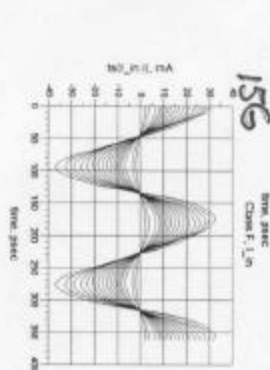
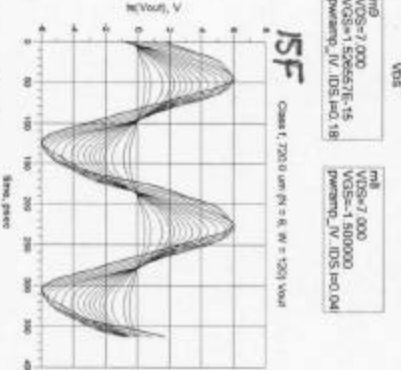
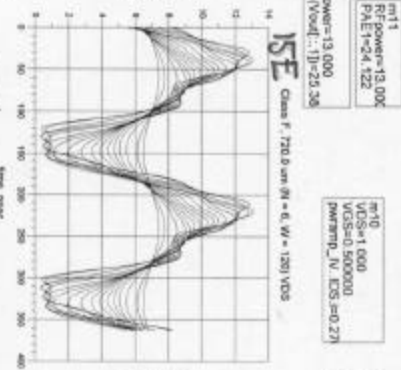
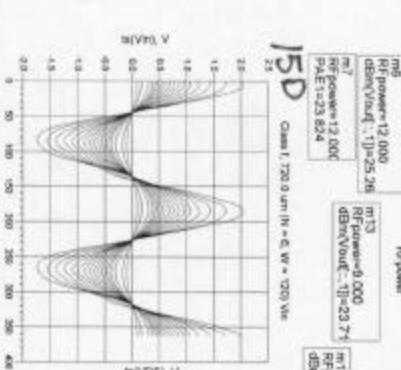
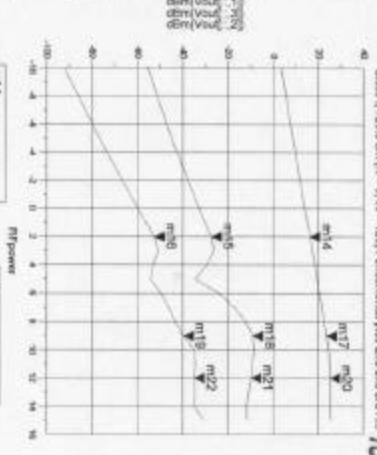
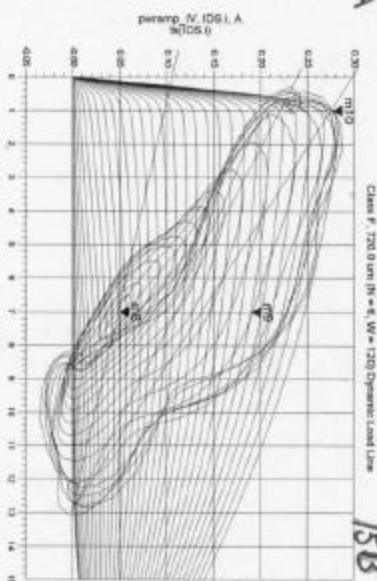
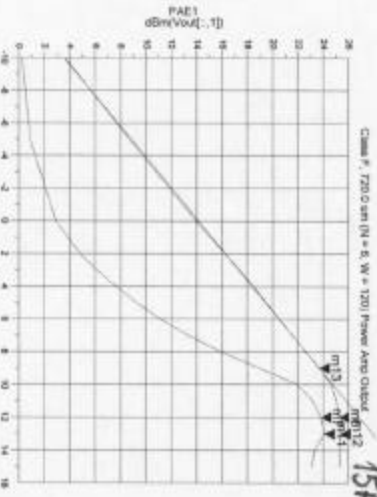
Class F Forward Transmission



Class F Amplifier Input/Output Reflection Coefficients



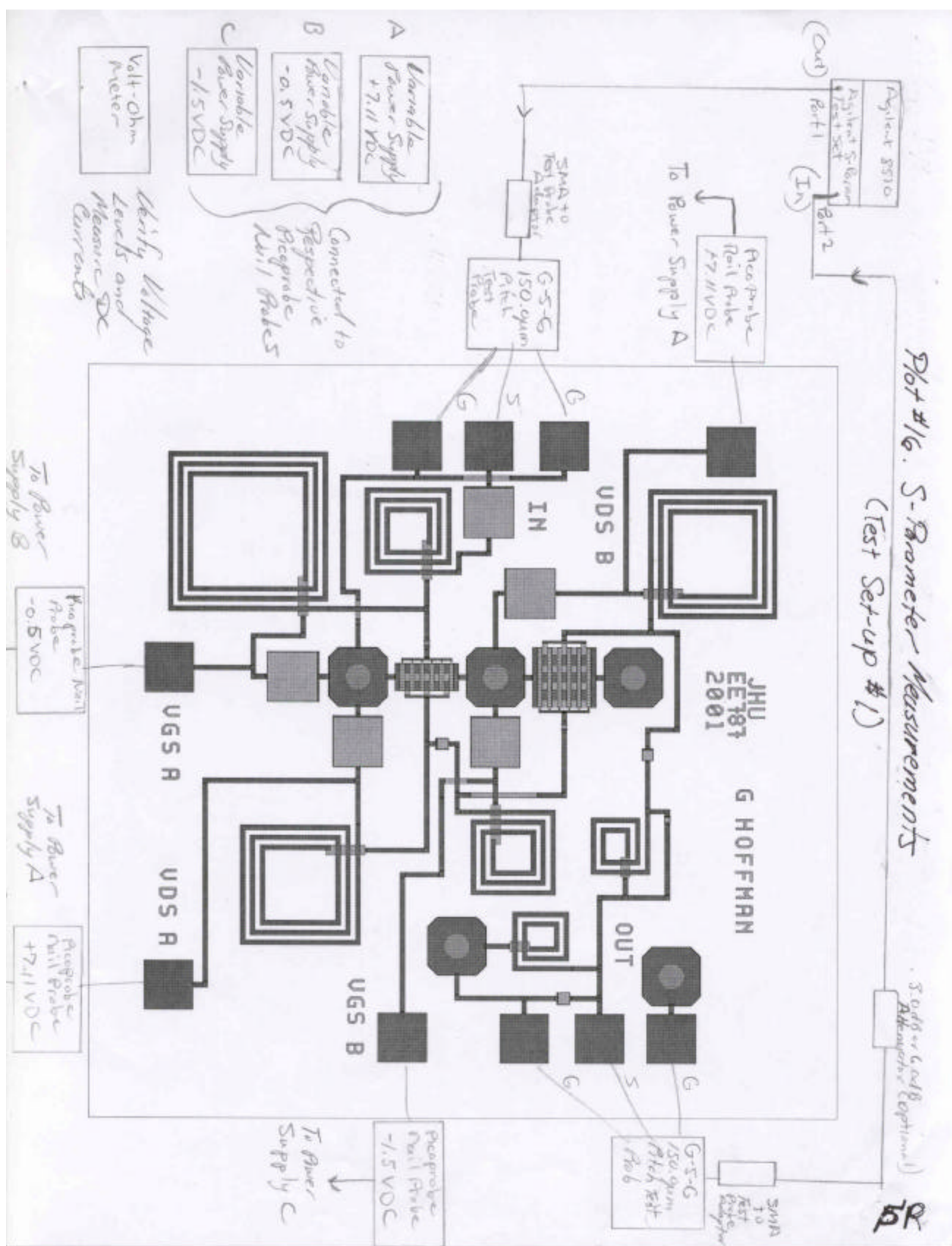
Plot # 15. Schematic # None. Class F Amplifier Final Layout Harmonic Balance Simulations



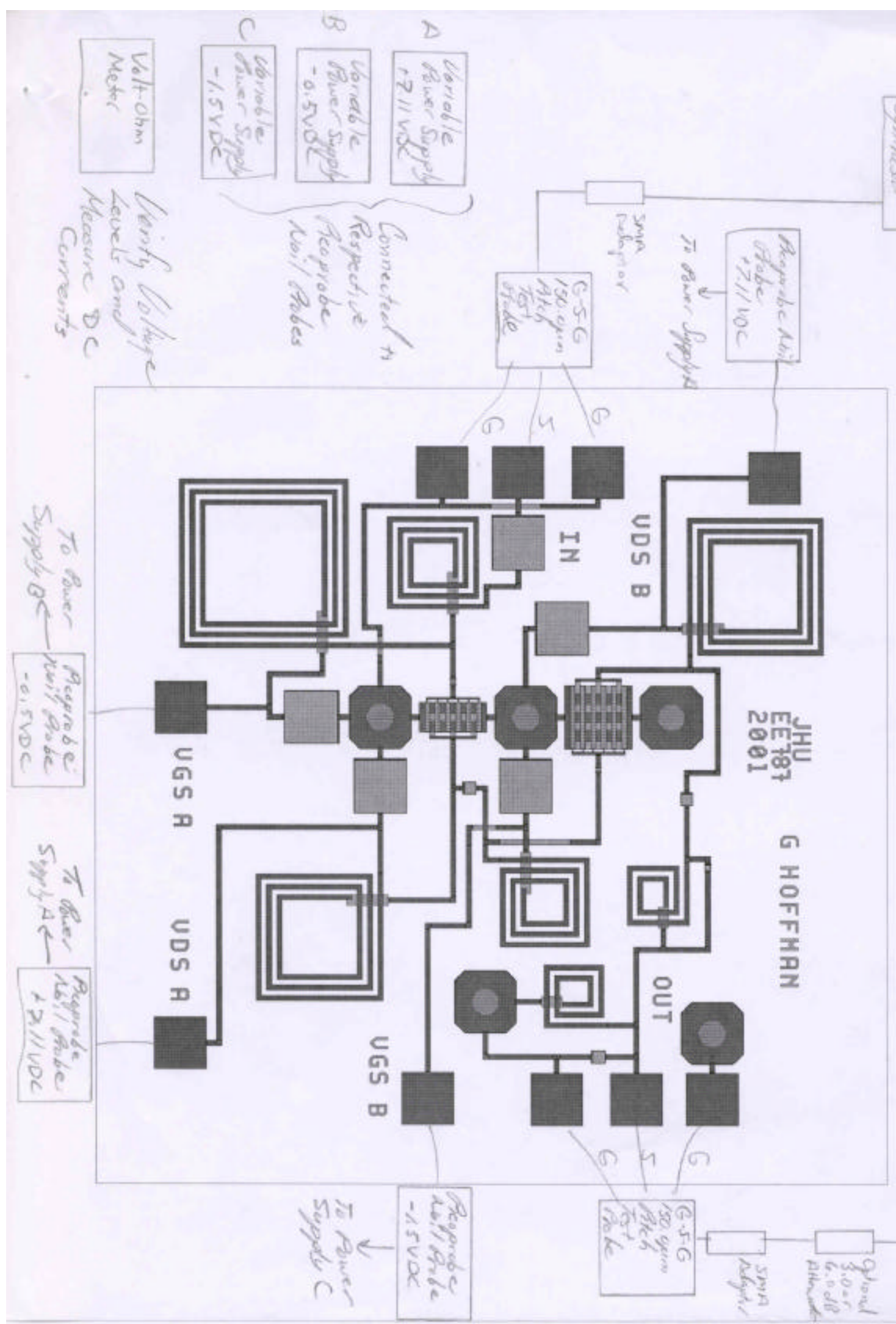
15
D

Plot #16. S-Parameter Measurements

(Test Set-up #1)



*Plot #17: 1.0dB Compression Point and (Test Set-up #2)
Power Input/Output Measurements.*



A Variable Power Supply +2.11VDC
 B Variable Power Supply -0.5VDC
 C Variable Power Supply -1.5VDC
 Volt-Ohm Meter
 Verify Voltage Levels and Measure DC Currents

Connected to Respective No./Gates
 To Power Supply A
 To Power Supply B
 To Power Supply C

Adjust Frequency Synthesizer

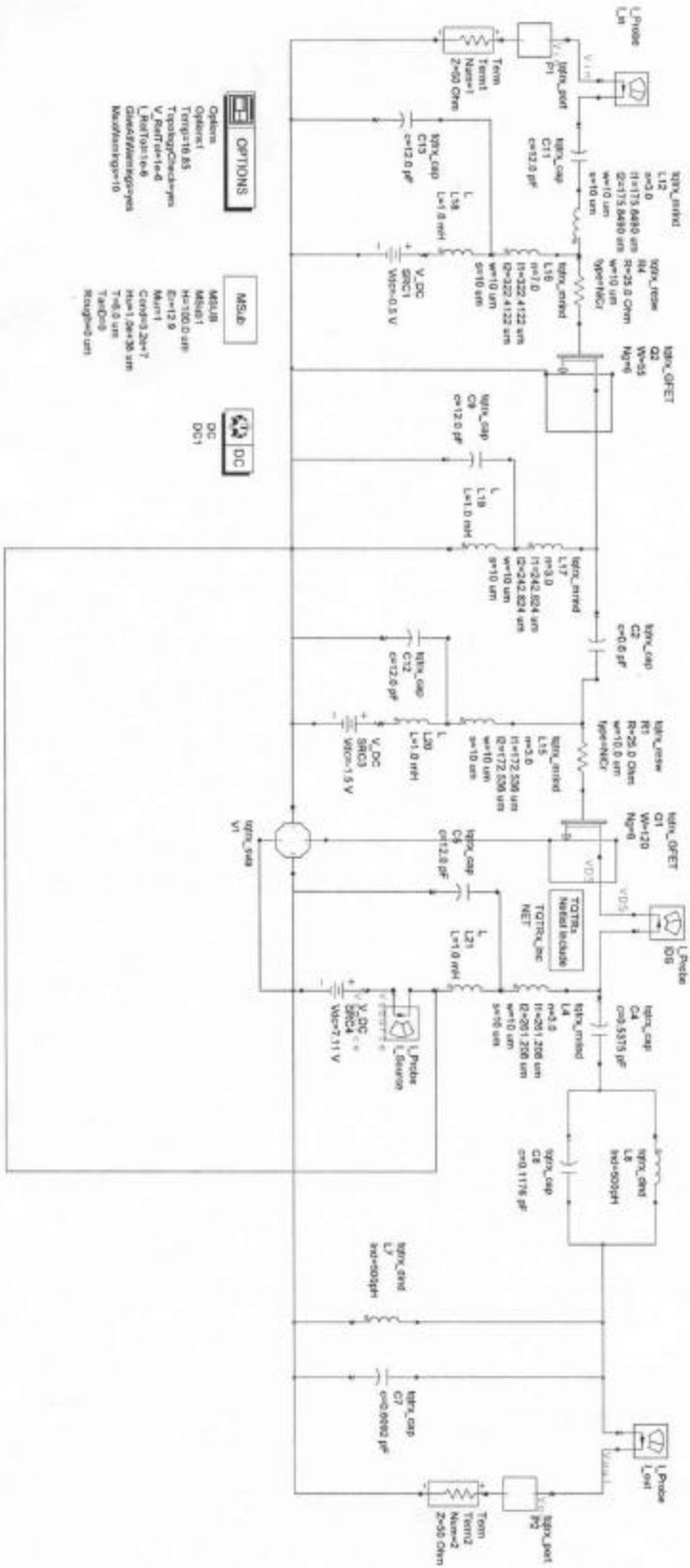
Adjust Spectrum Analyzer

50

4. SCHEMATIC DIAGRAMS

Schematics used in all discussions follow. Numbering for each schematic and its respective plot(s) is shown in the upper left-hand corner. A simplified schematic of the final layout is shown in Schematic #1 on page 6A. There are no corresponding plot(s) since this simplified schematic was not used in Sparameter or harmonic balance simulations.

Plot #None, Schematic # 1. Final Layout (Simplified Schematic) Component Values of Class F, 720.0 um (N = 6, W = 120) Power Amplifier with 330.0 um (N = 6, W = 55) Pre-Amp



OPTIONS

Options
 Optimize: 1
 Temp: 18.85
 TopologicCheck: yes
 V_Pull: 0.1
 L_Pull: 0.1
 GroundForming: yes
 MaxIterations: 10

MSLB

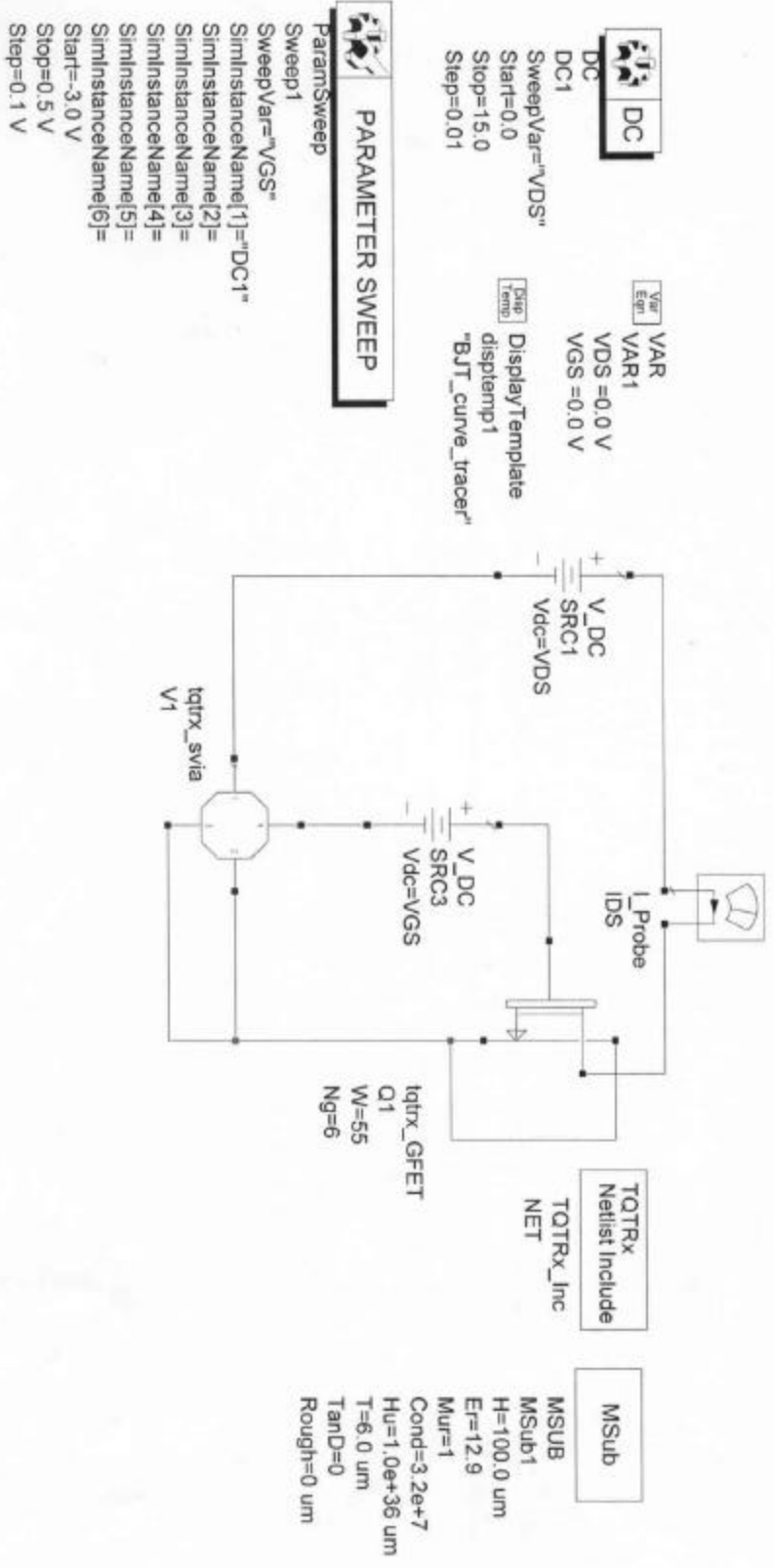
MSL: B
 Min: 100.0 um
 Et: 12.8
 Min: 1
 Core: 204
 Min: 1.5e+26 um
 T: 40.0 um
 T: 40.0 um
 Ring: 90.0 um

DC

DC
 DC1

6A

Plot # 1. Schematic # 2. Class F PRE-Amplifier GFET IV Curve Tracer



6C

Plot # 2. Schematic # 3. Class F Post Amplifier GFET IV Curve Tracer

DC

DC 1
SweepVar="VDS"
Start=0.0
Stop=15.0
Step=0.01

DisplayTemplate

displaymp1
"BJT_curve_tracer"

VAR

VAR1
VDS =0.0 V
VGS =0.0 V

PARAMETER SWEEP

Param:Sweep

Sweep1
SweepVar="VGS"
SimInstanceName[1]="DC1"
SimInstanceName[2]=
SimInstanceName[3]=
SimInstanceName[4]=
SimInstanceName[5]=
SimInstanceName[6]=
Start=-3.0 V
Stop=0.5 V
Step=0.1 V

MSUB

MSUB1
H=100.0 um
Er=12.9
Mur=1
Cond=3.2e+7
Hu=1.0e+36 um
T=6.0 um
TanD=0
Rough=0 um

TOTRX

Netlist Include
TOTRX_inc
NET

MSUB

MSUB1
H=100.0 um
Er=12.9
Mur=1
Cond=3.2e+7
Hu=1.0e+36 um
T=6.0 um
TanD=0
Rough=0 um



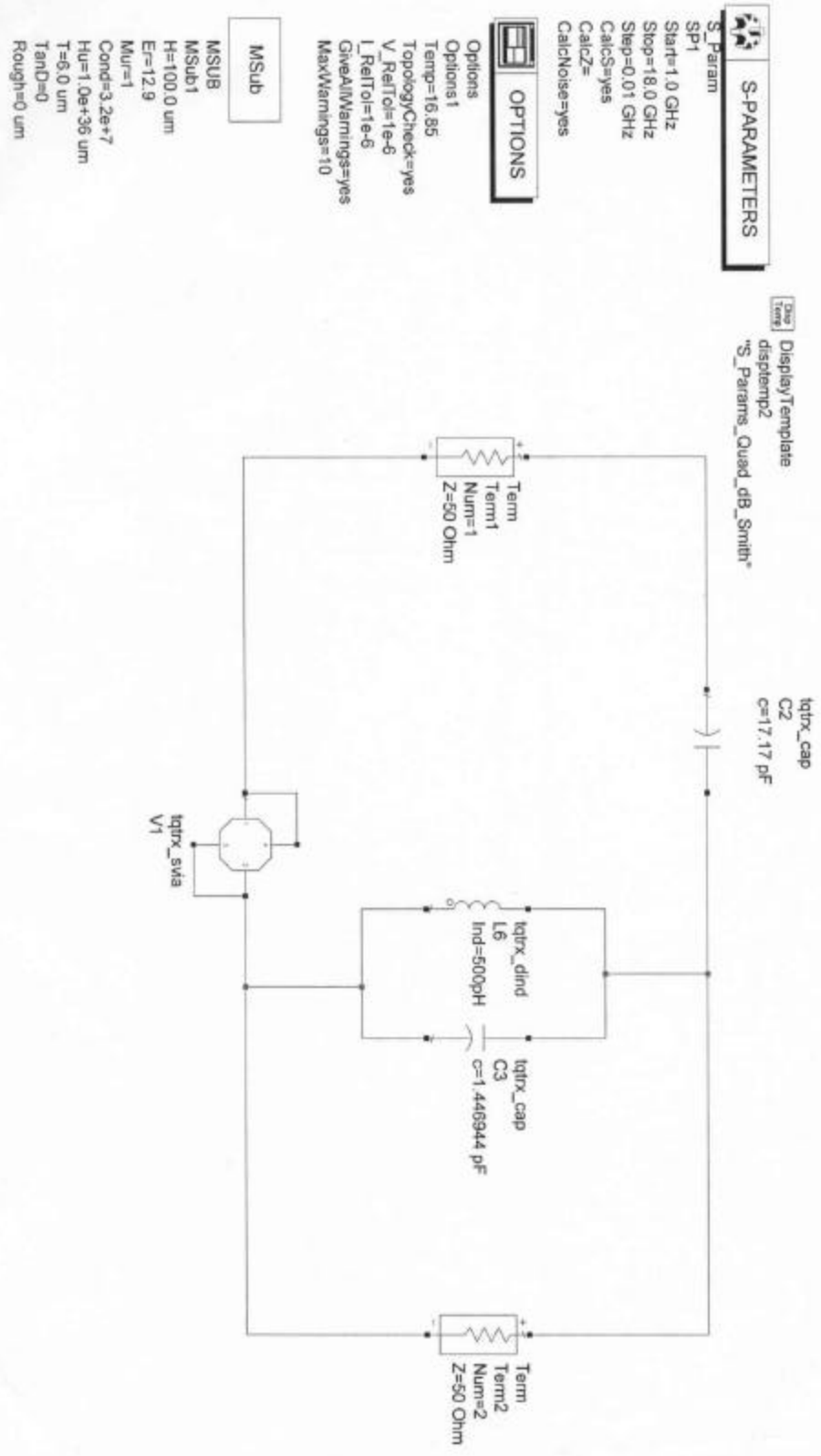
Chart # 720p camera & 90° 120° Power Amp & Chirp A 1000 series (L, W, S) Harmonic Balance Simulation

Schematic #4. Full Final Layout.

60

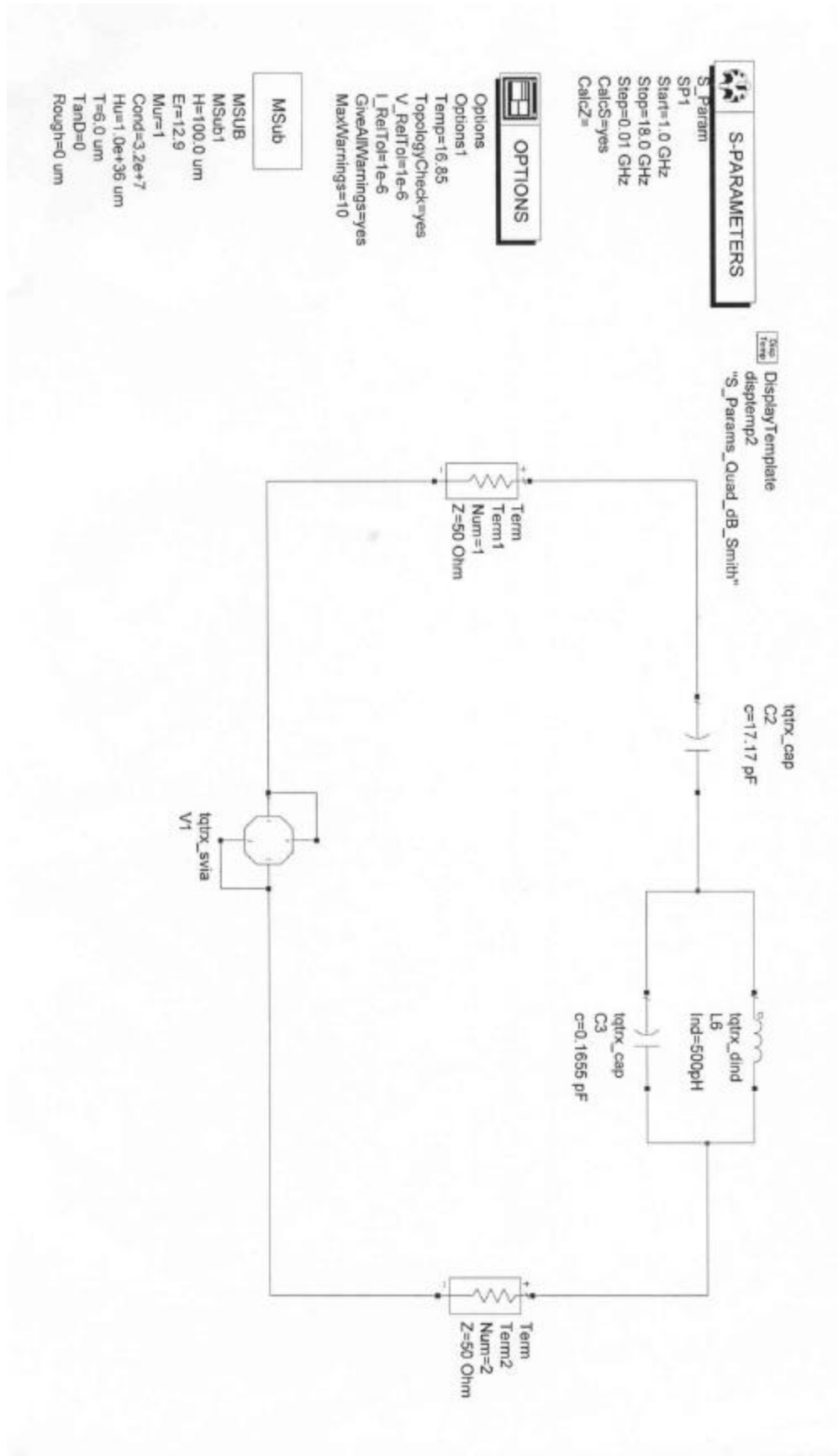
6E

Plot # 4. Schematic # 5. Class F Parallel Fundamental Frequency Resonant Tank Test Bed



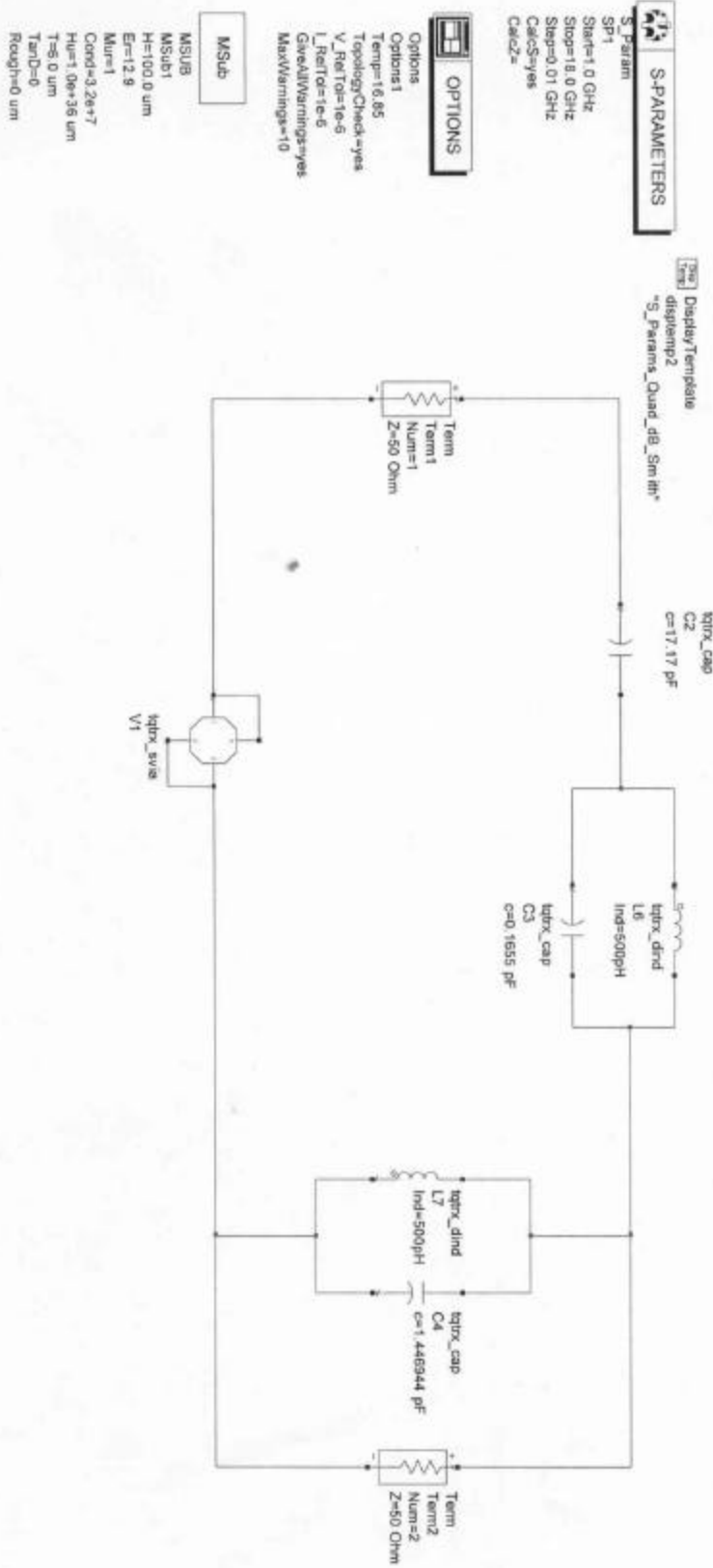
6F

Plot # 5. Schematic # 6. Class F Series 3Rd Harmonic of Fundamental Resonant Tank Test Bed



6G

Plot # 6. Schematic # 7. Class F Series and Parallel Resonant Tank Test Bed



6H

Plot # 7. Schematic # 8. Class F Pre-Amplifier GFET S22 and S11 S-Parameter Simulations

VAR
VAR1
VDS =7.0 V
VGS =-0.5 V

Display/Template
diaplenp2
_Params_Quad_db_Smith

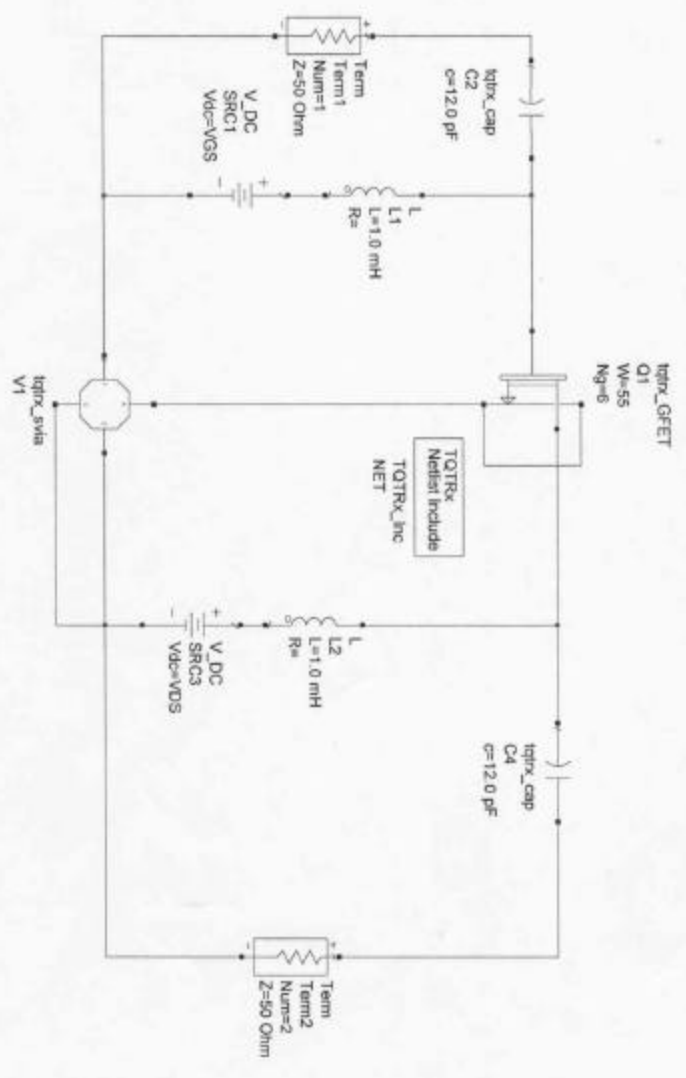
S-PARAMETERS

S_Param
SP1
Start=1.0 GHz
Stop=18.0 GHz
Step=0.01 GHz
CalcS=yes
CalcZ=

OPTIONS

Options
Options 1
Temp=16.85
TopologyCheck=yes
V_RetTol=1e-6
L_RetTol=1e-6
GiveAllWarnings=yes
MaxWarnings=10

MSub
MSUB
MSub1
H=100.0 um
E=12.9
Mur=1
Cond=3.2e+7
Hnr=1.0e+35 um
T=8.0 um
TanD=0
Rough=0 um



6J

Plot # 8. Schematic # 9. Class F Post Amplifier GFET S22 and S11 S-Parameter Simulations

VAR
VAR1
VDS =7.0 V
VGS =-1.5 V

DisplayTemplate
displaymp2
_S_Paramns_Quad_db_Smith

TOTRx
Nellist Include
TOTRx_inc
NET
W=-120
Ng=5

igfex_cap
C2
c=12.0 pF

MSub

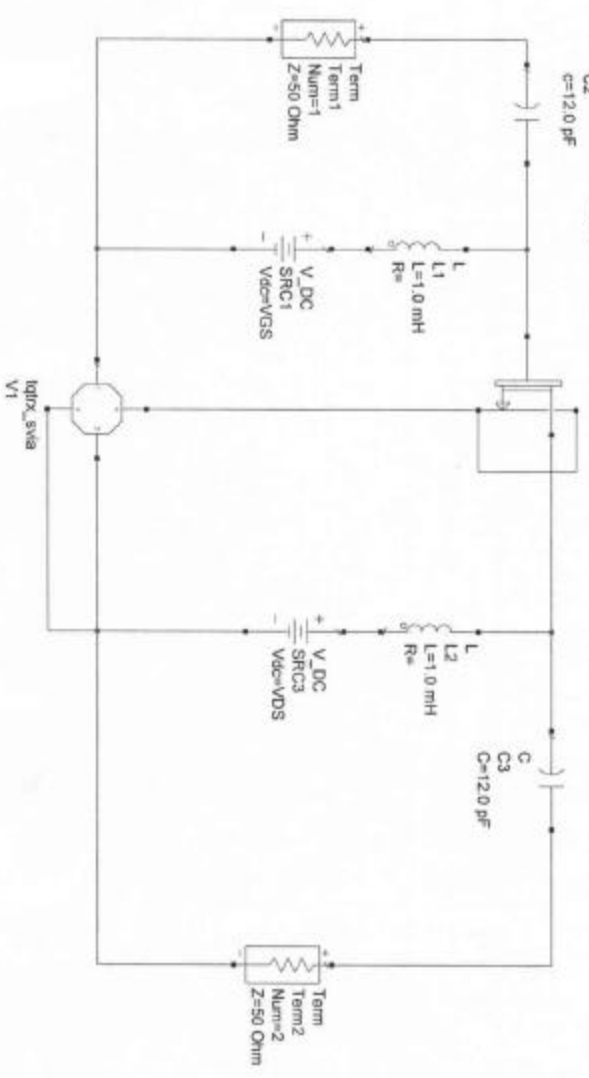
MSub
MSUB
MSUB1
H=1000.0 um
E=12.9
MUr=1
Conds=3.2e+7
HUr=1.0e+38 um
Tand=0
Rough=0 um

S-PARAMETERS

S_Param
SP1
Start=3.0 GHz
Stop=18.0 GHz
Step=0.01 GHz
CalcS=Yes
CalcZ=

OPTIONS

Options
Options1
Temp=16.85
TopologyCheck=yes
V_ReitDol=1e-6
L_ReitDol=1e-6
GiveAllWarnings=yes
MaxWarnings=10



Plot # 9. Schematic # 10. Class F Rcripp Output Matching Circuit to Post Amplifier
 720.0 um (N = 6, W = 120) GFET S22 S-Parameters

S-PARAMETERS

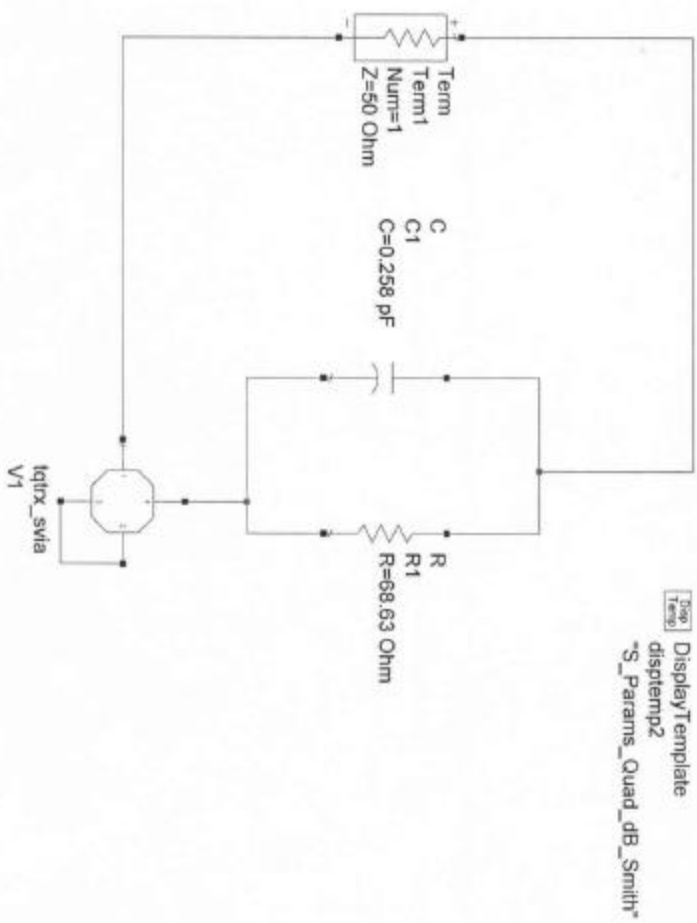
S_Param
 SP1
 Start=1.0 GHz
 Stop=18.0 GHz
 Step=0.01 GHz
 CalcS=yes
 CalcZ=
 CalcNoise=yes

OPTIONS

Options
 Options1
 Temp=16.85
 TopologyCheck=yes
 V_ReITol=1e-6
 I_ReITol=1e-6
 GiveAllWarnings=yes
 MaxWarnings=10

MSub

MSub
 MSub1
 H=100.0 um
 Er=12.9
 Mur=1
 Cond=3.2e+7
 Hu=1.0e+36 um
 T=6.0 um
 TanD=0
 Rough=0 um



6k

Plot # 10. Schematic # // Class F Rcripp Output Matching Circuit to Post Amplifier
 720.0 (n = 6, W = 120) GFET S22 S-Parameters

S-PARAMETERS

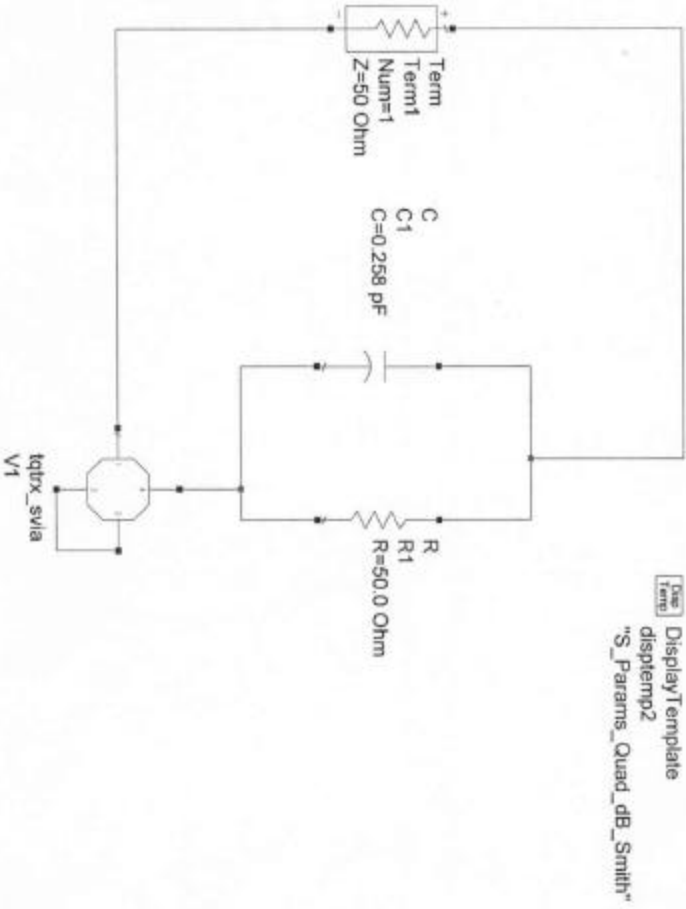
S_Param
 SPl
 Start=1.0 GHz
 Stop=18.0 GHz
 Step=0.01 GHz
 CalcS=yes
 CalcZ=
 CalcNoise=yes

OPTIONS

Options
 Options1
 Temp=16.85
 TopologyCheck=yes
 V_ReITol=1e-6
 L_ReITol=1e-6
 GiveAllWarnings=yes
 MaxWarnings=10

MSub

MSUB
 MSub1
 H=100.0 um
 Er=12.9
 Mur=1
 Cond=3.2e+7
 Hu=1.0e+36 um
 T=6.0 um
 Tand=0
 Rough=0 um



62

Plot # 11. Schematic # 12. Class F Rcripp Output Matching Circuit to Post Amplifier
 720.0 um (N = 6, W = 120) GFEET S22 S-Parameters

S-PARAMETERS

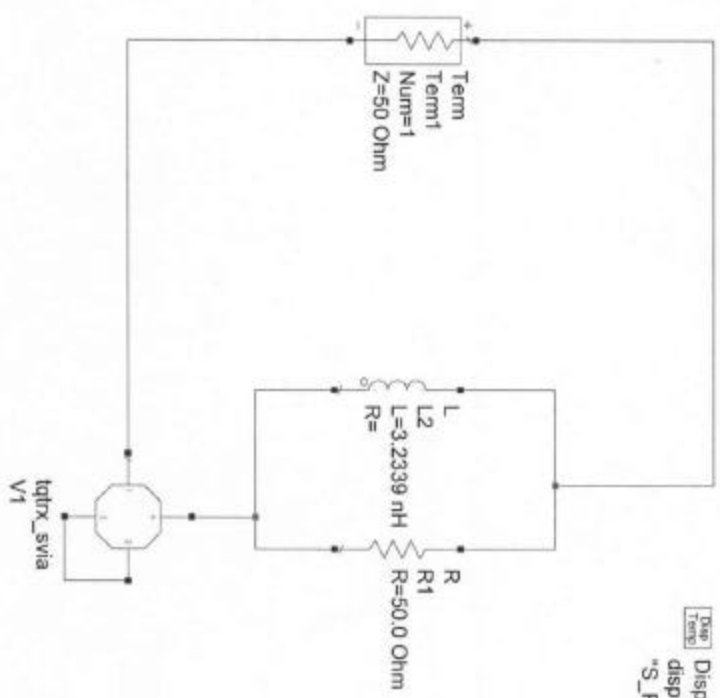
S_Param
 SP1
 Start=1.0 GHz
 Stop=18.0 GHz
 Step=0.01 GHz
 CalcS=yes
 CalcZ=
 CalcNoise=yes

OPTIONS

Options
 Options1
 Temp=16.85
 TopologyCheck=yes
 V_RelTol=1e-6
 L_RelTol=1e-6
 GiveAllWarnings=yes
 MaxWarnings=10

MSUB

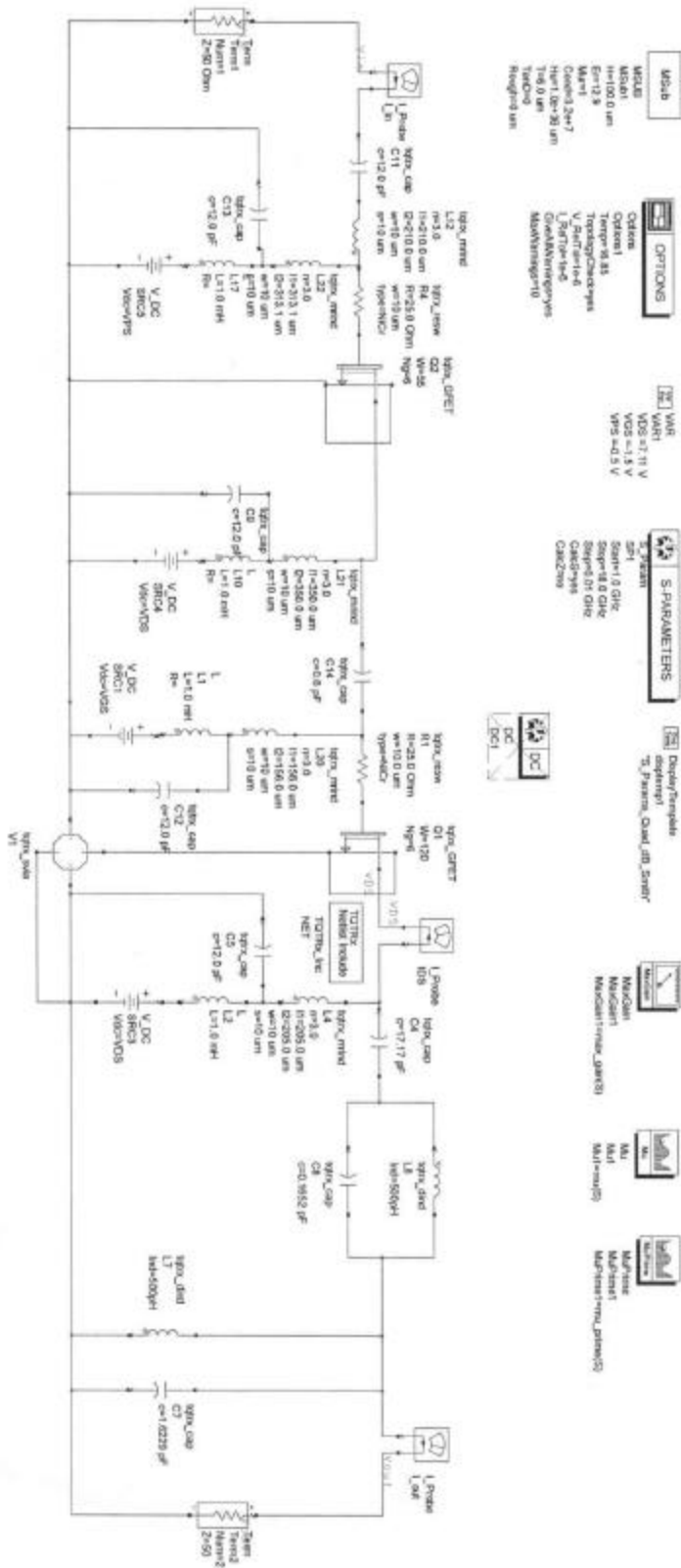
MSUB
 MSUB1
 H=100.0 um
 Er=12.9
 Mur=1
 Cond=3.2e+7
 Hu=1.0e+36 um
 T=6.0 um
 TanD=0
 Rough=0 um



Temp
 DisplayTemplate
 dispstemp2
 "S_Params_Quad_dB_Smith"

6M

Plot # 12. Schematic # 13. Pre-Layout Class F, 720.0 um (N = 6, W = 120) Power Amplifier with 330.0 um (N = 6, W = 55) Pre-Amp



Model

- Model: h=100.0 um
- Er=12.9
- Material: Cu
- Class: 2+1
- H=1.0e-20 um
- T=1e-20 um
- TempCo: 0
- Temp: 300 K
- Topology: 2D
- V: 2D
- Grid: 100 um
- Material: h=100.0 um
- TempCo: 0
- Temp: 300 K
- Topology: 2D
- V: 2D
- Grid: 100 um

Options

- Options: 1
- Topology: 2D
- V: 2D
- Grid: 100 um

Parameters

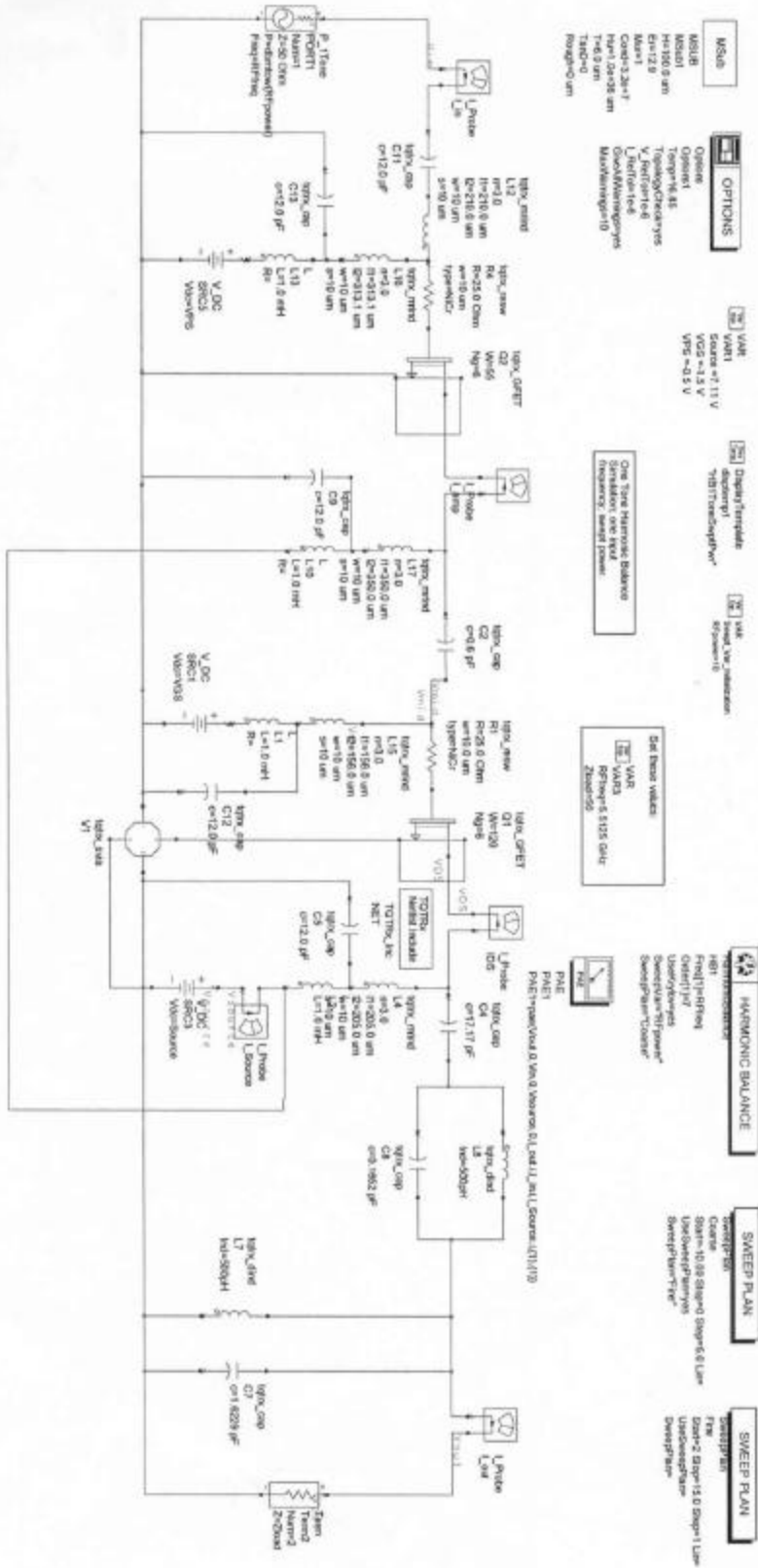
- Model: h=100.0 um
- Er=12.9
- Material: Cu
- Class: 2+1
- H=1.0e-20 um
- T=1e-20 um
- TempCo: 0
- Temp: 300 K
- Topology: 2D
- V: 2D
- Grid: 100 um

DC

- DC: 1

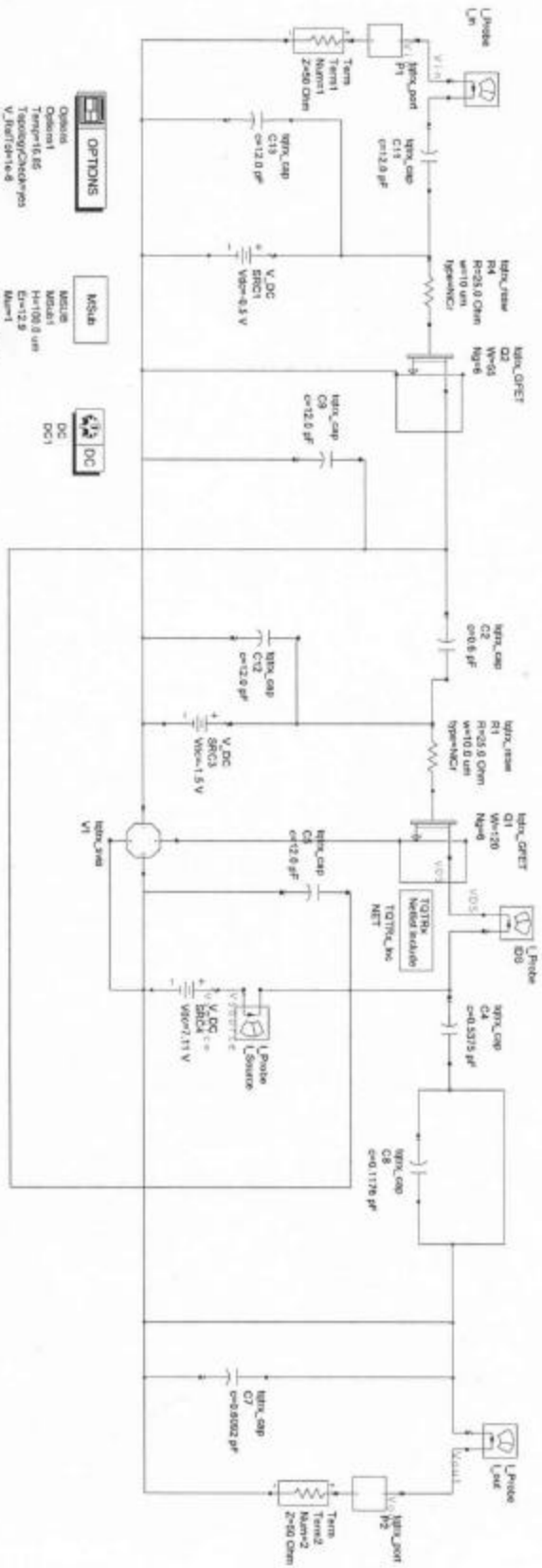
6N

Plot # 13. Schematic # 14. Pre-Layout Class F, 720.0 um (N = 6, W = 120) Power Amplifier with 330.0 um (N = 6, W = 55) Pre-Amp
 Harmonic Balance Simulations



6P

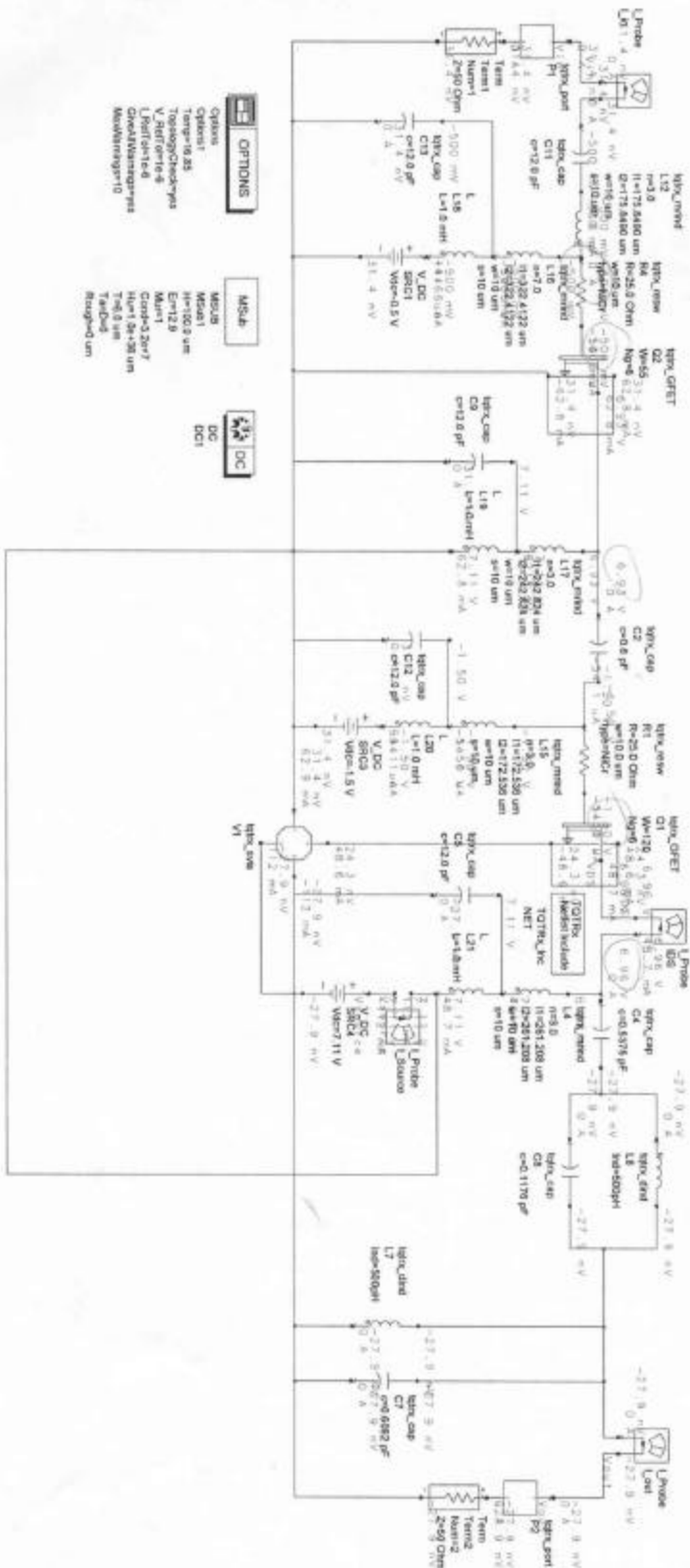
Plot # NonE Schematic # 15 Final Layout (Simplified Schematic) Component Values of Class F, 720.0 um (N = 6, W = 120) Power Amplifier with 330.0 um (N = 6, W = 55) Pre-Amp



- OPTONS**
- Options1
 - Options2
 - Options3
 - Options4
 - Options5
 - Options6
 - Options7
 - Options8
 - Options9
 - Options10
- MSUB**
- MSUB1
 - MSUB2
 - MSUB3
 - MSUB4
 - MSUB5
 - MSUB6
 - MSUB7
 - MSUB8
 - MSUB9
 - MSUB10
- DC**
- DC1
 - DC2
 - DC3
 - DC4
 - DC5
 - DC6
 - DC7
 - DC8
 - DC9
 - DC10

69

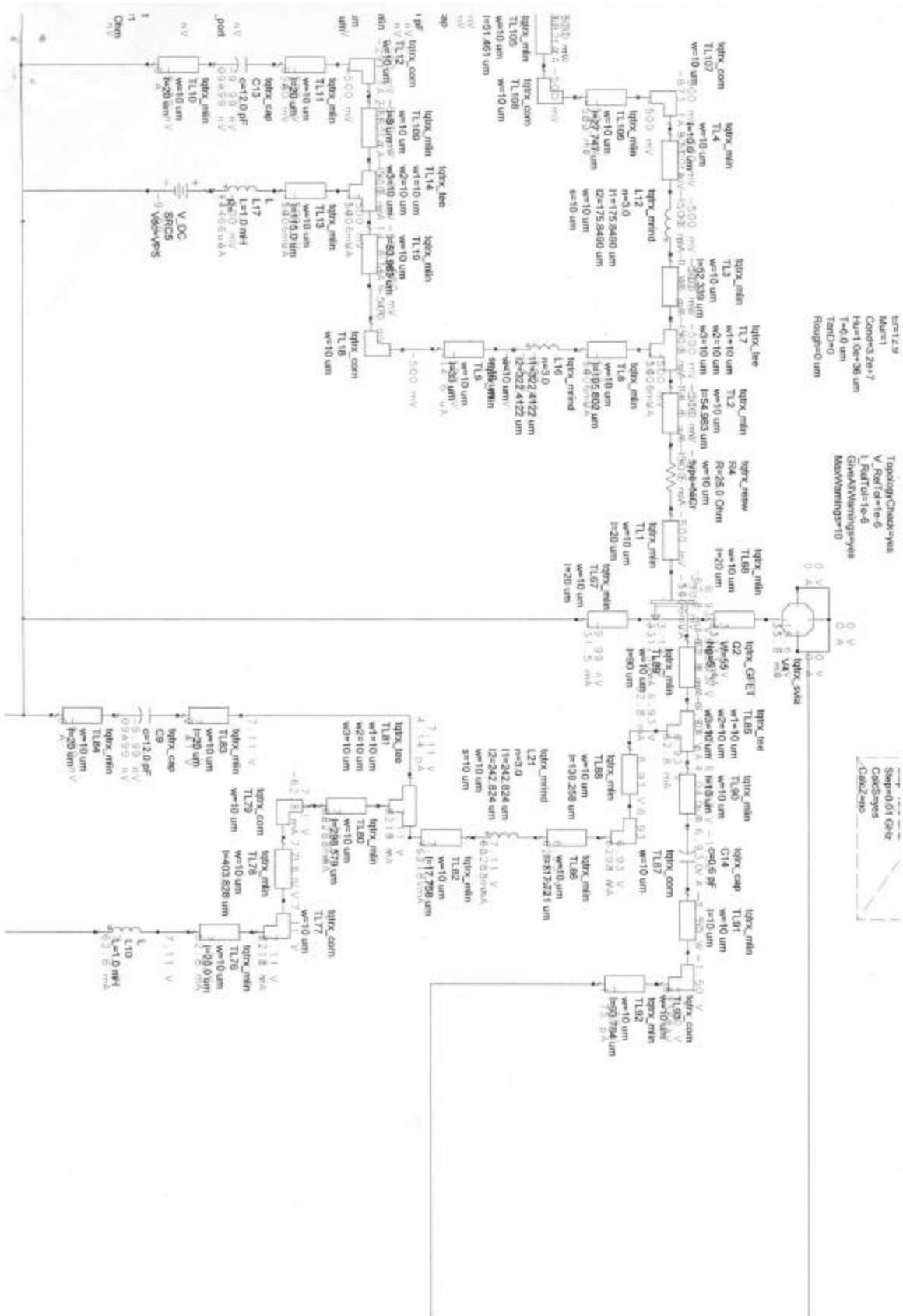
Plot # *None* Schematic # *16*. Final Layout (Simplified Schematic) Component Values of Class F, 720.0 um (N = 6, W = 120) Power Amplifier with 330.0 um (N = 6, W = 55) Pre-Amp



6R

Plot #18. Pre-Amplifier DC Simulation

19



5. DC ANALYSIS

SIMPLIFIED DC SCHEMATIC (No microstrip or inductors) – Schematic #15 on page 6Q is a “simplified” final layout schematic in-which all inductors were shorted. This, to see if any DC shorts existed but had not been previously noted. From Schematic #15, a possible problem found was a shorted C7 in the output resonant network. While this would not affect operation of this cascade Class-F power amplifier, it would affect a follow-on circuit without DC blocking on its input. No other possible problems were found.

BIAS CHECK – Schematic #16 on page 6R is a “simplified” final layout schematic on which fixed DC supplies were used and a DC bias simulation was performed. Schematics #17 and #18 on pages 6S and 6T are partial close-ups from DC bias simulations for the final layout shown in Schematic #4 on page 6D. VDS drain voltages for both GFET amplifier stages were designed to be +7.0V.

Comparisons between of these three schematics show losses for VDS from TriQuint inductors. DC simulations with a VDS supply voltage of 7.11 V gave a VDS of 6.96 V (loss of 0.15 V) for the post-amplifier and 6.93 V (loss of 0.18 V) for the pre-amplifier. It should be noted that the presence or absence of mlin components did change VDS drain voltages in these simulations.

INTERCONNECT AND COMPONENT DC CURRENT STRESS – Referring to Schematics #16, #17 and #18 on pages 6R, 6S and 6T; simulated IDS current draw from the common VDS supply for both GFETs was approximately 112.0 mA for a supply voltage of +7.11 VDC (approximately 0.8 Watts of DC power). From class it was given that TriQuint inductors could handle 27.0 mA/ μm , or a margin of 270.0 mA for 10.0 μm inductor trace widths. IDS bias current drawn by the Class-A pre-amplifier was approximately 62.8 mA through L17, and IDS bias current drawn by the Class-AB post-amplifier was approximately 48.7 mA through L4. These IDS currents drawn through their respective drain circuit inductors are < 270.0 mA.

From Plots #13B and #15B on pages 5N and 5Q respectively, it does not appear that this DC bias point is shifting appreciably due to the 25.0 Ohm de-Q'ing resistors, R1 and R4, on the gates of the pre- and post-amplifier GFETs shown in Schematic #1, on page 6A.

The VGS supplies draw approximately 14.6 μA through L16 for the -0.5 VGS supply and 54.1 μA through L15 for the -1.5 VGS supply, or 7.3 μWatts and 81.15 μWatts respectively. Both DC bias currents drawn for respective VGS supplies are << 270.0 mA.

6. TEST PLAN

TEST EQUIPMENT LIST

2-port S-parameters tests across frequency range of 1.0 to 18.0 GHz:

1. Agilent 8510 Network Analyzer;
2. S-Parameter test set and flexible test cables;
3. 2 ea., 150.0 μm pitch, G-S-G test probes;
4. 2 ea. test fixtures to hold G-S-G probes;
5. 2 ea. G-S-G test probe to SMA adapter connectors;
6. LRM calibration card;
7. Cleaning/flatness test card;
8. 4 ea. Picoprobe DC pin probes;
9. Microscope test bench with chuck to hold test die;
10. 3 ea. Variable power supplies for outputs of -0.5, -1.5 and 7.11 VDC;
11. VOM meter.

Power gain, 1.0 dB Compression Point, and PAE determinations at 5.5125 GHz:

1. #3 through #11 above plus a 3.0 dB or 6.0 dB SMA attenuator if power amplifier output exceeds input power level of spectrum analyzer;
2. Agilent spectrum analyzer.
3. Agilent frequency synthesizer.

PARAMETERS TO BE TESTED --

1. VSWR, 2-port,
2. S-Parameters, 2-port,
3. Bandwidth, 3.0 dB points,
4. Small Signal Gain,
5. Power Input and Output at the 1.0 dB Compression Point,
6. Power gain,
7. “Under load” DC voltage and current measurements,
8. PAE.

SIMULATION RESULTS FOR MEASUREMENT COMPARISON –

PARAMETER	PRE-LAYOUT	FINAL LAYOUT
PAE	20.51	23.82
Output 1.0 dB Comp. Pt., dBm	24.49	25.26
Power Gain, dB	14.21	14.71
Ctr. Freq. S11, dB	-22.99	-28.23
Ctr. Freq. S22, dB	-23.05	-22.47
Ctr. Freq. Input VSWR	1.15:1	1.08:1
Ctr. Freq. Output VSWR	1.15:1	1.16:1
Ctr. Freq. S21 Small Signal Gain, dB	13.32	13.61
VDS, V	7.11	7.11
VGS_A (Pre-Amp), V/ μ A	-0.5/14.6	-0.5/14.6
VGS_B (Post-Amp), V/ μ A	-1.5/54.1	-1.5/54.1
IDS_A (Pre-Amp), mA	62.8	62.8
IDS_B (Post-Amp), mA	48.7	48.7

TEST CONFIGURATIONS --

- A. For 2-port S-parameter and bandwidth tests from 1.0 to 18.0 GHz; refer to final layout Plot #16, Test Set-Up #1, on page 5R.
- B. For power gain and 1.0 dB compression point tests at 5.5125 GHz; refer to final layout Plot #17, Test Set-Up #2, on page 5S.

7. CONCLUSIONS & RECOMMENDATIONS

Cascade Class-F power amplifier operation and almost all stated performance specifications were obtained. The one exception was the required specification of ± 0.5 dB Max for gain flatness. Because of the output resonant network required for Class-F amplifier operation, roll-off from the low-pass filter action of this output network exceeded ± 0.5 dB Max for gain flatness. This roll-off can be seen in Plot #12B on page 5M, and again in Plot #14B on page 5P

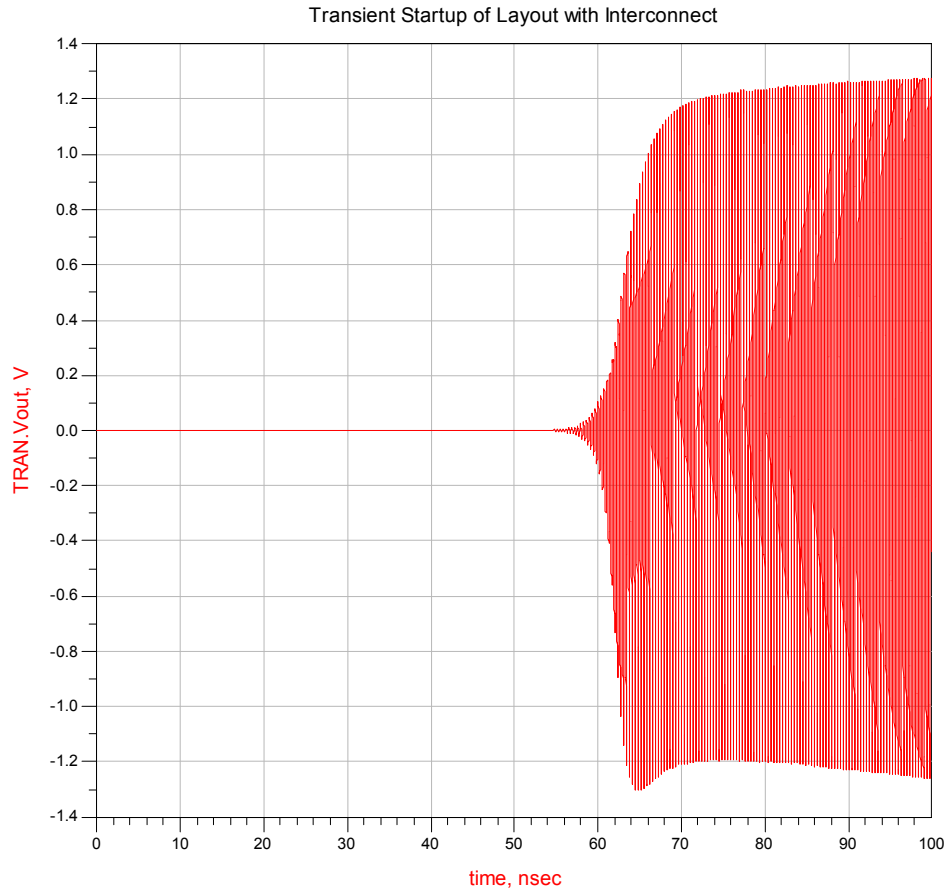
With regard to improvements in PAE, adjustments and/or changes to the matching network located between the amplifier stages could possibly reduce IDS current draw and DC power requirements from the VDS supply for both amplifier stages. Another possible change would be the use of self-biasing on the Class-A amplifier stage. Use of self-biasing on the Class-AB post-amplifier would interact with the output resonant network. These changes will be tested in future Class-F amplifier designs.

Overall, this cascade Class-F amplifier design followed theory and design given in references [1, 2, 3, 4, 5, 6]. The most time consuming aspects in this design were with inter-actions experienced from adjustments made to the input matching network and the matching network between the amplifier stages. Small changes to achieve one design specification would result in major changes in another design specification. Adjustments made to the output matching and resonant network did not have such dramatic effects on circuit operation. Future designs will explore other methods for biasing and matching networks in a cascaded amplifier design.

8. REFERENCES

- [1] Frederick H. Raab, “**Class-F Power Amplifiers with Maximally Flat Waveforms,**” IEEE Transactions on Microwave Theory and Techniques, Vol. 45, No. 11, November 1997, pp.2007-2012.
- [2] Chris Trask, “**Class-F Amplifier Loading Networks: A Unified Design Approach,**” 1999 MTT-S International Microwave Symposium Digest 99.1 (1999 Vol. 1 [MWSYM]): 351-354 Vol. 1.
- [3] William S. Kopp, “**High Efficiency Power Amplification for Microwave and Millimeter Frequencies,**” 1989 MTT-S International Microwave Symposium Digest 89.3 (1989 Vol. III [MWSYM]): 857-858.
- [4] Bernhard Ingruber, “**Reliability and Efficiency Aspects of Harmonic-Control Amplifiers,**” IEEE Microwave and Guided Wave Letters, Vol. 9, No. 11, November 1999.
- [5] Craig Moore and John Penn, **525.787 Microwave Monolithic Integrated Circuit (MMIC) Design,** Johns Hopkins University, Class Notes and Handouts, Fall 2001.
- [6] **Analysis and Design of Analog Integrated Circuits, Second Edition,** Paul R. Gray and Robert G. Meyer Copyright 1977 and 1984, ISBN 0-471-87493-0.

An S – Band, 0.6- μm GaAs, Voltage Controlled Oscillator



Gary Levy & Steve Williams

Johns Hopkins University

MMIC Design

525.787

12/17/01

I. Summary

An approach for the design of an S-Band Voltage Controlled Oscillator (VCO) for application in HyperLAN and ISM systems implemented in Triquint TQTRx 0.6- μm GaAs technology is presented. The VCO operates from 2596 MHz to 2893 MHz with output power ranging from 14.287 dBm to 12.259 dBm respectively. The VCO powered by a 5 Volt supply, features an on chip high Q resonator and tuning varactor controlled with a 0 to 5 Volt variable supply. The VCO has been used in the design of a frequency converter for a C-band HyperLAN simplex transceiver.

II. Introduction

A. Circuit Description

A simplex MMIC transceiver implemented in the Triquint TQTRx process (4 mil thick GaAs) with simulation and layout in Agilent ADS (ADS version 150) has been designed for C-Band HyperLAN wireless local area network (WLAN) and industrial, scientific, and medical (ISM) frequency applications.

The system utilizes a C-Band Up-Down Converter with a 275MHz intermediate frequency (IF) that can be down-converted to baseband with a second 275MHz local oscillator (LO). The second LO is upconverted to the C-Band in TX mode and modulation can be introduced onto the second LO or through direct frequency modulation of the VCO in the transceiver. The dual band usage VCO with high side or low side (HSLO/LSLO) injection to the mixer is specified for operation from 2712 MHz to 2813 MHz, which when doubled is between the WLAN and ISM frequencies.

Receive and transmit signals are routed by C-Band single-pole-double-throw (SPDT) switches. The receive chain consists of a cascaded low noise amplifier (LNA) and post amplifier. The transmit path employs a variable gain amplifier for level control and a driver amplifier preceding a 0.25 Watt power amplifier.

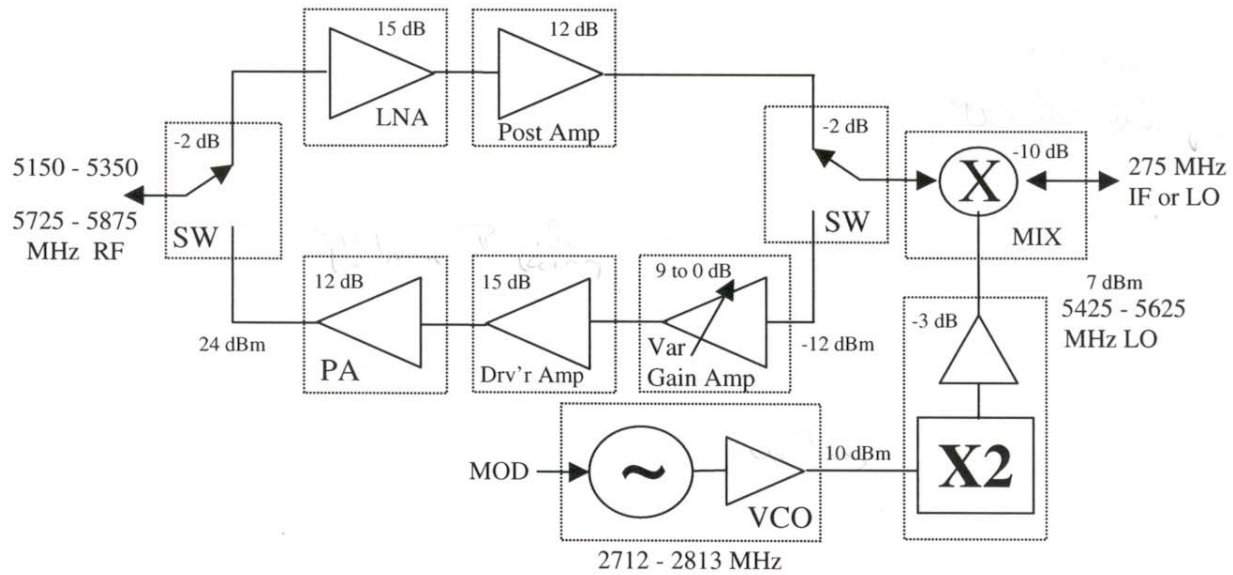


Figure 1. Chip-Set for the 5150 – 5350 MHz WLAN and 5725 – 5875 MHz ISM Bands.

The 5 Volt powered, 0 to 5 Volt voltage controlled oscillator, as shown in Fig. 2, operates from 2596 MHz to 2893 MHz with output power ranging from 14.287 dBm to 12.259 dBm respectively, while occupying only a 60 x 60 mil Anachip area. The VCO features a self-biased, $W=50\mu\text{m}$, $N=6$, TQTRx_DFET with an active current source utilizing a gate to source tied inductor for frequency dependent gain control which minimizes higher order harmonic components at the output. Common-source capacitive feedback is employed in the design to satisfy the required oscillation criteria with a series resonance applied at the gate of the VCO FET. The required output power is achieved by a $W=70\mu\text{m}$, $N=8$ source follower output stage.

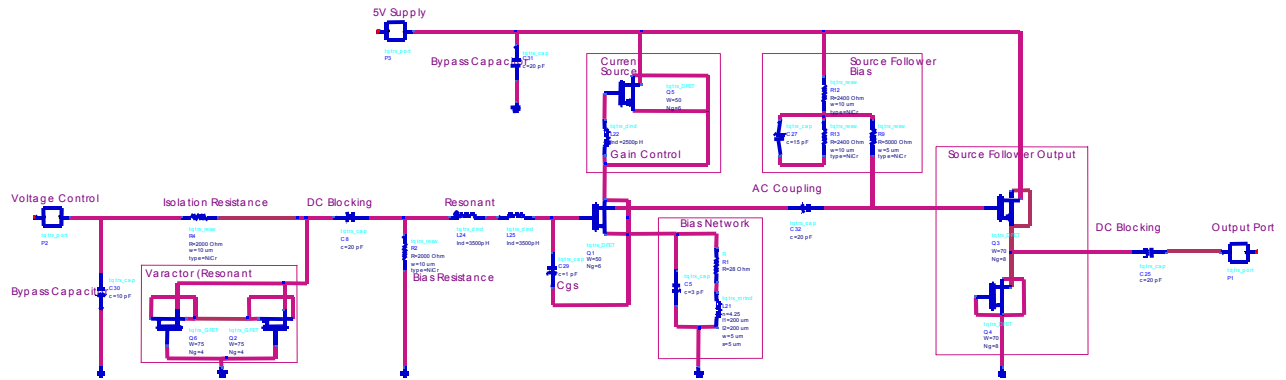


Figure 2. VCO Block Diagram.

B. Design Philosophy

The VCO architecture is based upon small signal negative impedance theory where the active circuit is represented by the impedance,

$$Z_a = R_a + jX_a$$

and the load circuit as

$$Z_1 = R_1 + jX_1$$

as shown in Fig. 3. Assuming that a steady state oscillation is occurring between the two networks then there must exist a loop current, I , that is non-zero. Using Kirchoff's law, the total loop voltage then must be zero which yields

$$Z_a + Z_1 = 0.$$

It can therefore be observed that

$$Z_a = -Z_1 \text{ (negative impedance)}$$

to ensure oscillation and hence the nomenclature of the theory and design technique. Furthermore, in small signal design, the imaginary portion of this relation is of particular interest and thus

$$X_a + X_1 = 0.$$

The large signal operation of a FET oscillator can then be predicted from its small signal characteristics since as the signal grows to steady state, the actual change of the imaginary portion of the active circuit is small.

The differential change in the active circuit impedance versus the operating point amplitude and frequency delta variations as described by Kurokawa is then,

$$[dR_a/dA][dX_1/d\omega] - [dR_1/d\omega][dX_a/dA] > 0$$

where R_a is the active device's negative resistance, A is the steady state amplitude, and ω is the frequency. As stated earlier, the change in X_a with respect to amplitude is small and considered to be zero. However, for GaAs FET oscillators, R_a increases positively with respect to amplitude since the negative resistance of the circuit decreases in magnitude with increasing amplitude. Therefore applying these conditions, then

$$[dX_1/d\omega]_{\omega_0} > 0$$

which implies that stable oscillations are ensured when the reactive component of the load impedance has a positive slope versus frequency, and the frequency of the oscillation corresponds to the zero crossing of the frequency axis.

Additionally, it has been shown that for a series resonant oscillator that

$$|R_a| \sim \geq 3R_1$$

to approximate a power impedance match between the load circuit and the large signal steady state oscillations. The factor of 3 is itself a compromise based upon the experimental trade-off between start-up conditions and final oscillation frequency.

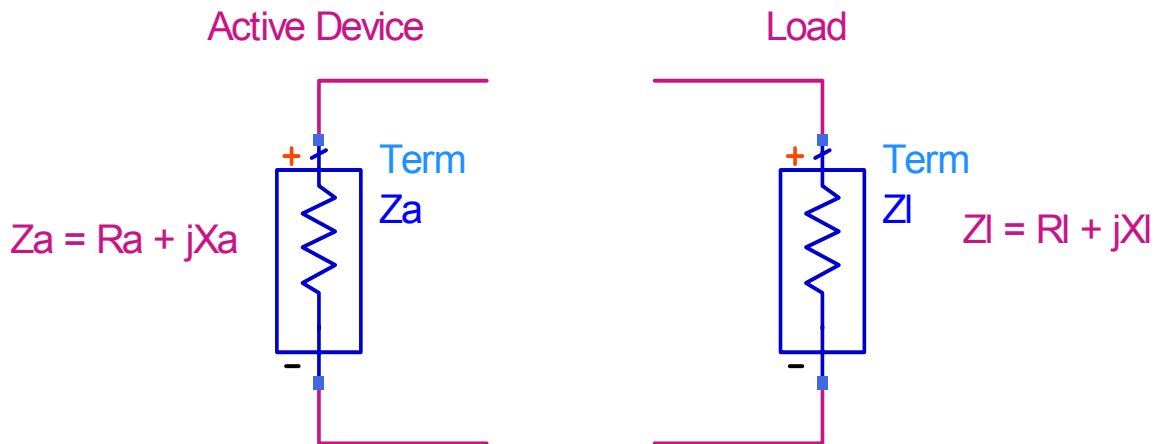


Figure 3. Conditions for oscillator startup.

To provide suitable output power for further amplification in a subsequent stage to achieve the output power specification, a $300\mu\text{m}$ ($W=50\mu\text{m}$, $N=6$) DFET (TQTRx DFET nonlinear model) was used to implement the oscillator and self-biased with a source resistor. The active current source is biased to provide $\sim 12\text{mA}$ to the oscillator FET and has an inductor tied between the gate and source to effect a rudimentary form of frequency dependent gain control. This is because at higher frequencies, the inductor opens up and tends to choke off current from the oscillating FET. This was added to help reduce the higher order harmonic component of the

output since otherwise the oscillations become limited. Additionally, the 5 Volt supply of the current source includes a 20pF bypass capacitor.

Common-source capacitive feedback sets the frequency of oscillation as given by

$$F_{osc} \cong [2\pi * \{L_r * (C_{VAR} || C_i)\}^{0.5}]^{-1}$$

where

$$C_i = (C_{gs} * C_f) / (C_{gs} + C_f)$$

and based upon start-up conditions, C_f was chosen to be 1pF.

The oscillator employs a series resonance at the gate to realize the negative resistance and was implemented as two 3500pH series inductors rather than one for ease of layout and tuning ability.

The Triquint varactor is implemented by two parallel 300 μ m ($W=75\mu$ m, $N=4$) GFET's with drain and source tied together and modeled as a parallel combination of a 0.04pF capacitor and a 5 Ω resistor in series with the tuning capacitor as shown in Fig. 4. (See Tuning Range in Fig. 5.) As a tuning voltage is increased on the tied drains, the depletion regions of the FET's are likewise increased. This causes an increase in the distance between the effective plates of the capacitor like structure and thus the capacitance decreases. A decrease in capacitance causes the oscillator to subsequently oscillate at a higher frequency with the converse true as well.

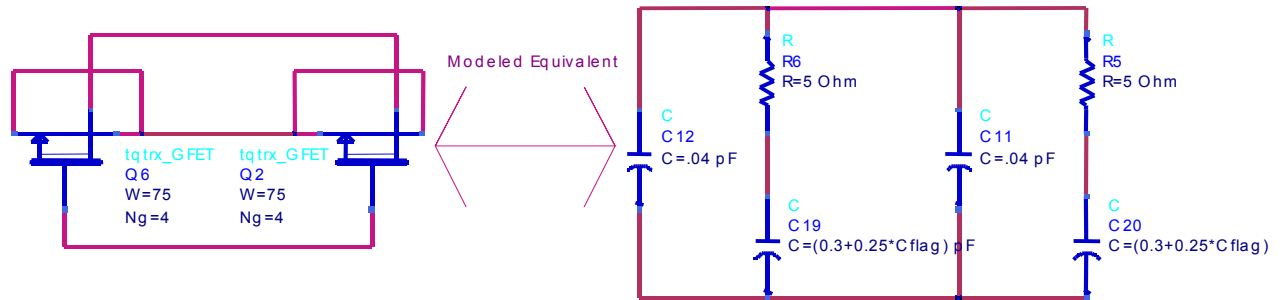


Figure 4. Varactor model.

Bias Voltage (V)	Tuned Capacitance (pF)
0	0.55
1	0.4
2	0.3

Figure 5. Single Varactor tuning range; 300 μ m ($W=75\mu$ m, $N=4$) GFET.

The input network also includes a series 20pF DC blocking capacitor, a 2K Ω resistor for isolation, and a 20pF bypass capacitor to filter power supply noise.

The oscillator FET is then AC coupled with a 20pF capacitor to a 560 μ m source follower output stage which provides the additional gain required for the output power specification. The source follower was implemented with a $W=70\mu$ m and $N=8$ DFET to support the large bias current required to meet and or exceed the greater than 10dBm output power goal. It is biased with a resistor divider network at the gate and a $W=70\mu$ m, $N=8$ DFET with gate tied to source. Additionally, the 5 Volt supply, which is applied to the resistor divider network, includes a 20pF bypass capacitor (same 5 Volt supply for the oscillator FET current source). A series 20pF capacitor was again added as a DC block at the output. The entire VCO architecture is illustrated in Fig. 2.

C. Trade-Offs

There were three major trade-off scenarios in the design of this VCO.

The first trade-off encountered was the inability to use an inductive load in the first stage of the VCO. This resulted from simulator convergence problems and rather than jeopardize the confidence level of the simulation results actually matching the fabricated circuit, the design was adapted to use a current source load so results could be better predicted with the simulator.

Design compromises were also made between the gain of the VCO and the contributions of harmonics at the output. The gain required to satisfy the start-up conditions was contrasted against the signal limiting occurring at the drain of the oscillator FET and at the output of the source follower stage, as signal compression resulted in an increased harmonic component in the output and decreased power efficiency.

Another compromise was made for the output match versus the power output. A smaller output device could have been used to match 50Ω since it could have been sized such that $1/g_m$ equaled 50Ω , but the design is current limited in driving the output. More current was thus run in the source follower stage to drive the output and it was deliberately chosen to not match the output to minimize power loss and save area.

III. Modeled Performance Specification Matrix

VCO with on chip high Q resonator and tuning varactor.

<i>Specification Description</i>	<i>Specification</i>	<i>Design Performance</i>	<i>Compliance</i>
Frequency	2712 - 2813MHz	2596 - 2893 MHz	Specification Achieved
Output Power	>+ 5dBm	14.287 - 12.259 dBm	Specification Achieved
Output Power Goal	+10dBm	14.287 - 12.259 dBm	Goal Achieved
Control Voltage	0 – 5 Volts	0 – 5 Volts	Specification Achieved
Supply Voltage	+/- 5 Volts	+5V	Specification Achieved
Supply Voltage Goal	+5V	+5V	Goal Achieved
Output Impedance	50Ω (nominal)	50Ω (nominal)	Specification Achieved
Size	60 x 60 mil ANACHIP	60 x 60 mil ANACHIP	Specification Achieved

Figure 6. Specification Compliance Matrix.

IV. Schematic Diagrams & Modeled Performance

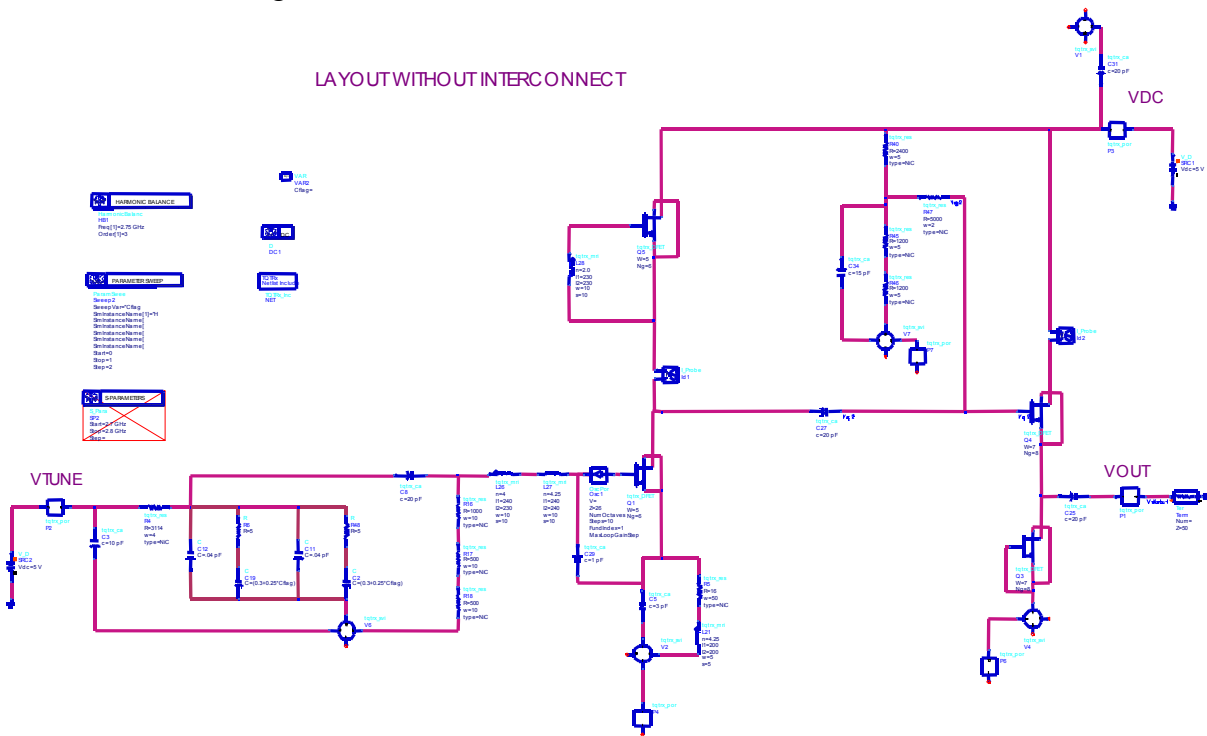
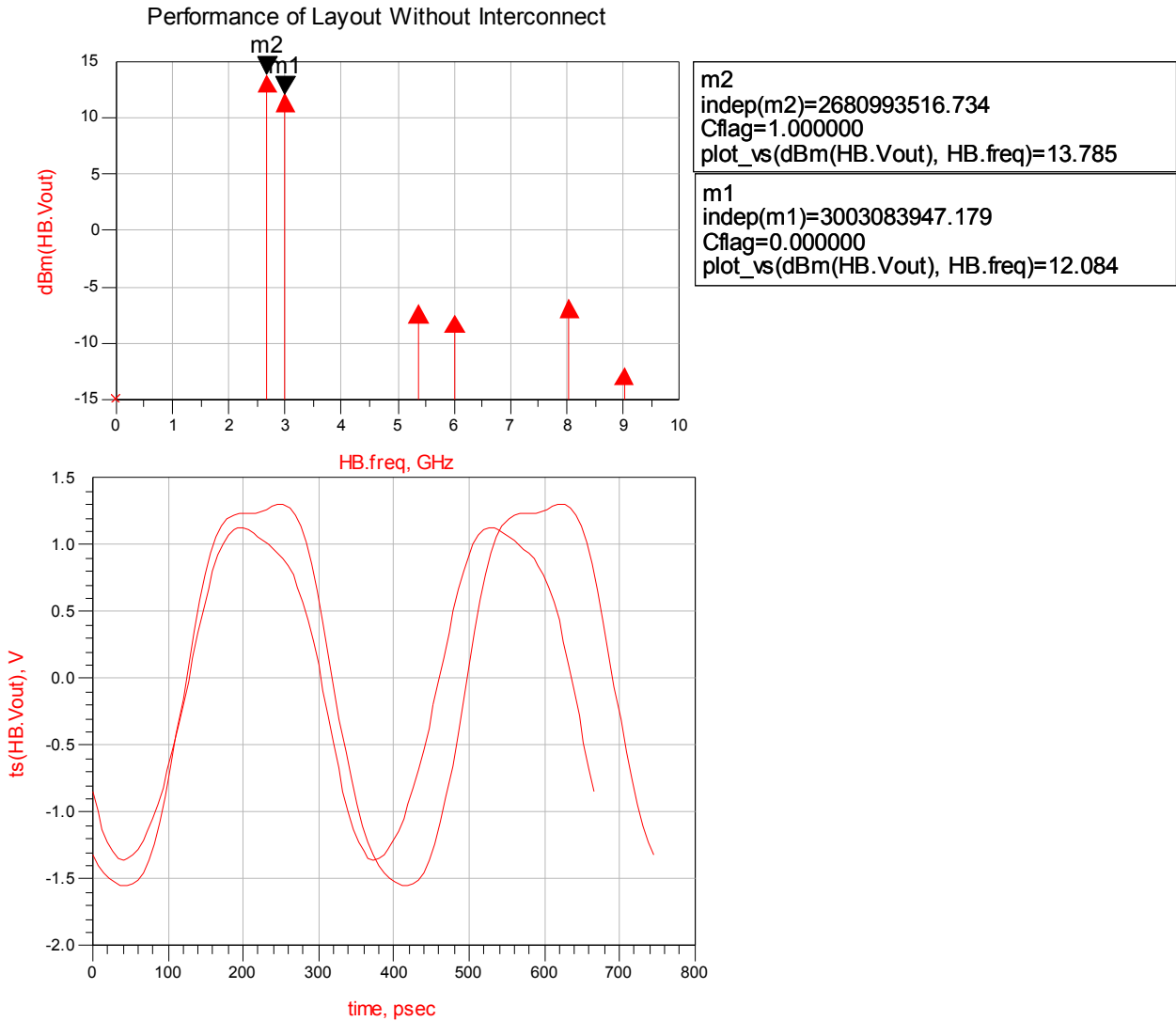


Figure 7. Pre-Layout: VCO Schematic without Interconnect.



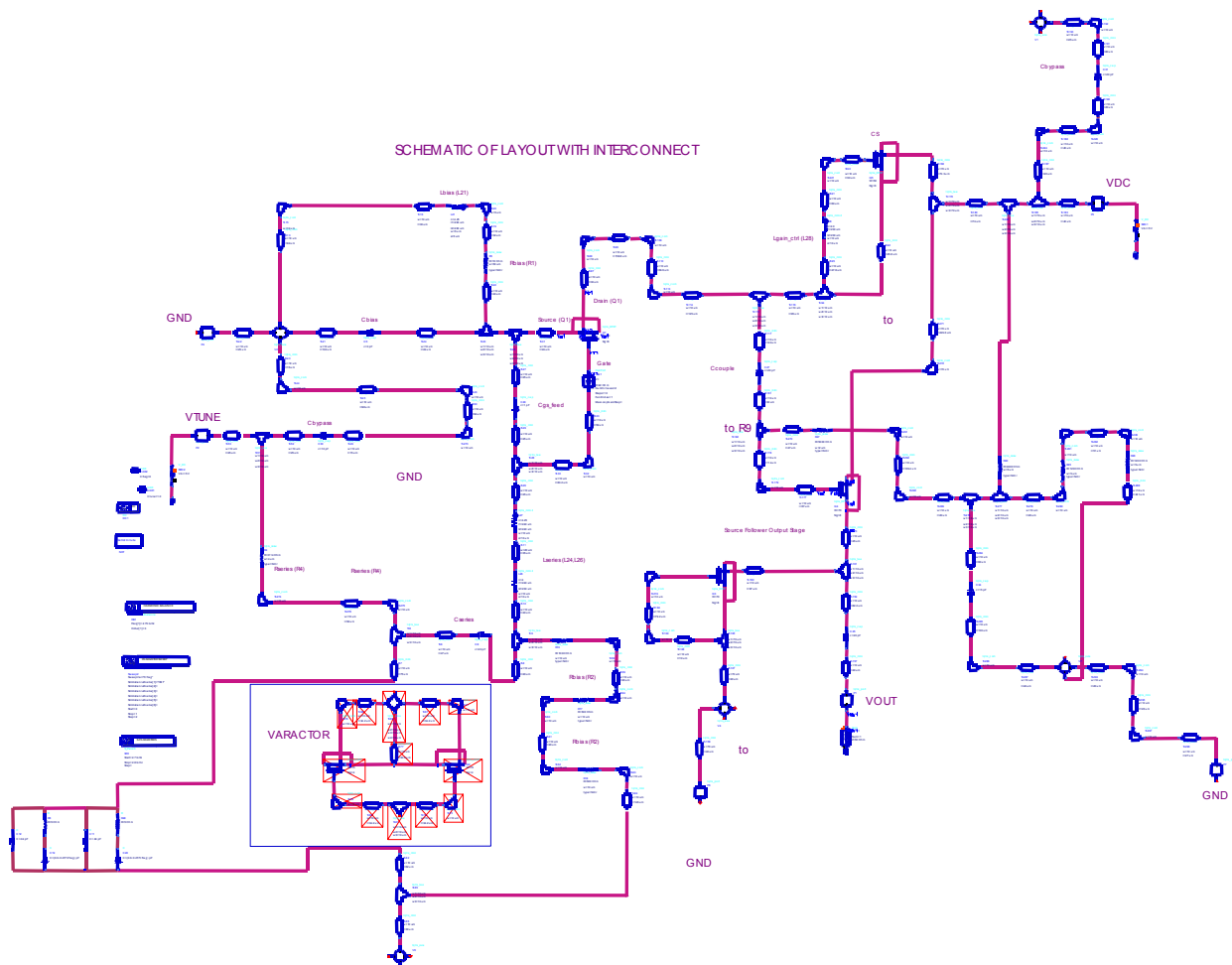


Figure 9. Post-Layout: VCO Schematic with Interconnect.

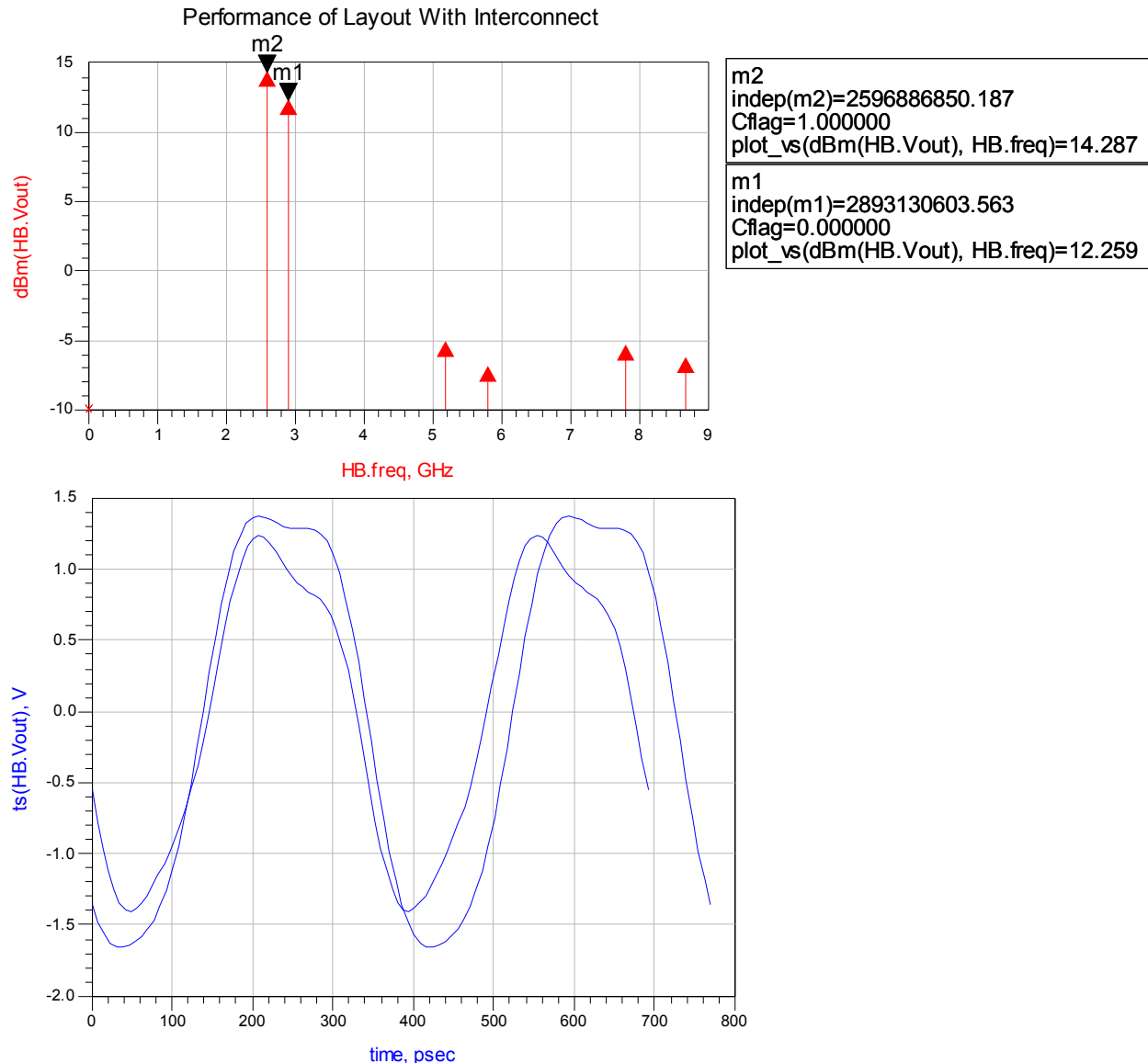


Figure 10. Post-Layout: VCO Performance with Interconnect.

When the results of an AC layout simulation with interconnect are examined as shown in Fig. 11, it can be seen that the VCO design satisfies both start-up conditions for steady state oscillation.

Marker M1 designates the real portion of the impedance looking into the resonant tank (Z_l ; the load resistance), whereas marker M2 is the real portion of the impedance looking into the gate of the oscillator FET (Z_a ; the negative active resistance). Note that the absolute value of the negative active resistance is approximately twice the value of the load resistance which is less than the factor of three desired. This is an effective compromise between gain and signal compression and still essentially satisfies the start-up condition where $|R_a| \sim \geq 3R_l$.

The minimum oscillation frequency occurs when the minimum control voltage (Cflag = 1.000) is applied and observed at marker M3 equal to 2.512GHz when the corresponding line crosses the frequency axis equivalent to $Z_a + Z_l = 0$. Conversely, when the maximum oscillation

frequency is applied (Cflag = 0.000), the maximum oscillation frequency is observed at M4 equal to 2.825 GHz. Note that the deviations in oscillation frequency as compared to previous simulation results are attributed to the differences in numerical solving methods between linear AC simulations and harmonic balance simulations.

Finally, observe that the top two unlabeled traces of Fig. 11 exhibit positive slopes for the imaginary portion of the impedance's looking into the resonant tank at both minimum and maximum control voltages (Cflag = 1.000, Cflag = 0.000) satisfying the condition where $[dX_1/d\omega]_{\omega_0} > 0$ is required.

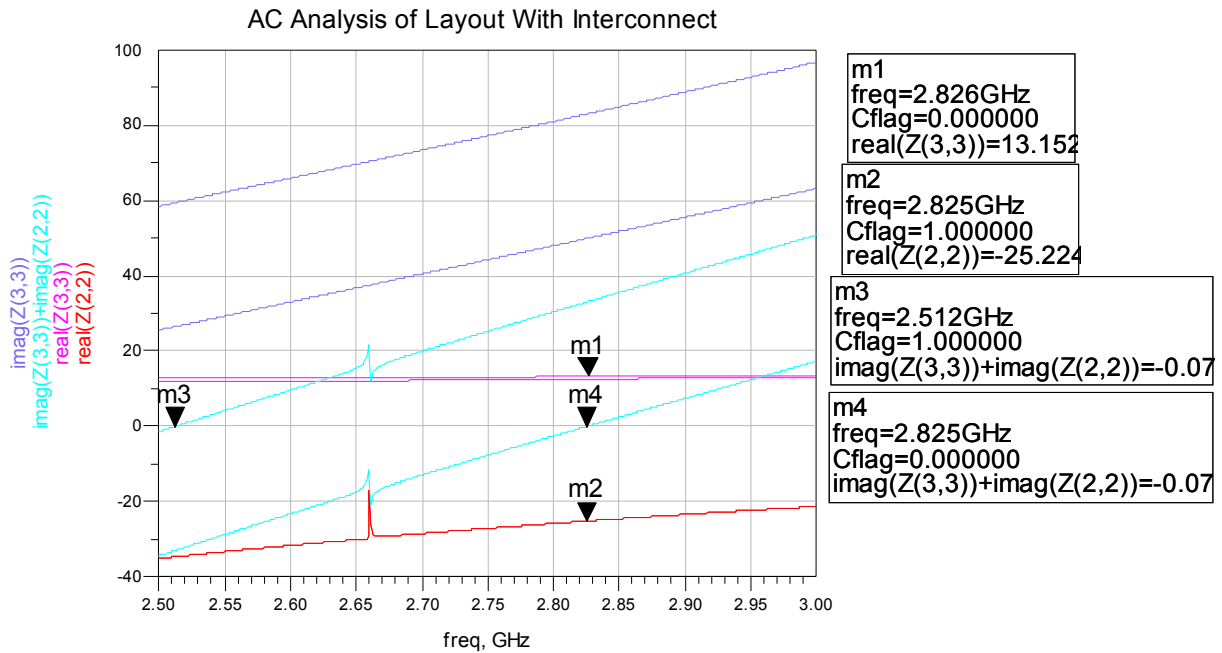


Figure 11. Post-Layout: AC Analysis of VCO with Interconnect.

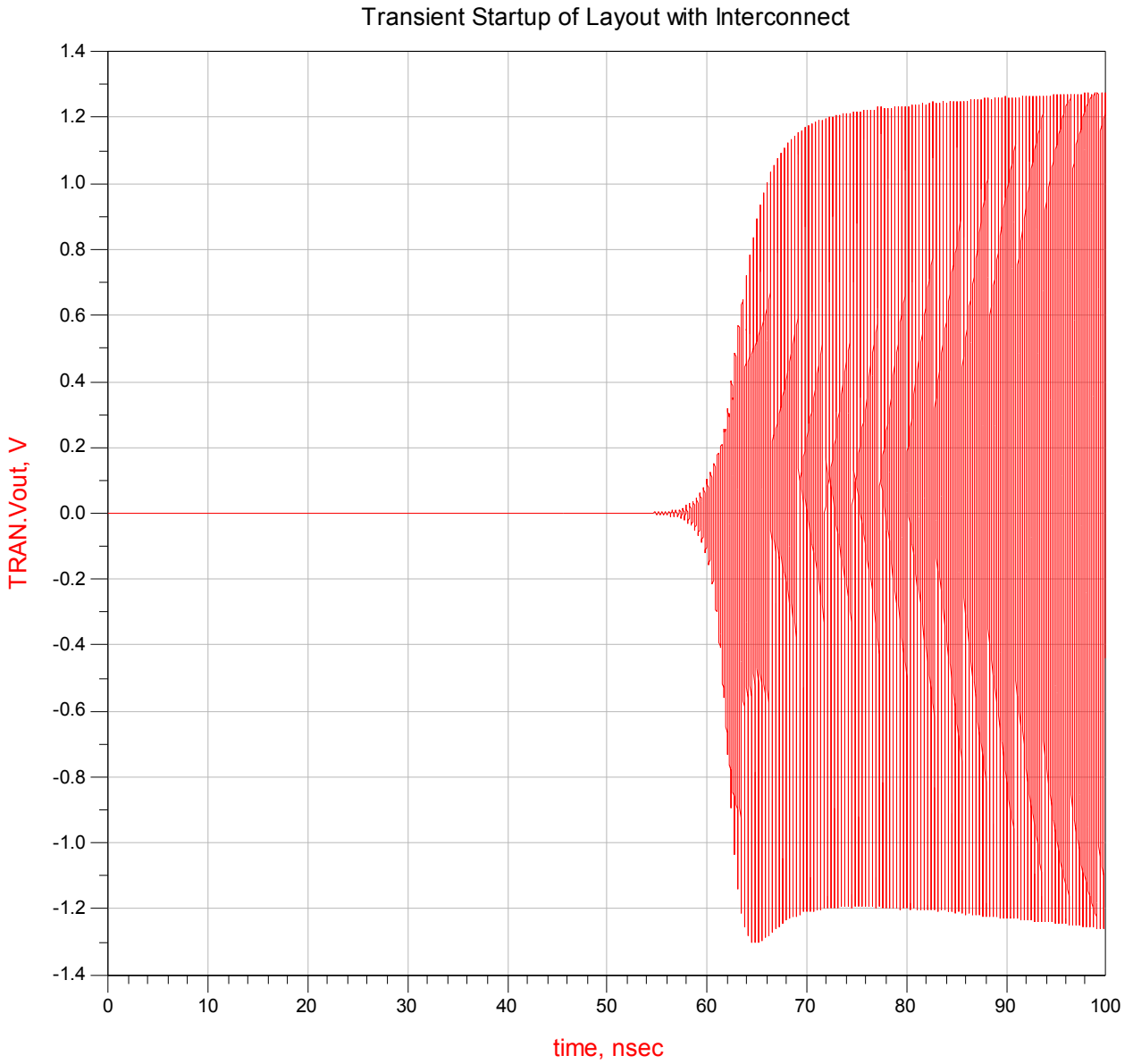


Figure 12. Post-Layout: Transient Analysis of VCO with Interconnect.

V. DC Analysis

A. Simplified DC Schematic

The original schematic without interconnect was edited such that all inductors were replaced with shorts and the capacitors opened, given that at DC, the frequency is zero. This is done to check for any inadvertent biasing shorts, shorting of the supplies, and to follow the biasing path.

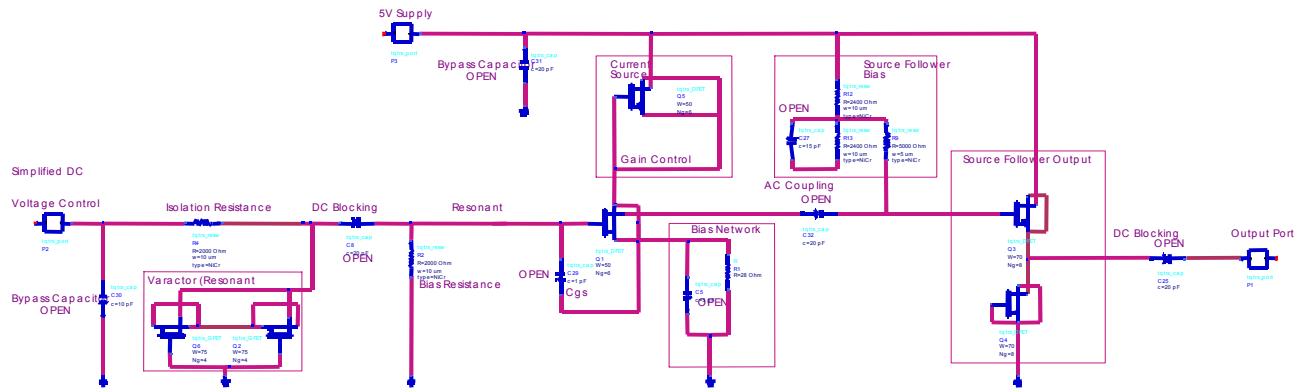


Figure 13. Simplified DC schematic of VCO.

B. Bias Check

<i>FET</i> (<i>tqtrx_DFET</i>)	<i>Function</i>	V_{GS} (mV)	V_{DS} (Volts)	I_{DS} (mA)
Q1	VCO FET	-203	4.5	12.8
Q5	VCO FET Current Source	0	0.290	12.8
Q4	Source Follower	0	2.5	40.9
Q3	Source Follower Current Source	0	2.5	40.9

Figure 14. DC Operating Points.

C. Interconnect and Component DC Current Stress

The VCO was simulated at DC and the current and voltage values at each of the circuit nodes were annotated upon the schematic. Based upon the TQTRx process design rules with respect to FET current handling, passive component current handling, and metal current density, no current thresholds appear to be violated.

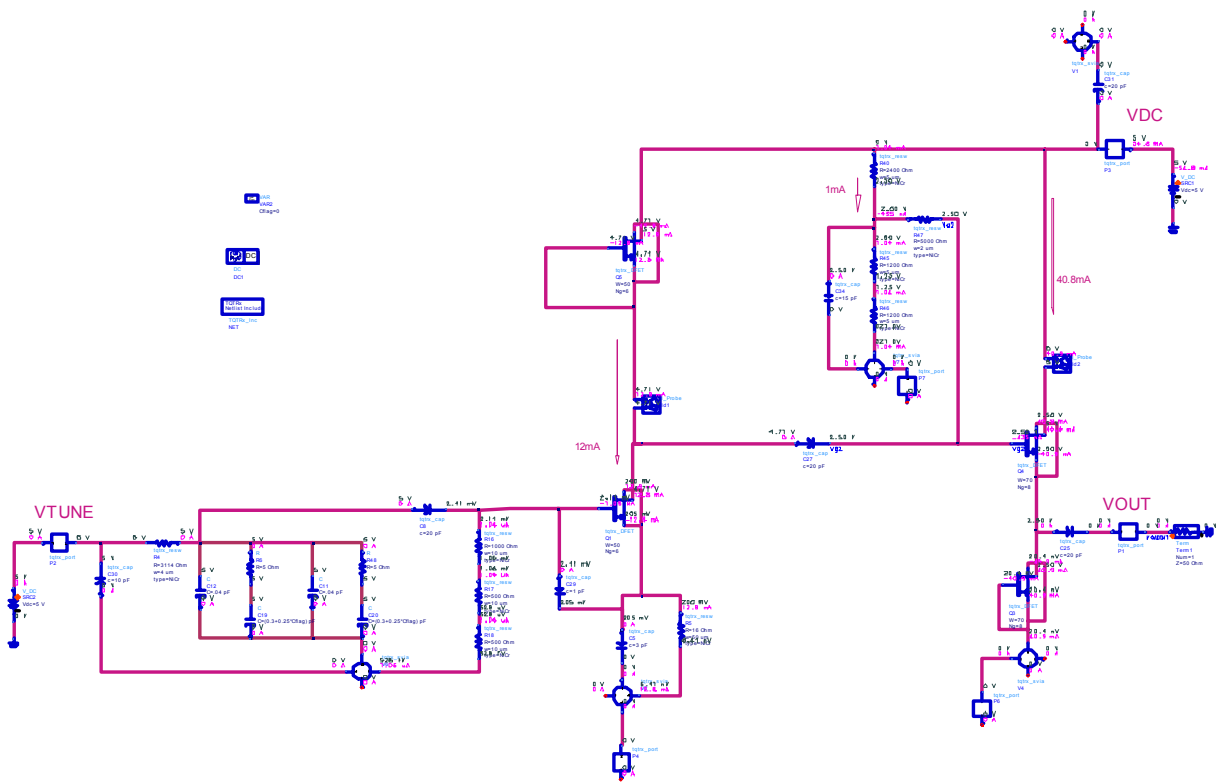


Figure 15. Interconnect and component DC current stress.

VI. Layout

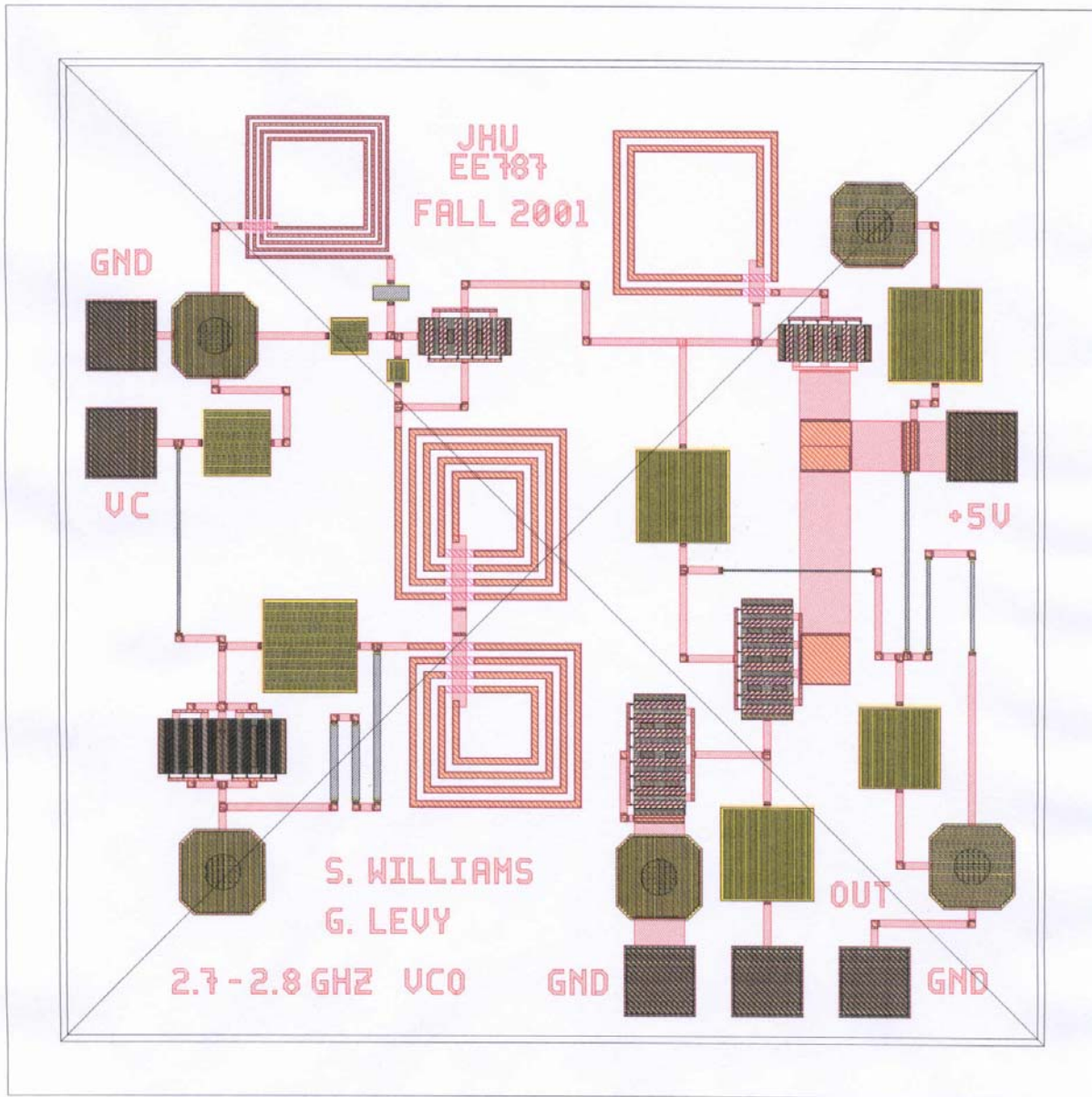


Figure 16. VCO layout.

VII. Test Plan

The bias (5 Volt supply) and frequency control (0-5 Volt variable supply) is applied to the designated pads on the layout with needle probes.

See Fig. 14 for the respective DC bias points for each transistor. Total DC current consumed by the VCO is ~55mA (the sum of each of the transistor bias currents at DC and the resistor ladder.)

The RF output should be extracted with ground-signal-ground (GSG) probes to a spectrum analyzer. The expected signal at the output should be a ~2 Volt peak to peak sinusoid, oscillating between 2596 MHz to 2893 MHz with corresponding power of 14.287 dBm to 12.259 dBm.

VIII. Conclusion & Recommendations

Given more time, a greater effort would have been spent to develop a more robust and innovative adaptive bias technique to limit the harmonic contribution to the output signal at the oscillation frequencies of interest while still maintaining a high gain at DC for startup.

Finally, given the design constraints for a HyperLan and or ISM frequency system, the VCO based upon schematic simulation results, layout simulation results, and peer and expert review, should both meet and or exceed each of the given VCO specifications.

IX. Acknowledgements

A special thanks is given to Craig Moore and John Penn of Johns Hopkins University for their assistance as well as to the class of 525.787 for their peer review. The use of ADS version 150 and tool and design kit support by Gary Wray of Agilent is also greatly appreciated. The authors would also like to graciously thank Triquint for process related information and the fabrication of this design in the TQTRx GaAs process.

X. References

J. Andrews, T. Holden, K. Lee, A. Podell, 2.5-6.0GHz Broadband GaAs MMIC VCO, IEEE MTT-S Digest, 1988.

W. Baumberger, M. Schmatz, A GaAs Single Chip 2.4GHz PLL Frequency Multiplier, IEEE Microwave & Millimeter-Wave Monolithic Circuits Symposium 1996.

H. Chen, A GaAs MESFET MMIC C Band Voltage Controlled Oscillator, Johns Hopkins University Course 525.787, Fall 2000.

F. Ellinger, U. Lott, w. Bachtold, Design of a Low-Supply-Voltage High Efficiency Class-E Voltage-Controlled MMIC Oscillator at C-Band, IEEE Transactions on Microwave Theory & Techniques, Vol. 49, No. 1, January 2001.

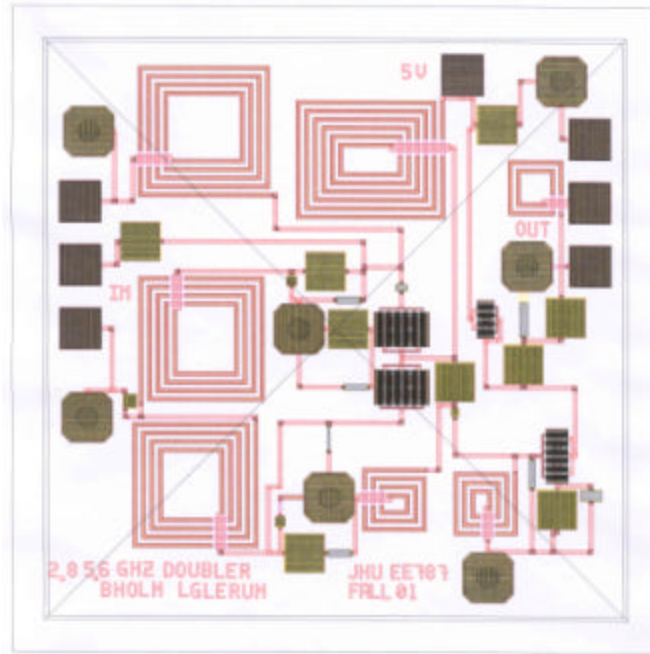
gEE-CAD User's Guide, Johns Hopkins University Courses 525.774 –775, Sept. 2000.

C. Lee, S. Han, B. Matinpour, J. Laskar, A Low Phase Noise X-Band MMIC GaAs MESFET VCO, IEEE Microwave & Guided Wave Letters, Vol. 10, No. 8, August 2000.

J. Shealy, J. J. Shealy, Low-Phase Noise AlGaIn/GaN FET-Based Voltage Controlled Oscillators (VCOs), IEEE Microwave & Wireless Component Letters, Vol. 11, No. 6, June 2001.

D. Warren, J. Golio, W. Seely, Large and Small Signal Oscillator Analysis, Microwave Journal, May 1989.

An S/C Band
Frequency Doubler Design
Using Agilent ADS with
TriQuint's Library



Design by
Lonnie Glerum and Brent Holm

December 10, 2001

Johns Hopkins University
Professors: Craig Moore and John Penn
EE525.787 MMIC Design Class

ABSTRACT

This paper details the design of an S/C band frequency doubler on a 60 mil square GaAs MMIC using HP Advanced Design Software and a TriQuint library. This frequency doubler was required to double an input frequency in the range of 2712.5 to 2812.5 MHz to 5424 to 5625 MHz. This frequency doubler is part of a simplex transceiver project for the C-band HiperLAN wireless local area network (WLAN) and the Industrial Scientific, and Medical ISM bands. The center frequency was selected to fall between the WLAN and ISM bands.

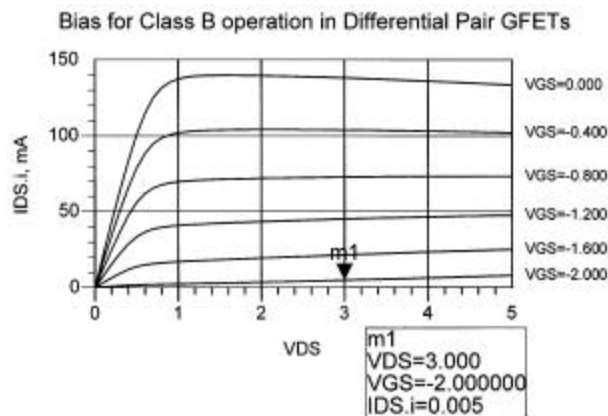
1 INTRODUCTION

1.1 Circuit Description

This MMIC frequency doubler consists of a differential pair of GFET's, a 180 degree phase shift network, and general purpose 2nd stage amplifier. The inputs of the differential pair are fed 180 degrees out of phase by a lumped element 180 degree phase shift network. Each transistor in the differential pair is biased class B that is to have a 50% conduction angle. The output appears as a full wave rectified version of the input, each transistor contributing every other "hump" in the output. Because of the symmetry of the output waveform (it is ideally even symmetric and half-wave even symmetric), it contains no odd harmonics. Therefore, the fundamental and third harmonics normally present in a nonlinear element doubler have been removed by symmetry. A second stage general purpose amplifier provides approximately 6 dB of gain to account for the conversion loss in the differential pair of GFETs.

1.2 Design Philosophy

The first step to designing this frequency doubler was to determine if the differential GFET pair would give the desired 2nd harmonic output while rejecting the 3rd harmonic and fundamental frequencies. A simple schematic consisting of a GFET differential pair with biasing power supplies and an ideal 180 degree transmission line was created and simulated with HP ADS. TriQuint 300 um GFET devices were selected initially since the 300 um device is TriQuint's standard device. A gate to source voltage (V_{gs}) of -2 V that is near the threshold voltage (see figure below) provided good results.



The next step in the design process was to create a 180 degree phase shift network from ideal lumped elements, since the operating frequency is too low for any practical transmission line elements.

To minimize the number of inductors required for a 180 degree lumped element, a double-Pi (two cascaded 90 degree lowpass networks) network was designed for a 50 ohm impedance. When the ideal 180 degree transmission line was replaced with the double-Pi 180 degree lumped element network the frequency doubler still provided good results.

The next step in the design process was replacing the ideal power supply biasing at the gate and drain with a self-bias scheme using a single 5 volt power supply. A large 10 pF shunt capacitor at the power supply and large series inductor of approximately 6000 pH provided adequate RF to DC isolation. Each gate of the differential pair was provided an approximate 0 Volt dc bias through a large resistor to ground. A shared 180 ohm source resistor bypassed with a large 10 pF shunt capacitor provided approximately minus 2.0 volts DC for V_{gs} .

Once proper biasing was obtained, the input matching network (IMN) and output matching networks (OMN) were designed. With the IMN and OMN networks added, the doubler contained a potentially unstable region at approximately 3.4 GHz. This oscillation was traced to a parallel resonance in the double-Pi 180 degree lumped element network. Professor Craig Moore suggested changing the double-Pi 180 degree lumped element network to a 100 ohm impedance and placing 100 ohm resistors at the gates of the differential pair to stabilize the circuit. This change worked very nicely and had the added benefit of a more broadband match at the IMN and OMN when the networks were retuned.

All ideal elements were replaced with TriQuint elements and the circuit was resimulated. This action degraded the performance of the frequency doubler. It was found that the resistive losses in the TriQuint discrete inductors caused a voltage difference between the right and left gates of the differential pair. To account for the resistive losses in the inductor, an 18 ohm series resistor was added at the left gate of the differential pair. The IMN and OMN were also tuned to optimize performance.

At this point in the design process, a rough layout design was performed to ensure that the current circuit would fit on a 60 mil square GaAs MMIC with some room to spare for a 2nd stage amplifier. The circuit layout left about 1/5 of the area for a 2nd stage amplifier which was needed to provide an additional 6 dB gain to reach the goal conversion loss of 0 dB. To fit a second stage amplifier in this area, an active bias network (a half-sized FET with its gate and source connected to create a current source) was selected for the second stage. Furthermore, the IMN and OMN's were kept physically

small by using 200 ohm shunt resistors at the input and output, and by choosing topologies that minimized the amount of inductance required.

1.3 Trade-Offs

The most significant and earliest tradeoff made was the choice of circuit architecture. By using a pair of GFET's driven out of phase for the doubler, it was possible to save a filter that would have been required to block the fundamental and third harmonic created by a more straightforward diode-connected-FET single non-linearity design. Of course, this choice meant it was necessary to construct a phase shift network. It wasn't possible to build both and do a comparison, but the dual transistor approach seemed more novel and elegant, so it was the one chosen. During the layout process, there were numerous small tradeoffs. Individual inductors only come in discrete sizes, so every time our design called for one, we had to add some microstrip line to tune the inductance. And every time we added microstrip line to physically connect things, we had to account for that additional inductance somewhere else. The post-amplifier circuit was designed to be small, not for high performance. Most notably, it has large stabilizing shunt loads on its input and output that made the circuit easier to match to 50 ohms without using large components, especially inductors. It also uses an active load for the bias circuit, which also saves space over that of an inductor used as an RF choke.

2 MODELED PERFORMANCE

2.1 Specifications Compliance Matrix

Characteristic	Specifications	Pre-Layout Results	Final Layout Results
Input Frequency Range	2712.5 – 2812.5 MHz	2712.5 – 2812.5 MHz	2712.5 – 2812.5 MHz
Output Frequency Range	5425 – 5625 MHz	5425 – 5625 MHz	5425 – 5625 MHz
Conversion Loss	3 dB max	5.4 dB	<0 dB
Spurious Fundamental Output	16dBc min, 25 dBc goal	32.8 dBc	39.8 dBc
Spurious 3 rd Order Output	20dBc min, 30 dBc goal	39.8 dBc	35.9 dBc
Input VSWR, 50 Ohms	2.5:1 max, 1.5:1 goal	1.19 max	1.28 max
Output VSWR, 50 Ohms	2.5:1 max, 1.5:1 goal	1.34 max	1.13 max
Supply Voltage	+/- 5 V, +5 V only goal	+5 V only	+5 V only
Size	60 x 60 mil ANACHIP	60 x 60 mil ANACHIP	60 x 60 mil ANACHIP

2.2 Predicted Performance

Figures 1- 3 show the predicted performance of the final layout for the 2.7 - 2.8 GHz frequency doubler.

2.2.1 Output Harmonic Content vs. RF Power In

Figure 1 details the expected output spectrum of the frequency doubler over a swept RF input level.

Marker m2 is the desired doubler output for an input level of +10 dBm. The final layout predicts a conversion gain of approximately 2 dB, and suppression of the fundamental and 3rd order products that exceeds the design goals.

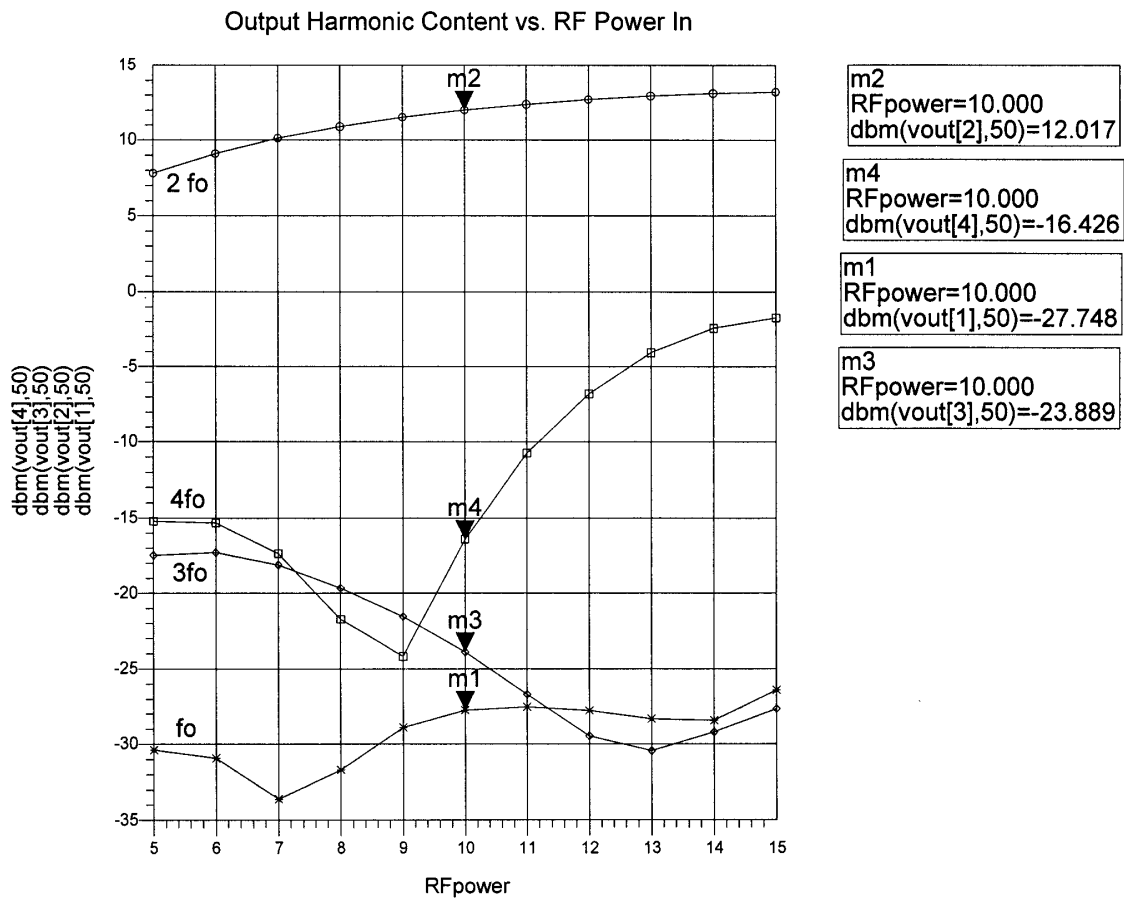


Figure 1

2.2.2 Input and Output Waveforms

Figure 2 shows the time domain representation of the input and output waveforms of the frequency doubler.

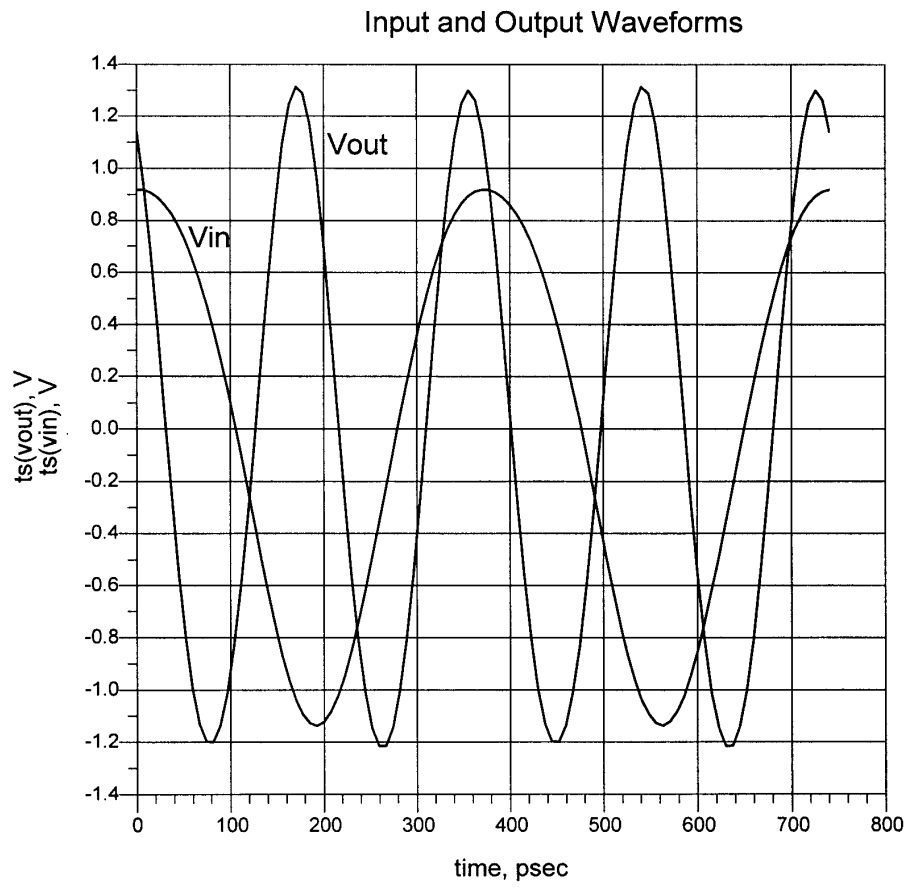


Figure 2

2.2.3 Input VSWR and Output VSWR

Figure 3 shows the predicted VSWR performance of the input and output ports.

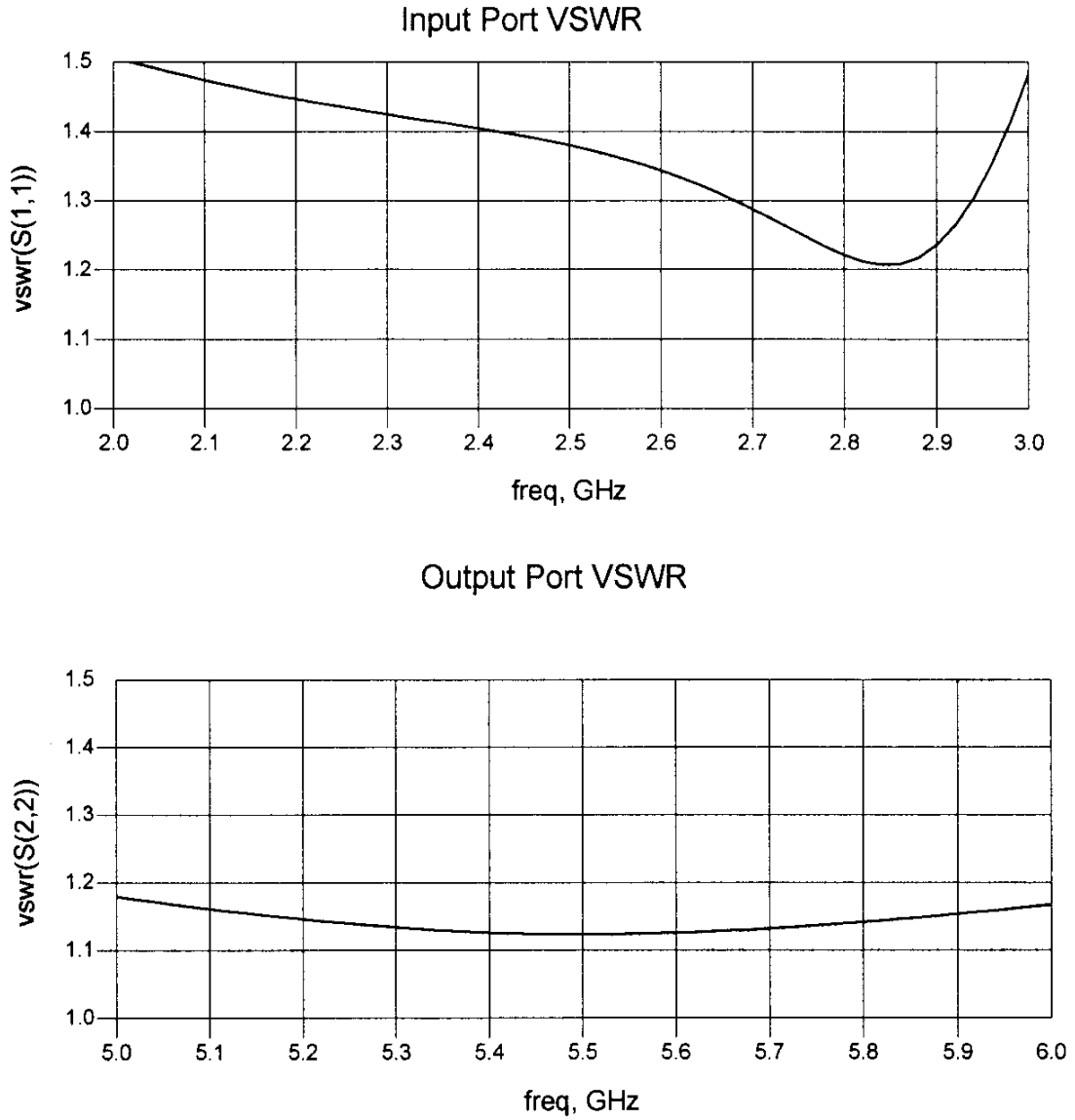
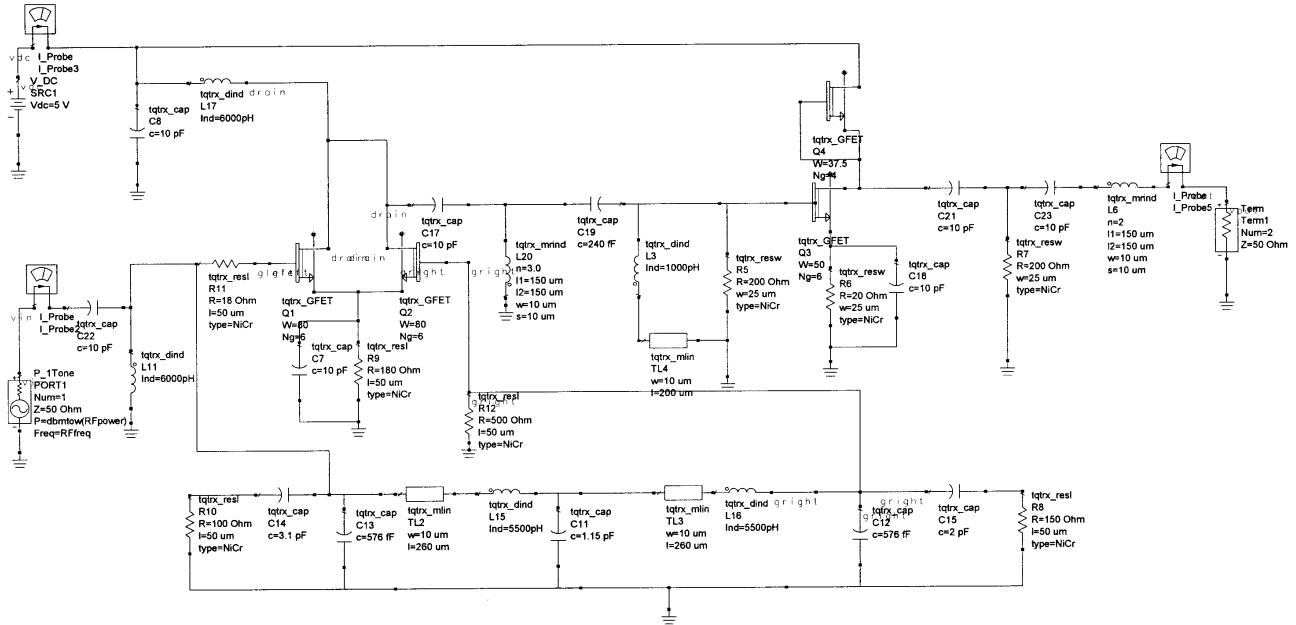


Figure 3

3 SCHEMATIC DIAGRAMS

3.1 Simplified Schematic

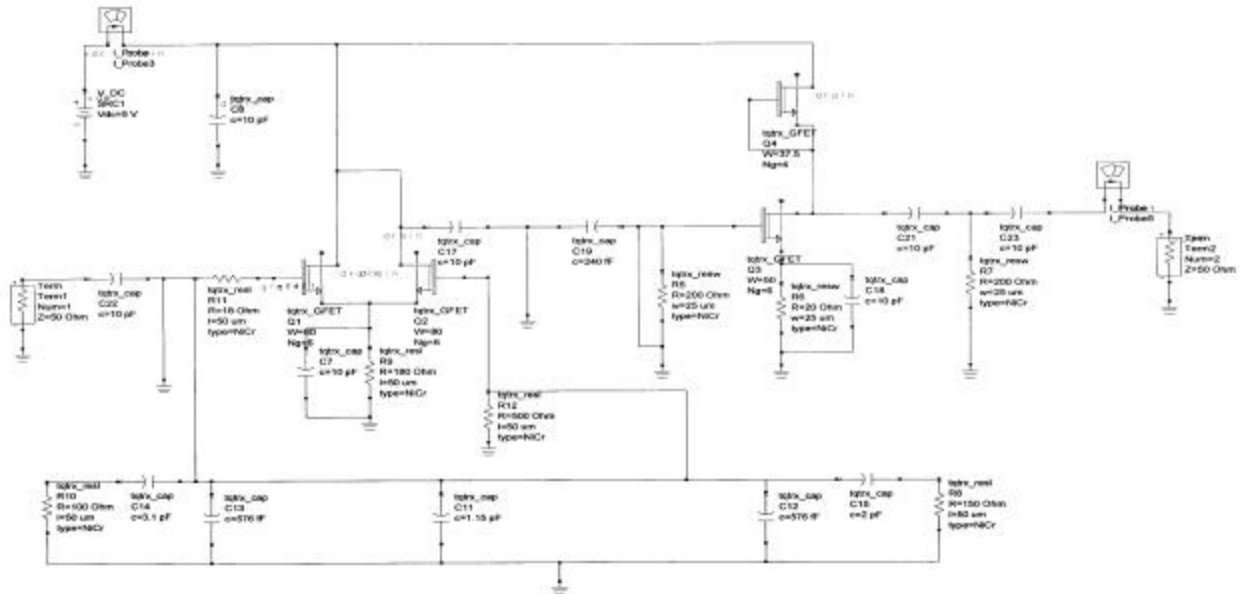
The schematic below has been simplified by removing all routing microstrip lines (bends tees and short MLINs), which did not significantly affect the simulated results.



4 DC ANALYSIS

4.1 DC Schematic

The DC schematic below has been simplified further by replacing inductors and microstrip lines with wires.



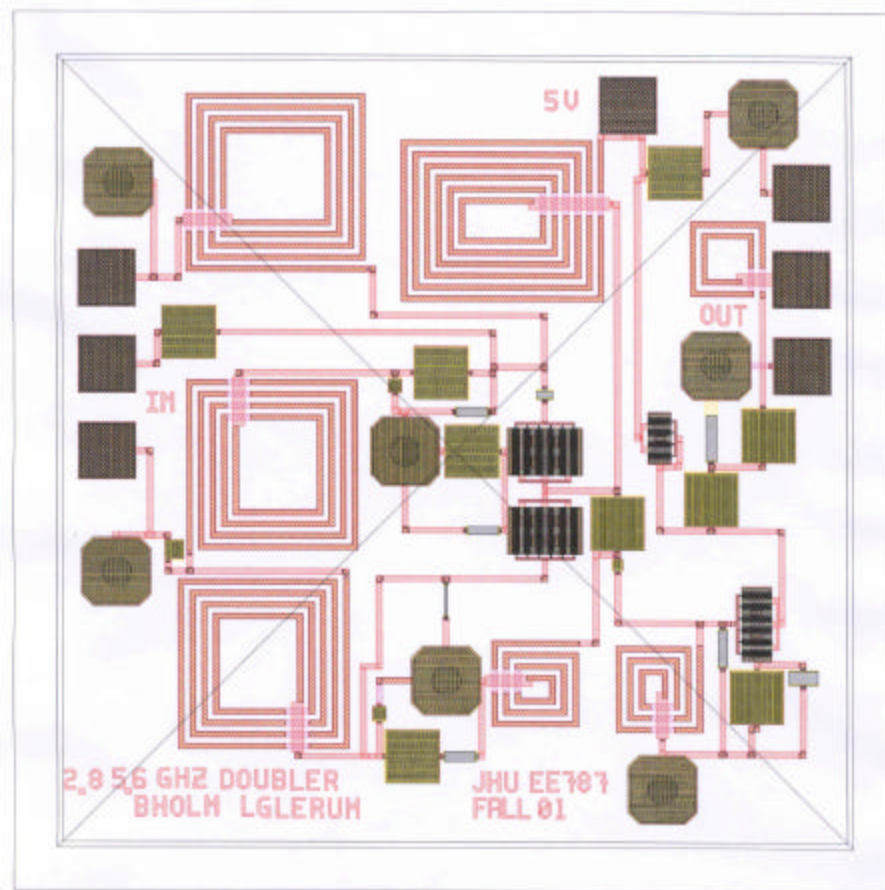
4.2 Bias Check

A bias check was performed on the simplified schematic to ensure that there was no inadvertent DC shorts to ground and that the circuit was biased properly. All biasing was correct, however it was discovered that blocking caps at the input and output ports were inadvertently left out of the schematic.

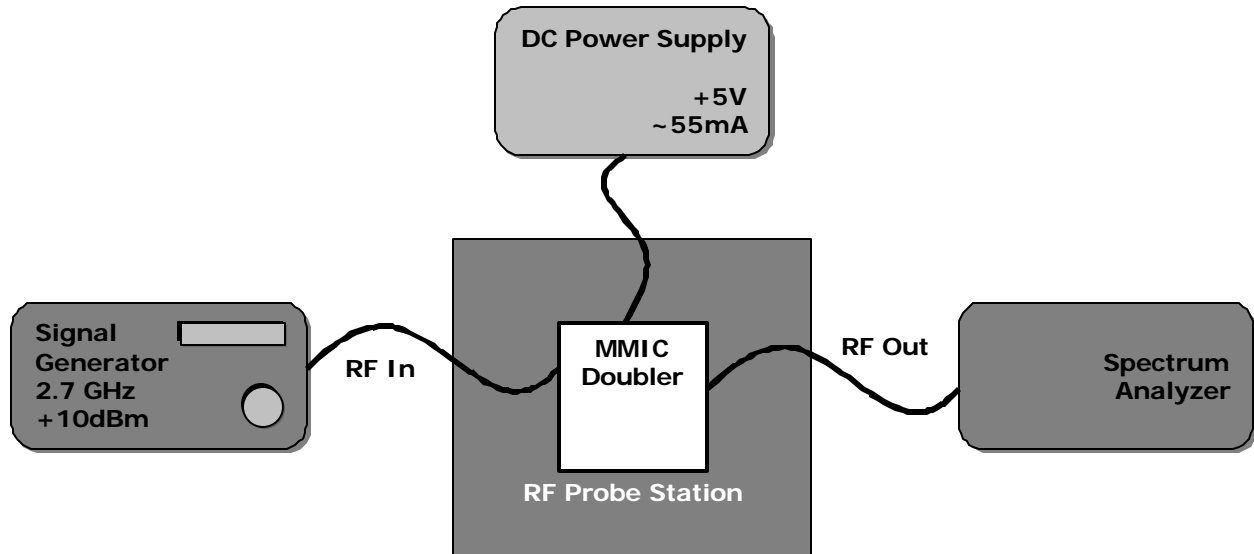
4.3 Interconnect and Component DC Current Stress

In performing the interconnect and component DC current stress analysis, instructors John Penn and Craig Moore discovered that resistor R6 located in series with drain of the output stage amplifier did not have sufficient width to support the current. All other components were satisfactory.

4.4 Final Layout



5 TEST PLAN



Test Equipment Required:

- 1 Glerum/Holm GaAs MMIC Doubler
- 1 RF Signal Generator, 2.7-2.8GHz, +5-15dBm output, (+10dBm minimum)
- 1 Spectrum Analyzer, 1-12GHz (6 GHz minimum). Power out of device could exceed +15dBm, use attenuator if necessary.
- 1 DC Power Supply (+5Vdc, 100mA) with DC milliammeter
- 1 Needle Probe for DC bias
- 2 RF Ground-Signal-Ground Probes

Test Plan:

1. **Visual Inspection.** Verify the chip's identity against the paper printout and check for obvious physical defects. Look for missing elements, inverted components, and chips and cracks.
2. **Bias Current Test.** With power supply off and set to 0V, connect the supply leads to the MMIC doubler chip. Turn supply on and slowly raise the voltage toward +5V. Monitor the current and shut the supply off if it goes above 70mA. (55mA is predicted draw.) Record the actual current draw here _____mA.
3. **RF Connections.** Install MMIC in RF test fixture with its text oriented right side up. Connect the RF input on the left and the RF output on the right.
4. **Functional Test.** Turn on the signal generator and set it to +10dBm, 2.7GHz. Verify that there is a $2F_0$ component on the spectrum analyzer within ~6dB of the input level.
5. **Swept Power Test.** Sweep the input power from +5dBm to +15dBm in 1dB steps and note the power in the frequency doubled term for each step. Also note the power in the fundamental, third, and fourth harmonics. Graph the results and compare them to theoretical.
6. **Input and Output Match.** If time permits, use a network analyzer to check the input impedance around 2.7-2.8GHz and the output match around 5.4-5.6GHz. Compare to theoretical.

6 CONCLUSION AND RECOMMENDATIONS

Using a differential pair of GFETs in class B operation proved to be good topology for a frequency doubler when proper balance was maintained. Careful selection of the bias point near cutoff is required such that each transistor only conducts for 180 degrees of the input wave. The double-Pi 180 degree lumped element network had the potential to cause instability in the differential pair when it was originally designed for an impedance of 50 ohms. By designing the double-Pi 180 degree network for a 100 ohm impedance and placing 100 ohm resistors to ground at each end of the network, the circuit was made stable. Further tweaking of the first and last series capacitors in the double-Pi 180 degree network allowed tuning to ensure a 180 degree phase shift.

When laying the frequency doubler schematic out using Agilent ADS several common mistakes could have been avoided. It is recommended to carefully consider placement of inductors. Try to allow for at least 50 mils of space between an inductor and other microstrip lines, vias, or other inductors. Also try to keep a spacing of 60 mils between capacitors and vias. The instructors caught most of the errors in the initial frequency doubler layout using a Design Rule Check (DRC) program.